TYROSINE KINASE SIGNALING PATHWAYS IN EXPERIMENTAL AUTOIMMUNE SKIN BLISTERING MODELS

Ph.D. thesis

Kata Petra Szilveszter, M.D.

Molecular Medicine Doctoral School

Semmelweis University

Supervisor: Attila Mócsai, M.D., D.Sc

Official reviewers: Éva Ruisanchez, Ph.D.
Ralf Ludwig, M.D., Ph.D.

Head of the Complex Examination Committee:
Edit Buzás, M.D., D.Sc

Members of the Complex Examination Committee:
Anna Erdei, D.Sc
Miklós Sárdy, M.D., D.Sc

Budapest
2022

Table of Contents

List of Abbreviations **6**

1. Introduction **9**

1.1. General overview of neutrophils **10**

1.1.1. Extravasation 10

1.1.2. Effector functions of neutrophils 11

1.1.2.1. Phagocytosis 12

1.1.2.2. Production of reactive oxygen species 12

1.1.2.3. Degranulation 13

1.1.2.4. De novo production of proinflammatory mediators 13

1.1.2.5. Extracellular vesicles 14

1.1.2.6. Neutrophil extracellular traps 14

1.1.3. Neutrophils in disease 14

1.2. Tyrosine kinase-coupled signaling in immune cells **15**

1.2.1. Immunoreceptor signaling 15

1.2.2. Signaling downstream of integrins 18

1.2.3. Cytokine receptors 20

1.2.4. Other tyrosine kinase-coupled signaling mechanisms 22

1.3. PLCγ enzymes **22**

1.3.1. Structure, function and expression of PLCγ enzymes 23

1.3.2. Mutations in the *Plcg2* gene in mice 25

1.3.2.1. Loss-of-function mutations in the Plcg2 gene 25

1.3.2.2. Gain-of-function mutations 26

1.3.3. *PLCG2* variants in humans 27

1.3.3.1. Inherited PLCG2 mutations 27

1.3.3.2. Acquired PLCG2 mutations in malignancies 29

1.3.3.3. PLCG2 variants in neurodegeneration 29

1.3.4. Role of PLCγ2 in autoimmune and inflammatory diseases 30

1.4. Tyrosine kinases in autoimmune and inflammatory skin diseases **31**

1.4.1. Atopic dermatitis 31
1.4.2. Psoriasis 32
1.4.3. Alopecia areata and vitiligo 33
1.4.4. Systemic lupus erythematosus 33
1.4.5. Neutrophilic dermatoses 33
1.5. Autoimmune blistering skin diseases 34
1.5.1. General characterization of pemphigoid diseases 34
1.5.1.1. Incidence and target antigens 34
1.5.1.2. Clinical presentation and associated diseases 36
1.5.1.3. Diagnosis 37
1.5.2. Experimental models of pemphigoid diseases 38
1.5.2.1. In vitro cellular assays 38
1.5.2.2. Ex vivo models 39
1.5.2.3. Autoantibody-induced in vivo models 40
1.5.2.4. Active immunization-induced in vivo models 42
1.5.2.5. Spontaneous development of pemphigoid diseases in mice 43
1.5.3. Pathogenesis of pemphigoid diseases 43
1.5.3.1. The immunization phase 43
1.5.3.2. Importance of complement components 45
1.5.3.3. Recruitment of effector cells 46
1.5.3.4. Fc receptor signaling 47
1.5.3.5. Neutrophils 49
1.5.3.6. Eosinophils and mast cells 50
1.5.3.7. Jak-Stat signaling 51
1.5.4. Therapeutic opportunities and prognosis 51
1.5.4.1. Prognosis 52
2. Objectives 53
3. Methods 54

3.1. Experimental animals 54
3.1.1. Utilized mouse strains 54
3.1.2. Generation of bone-marrow chimeras 55
3.1.2.1. Generation of mixed bone-marrow chimeras 55
3.2. Analysis of the survival rate of mice 56
3.3. Analysis of PLCγ2 expression with western blot 56
3.4. Flow cytometry measurements of circulating leukocyte subsets 57
3.4.1. Sample preparation 57
3.4.2. Flow cytometry and gating strategy 57
3.5. Production of tagged C7 fusion proteins 58
3.5.1. Production of GST-C7 and C7 59
3.5.2. His-C7 production 60
3.6. Production of anti-C7 antibodies 60
3.7. Anti-C7-induced skin blistering in mice 61
3.7.1. Disease induction 61
3.7.2. Evaluation 62
3.8. Histological analysis of the ear tissue 63
3.9. Analysis of leukocyte infiltration and inflammatory mediators 64
3.10. Competitive in vivo migration assay 64
3.11. In vivo chemiluminescence assay 65
3.12. In vitro experiments using murine neutrophils 65
3.12.1. Isolation of murine neutrophils 65
3.12.2. In vitro Transwell migration assay 66
3.12.3. In vitro immune complex-induced proinflammatory mediator release 66
3.13. Experiments using human cells and tissue 67
3.13.1. Isolation of human neutrophils 67
3.13.2. Ex vivo human skin separation assay 67
3.14. Presentation of the data and statistical analysis 68
4. Results 69
4.1. General characterization of *Plcg2*$^{-/-}$ mice 69
4.2. Setting up the anti-C7-induced skin blistering model 71
4.2.1. Purification of antigens and antibodies 72

4.2.2. Disease induction 74
4.3. The role of PLCγ2 in antibody-induced skin blistering 75
4.3.1. Anti-C7-induced skin blistering in intact *Plcg2*$^{-/-}$mice 75
4.3.2. Anti-C7-induced skin blistering in *Plcg2*$^{-/-}$ bone-marrow chimeras 77
4.3.3. Circulating anti-C7 levels and antibody deposition 80
4.3.4. Dermal infiltration of leukocytes 81
4.3.5. Intrinsic migratory capacity of leukocytes 83
4.3.6. Development of the proinflammatory microenvironment in vivo 87
4.4. In vitro functional responses of PLCγ2-deficient neutrophils 92
4.4.1. Migration capacity 92
4.4.2. Immune complex-induced release of proinflammatory mediators 93
4.5. Lineage-specific analysis of PLCγ2 in anti-C7-induced skin blistering 94
4.5.1. Efficacy and specificity of *Plcg2* deletion in *Plcg2*$^{\Delta PMN}$ mice 95
4.5.2. Anti-C7-induced skin blistering in *Plcg2*$^{\Delta PMN}$ mice 97
4.5.3. Infiltration of leukocytes in *Plcg2*$^{\Delta PMN}$ mice 99
4.6. Human ex vivo dermal-epidermal separation 100
4.7. Effect of tofacitinib treatment on anti-C7-induced skin blistering 102
5. Discussion 105
5.1. Characterization of *Plcg2*$^{-/-}$ mice 105
5.2. Anti-C7-induced skin blistering in *Plcg2*$^{-/-}$ mice 106
5.3. Neutrophil-specific analysis of PLCγ2 during experimental EBA 110
5.4. Human relevance of our studies 113
5.5. Relevance of our studies regarding other autoimmune diseases 115
5.6. Effect of Jak inhibition in experimental EBA 115
6. Conclusions 117
7. Summary 118
8. Összefoglalás 119
9. References 120
10. Bibliography of Candidate's Publications 149
10.1. Publications related to thesis 149
10.2. Publications not related to thesis 149
11. Acknowledgements 150

LIST OF ABBREVIATIONS

ANOVA	analysis of variance
APLAID	autoinflammation and PLAID
BCR	B cell receptor
bid	bis in die, twice a day
BLT1	leukotriene B4 receptor
BP	bullous pemphigoid
Btk	Bruton tyrosine kinase
C5a	complement component 5a
C5aR	complement component 5a receptor
C7	collagen type VII
CARD9	caspase recruitment domain family member 9
CD	cluster of differentiation
CD11a	αL integrin
CD11b	αM integrin
CD18	Integrin β chain 2
CR3	complement receptor 3 (also known as CD11b/CD18 or Mac-1)
DAPI	4′,6-Diamidino-2-phenylidole
D-E	dermal-epidermal
DEJ	dermal-epidermal junction
DMF	dimethylformamide
EBA	epidermolysis bullosa acquisita
ELISA	enzyme-linked immunosorbent assay
ENU	N-ethyl-N-nitrosourea
FCS	fetal calf serum (same as fetal bovine serum or FBS)
GM-CSF	granulocyte-monocyte colony-stimulating factor
GST	glutathione-S-transferase
HBSS	Hank’s Balanced Salt Solution
HBSS/H	HBSS supplemented with 20 mM HEPES
H&E	haemotoxylin and eosin dye
HEPES	4-(2-hydroxyethyl)-1-piperazineethanesulfonic acid

HRP	horseradish peroxidase
HSA	human serum albumin
ICAM	intercellular adhesion molecule
IL	interleukin
ITAM	immunoreceptor tyrosine-based activation motif
ITIM	immunoreceptor tyrosine-based inhibitory motif
Jak	Janus kinase
LFA-1	lymphocyte function-associated antigen 1 (CD11a/CD18)
LTB_4	leukotriene B4
Ly6G	lymphocyte antigen 6 complex locus G
Mac-1	macrophage antigen 1 (also known as CD11b/CD18 or CR3)
MCP	monocyte chemoattractant protein
MFI	mean fluorescent intensity
MHC	major histocompatibility
MIP-2	macrophage inflammatory protein 2; CXCL2
MMP	mucous membrane pemphigoid
MPO	myeloperoxidase
MRP8	myeloid-related protein 8
NADPH	Nicotinamide adenine dinucleotide phosphate
NC	noncollagenous domain
NF-κB	Nuclear factor kappa-light-chain-enhancer of activated B cell
PAGE	polyacrylamide gel electrophoresis
PBS	phosphate buffered saline
PCR	polymerase chain reaction
PH	pleckstrin homology domain
PLAID	PLCG2-associated antibody deficiency and immune dysregulation
PLC	phospholipase C
ROS	reactive oxygen species
SDS	Sodium dodecyl sulphate
SEM	Standard error of the mean
SH	Src homology
SHP-1	SH2 domain-containing protein phosphatase

Siglec-F	sialic acid-binding immunoglobulin-like lectin-F
Stat	signal transducer and activator of transcription
Syk	spleen tyrosine kinase
TCR	T cell receptor
TNF	tumor necrosis factor
VCAM-1	vascular cell adhesion molecule 1
VLA-4	very late antigen4
WT	wild-type

1. INTRODUCTION

Autoimmune diseases are quite prevalent conditions with increasing incidence due to mostly unknown reasons, creating a serious burden to the medical system and the overall society worldwide [5]. Although there is an expanding palette of targeted therapeutic approaches like biologic agents and small molecule inhibitors [1, 6, 7], treatment of several autoimmune diseases are far from being solved. Multiple aspects of their complex pathology are still not fully elucidated, underlining the importance of further research in this field.

There are two major phases in the pathogenesis of diseases of autoimmune origin. In the so-called immunization phase, the immune system loses tolerance to particular self-antigens due to multifactorial etiology consisting of several, mainly unknown genetic and environmental factors. Adaptive immune cells like autoreactive B and T cells are central players during this phase. They can exert direct cytotoxicity (CD8 positive cytotoxic T cells) or produce autoantibodies (plasma cells differentiated from autoreactive B cells).

Circulating autoantibodies typically get deposited in tissues recognizing their specific autoantigens creating immune complexes, which can initiate the second, so-called effector phase of autoimmune diseases. Here, deposited immune complexes initiate an acute inflammatory response driven mainly by innate immune cells like neutrophils. Tissue damage and further amplification of inflammation finally result in the clinical manifestation of the disease.

Our workgroup has been investigating immune cell signaling mechanisms driving inflammation and tissue damage during the effector phase of autoimmune diseases focusing on innate immune cells, especially neutrophils. We showed that tyrosine kinases involved in immune complex-recognizing immunoreceptor signaling play an essential role in the effector phase of animal models reminiscing rheumatoid arthritis and autoimmune blistering skin diseases [4, 8-10].

In addition, the developing proinflammatory milieu consists of several cytokines, which signal through tyrosine kinases, namely Janus kinases (Jaks) [11]. Inhibition of Jaks has revolutionized disease therapy in rheumatoid arthritis and other inflammatory and autoimmune diseases [12]. However, there are scarce information about this pathway in autoimmune blistering skin diseases [1].

During my PhD studies, I aimed to further elucidate the immunoreceptor signaling cascade downstream of tyrosine kinases driving autoimmune skin blistering using an in vivo mouse model and in vitro cellular assays, mainly focusing on the phospholipase Cγ2 (PLCγ2) enzyme. Moreover, we translated our studies to human pathology using an ex vivo human skin separation assay, as well. I also intended to investigate the role of Jak kinases in the mouse model of autoimmune skin blistering, of which I will present my initial findings in this thesis.

1.1. GENERAL OVERVIEW OF NEUTROPHILS

Neutrophils are short-lived innate immune cells of myeloid origin representing the first line of defense against various external pathogens or intrinsic potential harmful stimuli. They are the most abundant leukocyte subtype in the human blood (40 – 70% of circulating leukocytes) and a smaller but significant portion (20 – 30% [13]) in the circulation of mice. They are capable of migrating out to the interstitium under chemotactic stimuli (a process called extravasation), being among the very first cells to be recruited to the site of inflammation [14].

1.1.1. Extravasation

Extravasation of neutrophils is a multi-step, tightly controlled mechanism allowing neutrophils to leave the circulation and enter the interstitium. The process contains the following steps summarized briefly based on recent reviews [14-16] and also shown in **Figure 1**.

Circulating neutrophils can bind to P-selectin expressed by endothelial cells. This weak link allows the neutrophils to slow down and tether at the endothelial layer ("rolling"). Upon inflammation, neighboring endothelial cells begin to express E-selectins, as well, which will further tighten neutrophil-endothelial cell binding and slow down neutrophil rolling even more ("slow rolling").

Further chemotactic stimuli from the inflamed tissue (e.g. LTB_4 through BLT1 receptor [17]) immobilized on the surface of the endothelial cells can initiate intracellular signaling in neutrophils leading to conformational change of plasma membrane β_2-integrins (also known as inside-out signaling process [16]). This conformation of β_2-

integrins will allow binding to their ligands (cell adhesion molecules from the immunoglobulin superfamily; present on endothelial cells) with high affinity, allowing the arrest and firm adhesion of neutrophils. Remaining firmly attached, they slowly crawl along the endothelial layer, searching for proper place for exiting the circulation, a process also controlled by β_2-integrins.

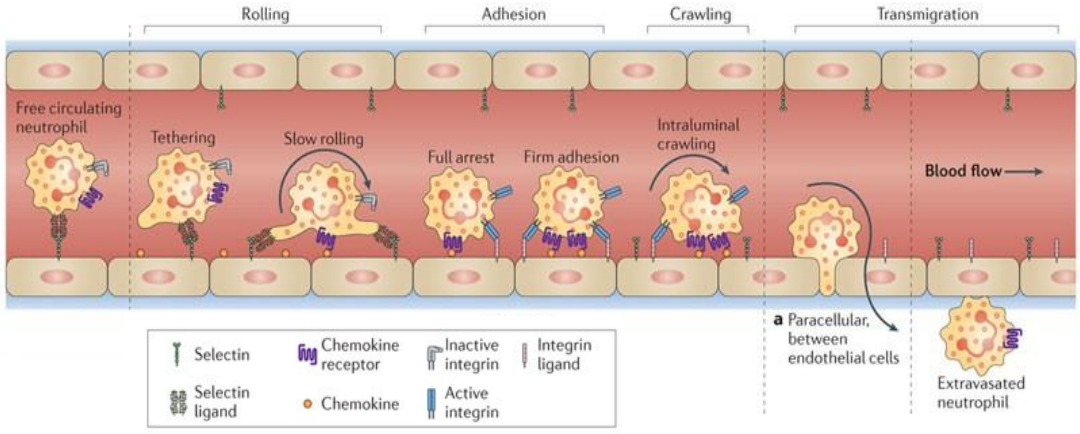

Figure 1. Extravasation of neutrophils.
From Kolaczkowska and Kubes, Nat Rev Immunol, 2013 [14]

Finally, transmigration can occur paracellularly between endothelial cells, or even transcellularly requiring integrins and different cellular and junctional adhesion proteins. After entering the interstitial tissue, neutrophils migrate via amoeboid movement along the chemotactic gradient such as microbial substances, the complement components, lipid mediators, or chemokines.

The classical dogma is, that neutrophils are short lived cells that undergo cell death quickly after entering the tissue. Contrarily, it has been revealed that neutrophils can have prolonged lifespan under certain inflammatory stimuli [18] and sometimes even return to the circulation by reverse migration. However, the mechanism and the exact relevance of the latter process is not fully understood yet [19].

1.1.2. Effector functions of neutrophils

Activation of neutrophils through various signaling pathways leads to the initiation of their extensive effector function repertoire. It drives the acute inflammatory response, aiming to eradicate pathogens and intrinsic danger signals. **Figure 2** shows the most important functions of neutrophils discussed briefly below.

1.1.2.1. Phagocytosis

Neutrophils can efficiently eliminate invading pathogens through phagocytosis. Ligand binding through Fcγ receptors or complement receptors initiates cytoskeletal reorganization leading to phagocytic cup formation and eventually the engulfment of the invading microorganism. The phagosome fuses with preformed intracellular granules resulting in rapid degradation of phagocytosed substances using hydrolytic enzymes, NADPH-oxidase and myeloperoxidase (MPO) [20].

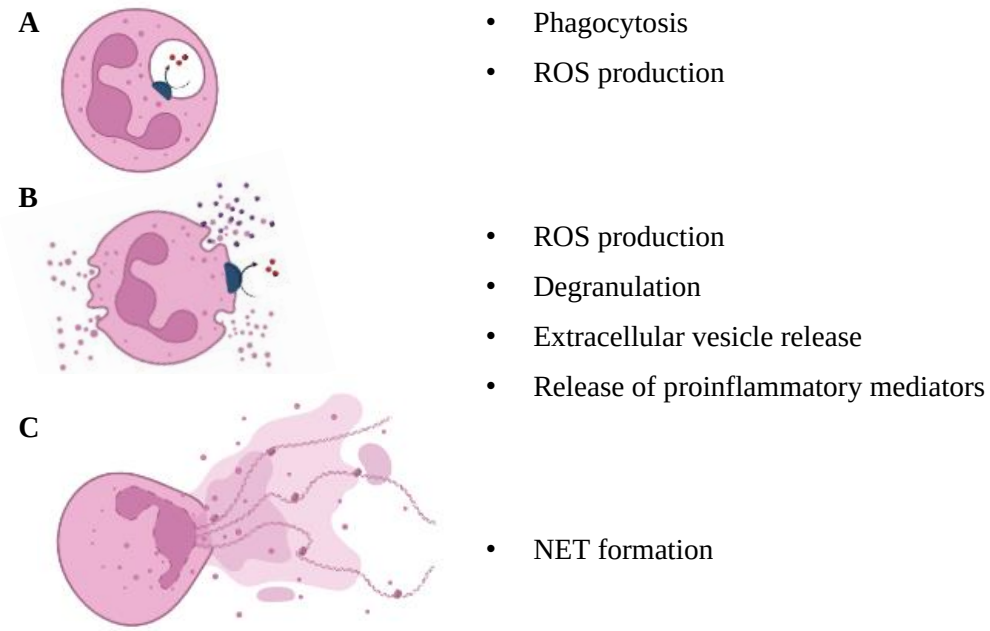

Figure 2. Effector functions of neutrophils.
Activation of neutrophils can result in cytoskeletal rearrangements leading to the phagocytosis and intracellular degradation of pathogenic particles (**A**); the production of reactive oxygen species released to the phagosome (**A**) or to the extracellular space (**B**); exocytosis of granule components and the release of several proinflammatory mediators (chemokines, cytokines and lipid mediators), as well as extracellular vesicles (**B**), or the formation of neutrophil extracellular traps (NETs) by releasing chromatin structure and granule components (**C**). *Created in BioRender.*

1.1.2.2. Production of reactive oxygen species

A relatively unique effector function of neutrophils is that they can produce a wide variety of oxidant molecules, collectively called reactive oxygen species (ROS), which can interact with high reactivity with surrounding proteins, lipids and nucleic acids, thus damaging invading microorganisms.

Upon activation, neutrophils undergo a respiratory burst, when oxygen consumption

increases due to an increased activity of the phagocyte NADPH oxidase complex [21]. This enzyme complex consists of several subunits assembling in the membrane of granules or sometimes in the plasma membrane, generating superoxide anion using the electron from NADPH oxidation. Superoxide anions then can turn into different reactive oxygen species. For instance, in the phagosome typically hydrogen peroxide is produced (catalyzed by superoxide dismutase), which is further converted to hypochloric acid (HOCl) with the help of MPO [22].

1.1.2.3. Degranulation

Neutrophils contain multiple types of preformed granules containing various antimicrobial agents, degrading enzymes and even signaling molecules.

Primary (azurophilic) granules specifically contain myeloperoxidase, critical for ROS-mediated degradation of phagocytosed particles [23]. In addition, they accumulate different serine proteases like elastase and cathepsins, as well as bactericidal proteins like lysozyme and defensins. They typically fuse with phagosomes in order to eliminate phagocytosed pathogens [22].

Secondary (specific) granules are characterized by containing lactoferrin among other antimicrobial compounds, while tertiary (gelatinase) granules store mostly proteolytic enzymes such as gelatinase, collagenase or other matrix metalloproteinases [24]. Besides fusing with phagosomes, granule content can also be released into the extracellular space to help the movement of neutrophils in the interstitium.

Secretory vesicles are somewhat different from granules. They are formed by endocytosis from the plasma membrane of neutrophils and therefore contain plasma-derived proteins like albumin [25]. They also serve as a pool of various transmembrane receptors important in adhesion and chemotaxis, which can be translocated to the plasma membrane upon inflammatory stimuli [23].

1.1.2.4. De novo production of proinflammatory mediators

In addition to processes involving direct antimicrobial killing and tissue damage, neutrophils are capable of releasing and producing a variety of different mediators upon activating stimuli, thus modulating immune response by interacting with other immune cells and creating an inflammatory microenvironment [26, 27]. It has been shown that gene expression is also actively happening in activated neutrophils leading to the increased de novo synthesis of several proinflammatory chemokines, and cytokines like

IL-1β and MIP-2 [28].

1.1.2.5. Extracellular vesicles

Neutrophils can also release extracellular vesicles, with a different mechanism than degranulation. Neutrophil-derived extracellular vesicles can be released both at rest and upon activation, having specific content according to stimuli [29]. They are implicated in antimicrobial killing and in the communication with other immune cells, however, their proper function is not fully characterized [30].

1.1.2.6. Neutrophil extracellular traps

Neutrophils are capable of forming extracellular traps (NETs) extruding their chromatin with granule proteins (like myeloperoxidase, elastase and other antimicrobial peptides) [31]. To our current knowledge, it has a role in trapping extracellular pathogens by the sticky net formed by DNA and histones. It results in their enhanced elimination via the high local concentration of granule components within the net. There are more and more data appearing about the role of NETs in health and disease [32, 33]. However, the mechanism of NET formation is incompletely understood and there are still many uncertainties and controversies about their specific functions [34].

1.1.3. Neutrophils in disease

In line with the above detailed anti-microbial functions of neutrophils, decreased number or impaired function of neutrophils results in the increased susceptibility to infections. Insufficient clearance of pathogens can result in chronic unresolving infections like in chronic granulomatous disease, or can lead to possibly life-threatening systemic spread of microbes [35].

Despite their essential role during host defense, overactivation or aberrant behavior of neutrophils were associated with diverse pathologic conditions. Neutrophils play a role in the development of several autoimmune diseases, like systemic lupus erythematosus, rheumatoid arthritis and vasculitis [36, 37]. Moreover, neutrophils were implicated in the pathomechanism of inflammatory skin diseases like psoriasis [38]; atherosclerosis [39], chronic inflammatory lung diseases associated with smoking [40], asthma [41], and even thrombosis [42] or cancer [43] . Therefore, investigation of neutrophil function and proper elucidation of signaling mechanisms in health and disease can lead to a better understanding of these diseases, and may identify new therapeutic options.

1.2. TYROSINE KINASE-COUPLED SIGNALING IN IMMUNE CELLS

Tyrosine kinase-coupled signaling in immune mediated disorders has been in the center of attention in medical research in the past decades. They have critical role in immune complex-mediated and many other inflammatory processes, representing a plausible therapeutic target showed by the success story of Jak inhibitors [12]. Therefore, I shortly summarize the key tyrosine kinase-coupled pathways in this section and point out their relevance during immune cell activation. I will focus on the immunoreceptor and integrin signaling in innate immune cells, and the Jak-Stat pathway, since these stood in the center of attention during my PhD studies.

1.2.1. Immunoreceptor signaling

B cell receptors (BCR), T cell receptors (TCR) and Fc-receptors belong to a group collectively termed as immunoreceptors. They bear a conserved immunoreceptor tyrosine-based activation motif (ITAM sequence) located on the cytoplasmic tail of the receptor itself, or on associated adaptor molecules. The motif contains four separated Tyr residues, which become phosphorylated by Src-family tyrosine kinases upon ligand binding. Phosphorylated ITAMs then serve as a docking site for several further adaptor proteins and tyrosine kinases through their Src homology 2 (SH2) domains. A crucial molecule recruited and activated through this process is the spleen tyrosine kinase Syk (or in case of TCR signaling, a similar molecule, called ζ-chain-associated protein kinase of 70 kDa, or ZAP-70). Activated Syk initiates downstream signaling (shown in **Figure 3**) including the Bruton tyrosine kinase (Btk), phospholipase Cγ (PLCγ) enzymes, the Vav family of guanine nucleotide exchange factors, Rac GTPases and phosphoinositide-3-kinases (PI3Ks). Finally, it leads to increased intracellular Ca^{2+} concentration and activation of the mitogen-activated protein kinase (MAPK) cascade, among others [44]. Importantly, SH2 domain-containing protein phosphatase (SHP-1) is a crucial component limiting ITAM-based signaling [45].

BCR and TCR signaling has an essential role in recognition of foreign and self-antigens by the adaptive immune system and is indispensable for the proper development, maturation and activation of B and T cells. Disruption of BCR signaling in case of Syk deficiency leads to the complete absence of mature B cells in mice [46, 47].

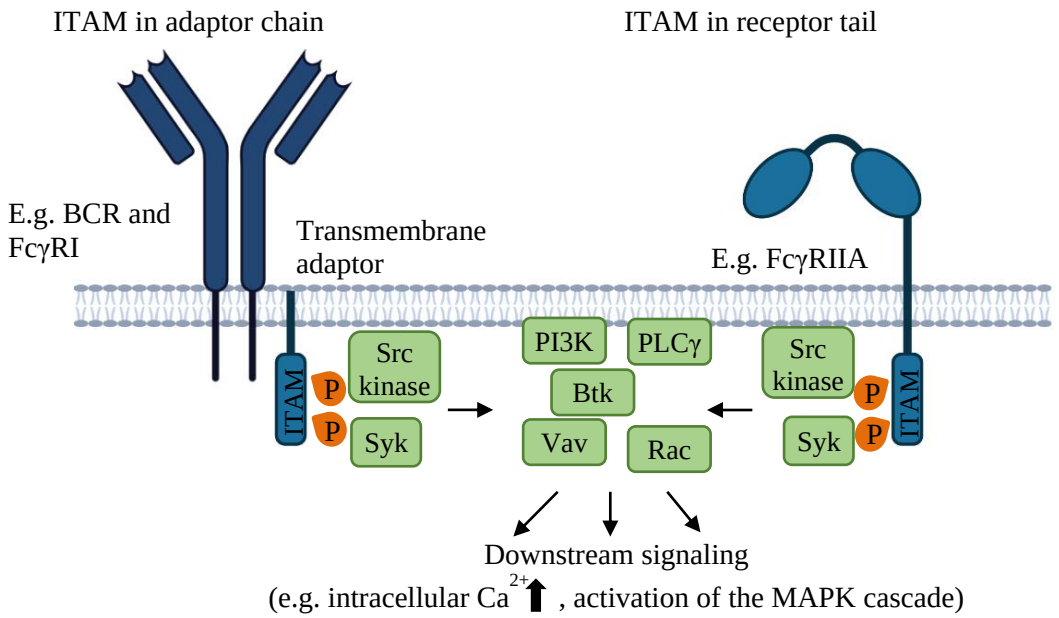

Figure 3. Scheme of immunoreceptor signaling.
Immunoreceptors signal through a tyrosine-based activation motif (ITAM sequence) located on an associated adaptor molecule (in case of BCR or human FcγRI for example) or on the cytoplasmic tail of the receptor itself (like in human FcγRIIA). Ligand binding leads to the phosphorylation of tyrosine residues by Src-family kinases, leading to the recruitment and activation of the Syk tyrosine kinase. It is followed by the recruitment of other components including phosphoinositide-3-kinases (PI3Ks), the Bruton tyrosine kinase (Btk), phospholipase Cγ (PLCγ) enzymes, the Vav family of guanine nucleotide exchange factors and Rac GTPases. Downstream signaling involves, among others, the increase of intracellular Ca^{2+} and the activation of the mitogen-activated protein kinase cascade, leading to functional responses. *Based on [44], created in BioRender.*

Several types of Fc receptors are present both in humans and mice recognizing the Fc portion of different antibody classes, therefore involved in the recognition and elimination of antibody-opsonized particles or aggregated antigen-antibody immune complexes. They are expressed by a wide variety of hematopoietic cells, like B cells, NK cells, dendritic cells, neutrophils, monocytes/macrophages, eosinophils, basophils and mast cells [48].

There are also inhibitory Fc-receptors which contain immunoreceptor tyrosine-based inhibitory motifs (ITIM sequences) activating phosphatases. They modulate ITAM-mediated activation of leukocytes to avoid uncontrolled activation of immune responses.

Immunoglobulin class G (IgG) is recognized basically by Fcγ-receptors (FcγRs). In humans, there are five main activating FcγRs [49] (see also in **Table 1**). FcγRI serves as

the high affinity receptor associated with an ITAM-containing adaptor called FcR γ-chain (FcRγ). The low affinity receptors are FcγRIIA and FcγRIIC. They carry ITAMs on their own cytoplasmic tail, while FcγRIIIA also associates with the ITAM-bearing FcRγ chain. Uniquely, FcγRIIIB is anchored to the plasma membrane only with a glycosylphosphatidylinositol (GPI) link and expressed exclusively by neutrophils. FcγRIIB is the inhibitory receptor containing ITIM sequences in the cytoplasmic tail [49].

Mice express three activating (FcγRI, FcγRIII and FcγRIV) receptors associated with FcRγ (see also in **Table 1**). FcγRI is a high-affinity receptor similar to the human one, expressed mainly on tissue resident macrophages and dendritic cells. The low-affinity FcγRIII (its human orthologue is FcγRIIA) and the inhibitory FcγRIIB are expressed widely in most of the myeloid cells, while FcγRIV (which is similar to human FcγRIIIA) is expressed predominantly by neutrophils and certain monocyte/macrophage subtypes [49]. Importantly, there are multiple differences in the structure of these orthologue receptors in humans and mice, making it difficult to directly compare them.

Table 1. Types and schematic structure of human and mouse FcγRs (based on [49])

	Human orthologue	Mouse orthologue
Activating receptors	FcγRI 	FcγRI 
	FcγRIIA 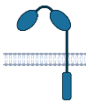	FcγRIII 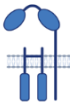
	FcγRIIC 	-
	FcγRIIIA 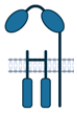	FcγRIV 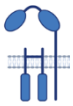
	FcγRIIIB 	-
Inhibitory receptor	FcγRIIB 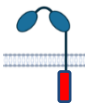	FcγRIIB 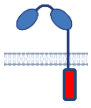

There are FcRs recognizing other Ig classes like IgE-sensing Fcε-receptors on the surface of basophils and mast cells. They are involved in anaphylactic reactions like

allergies and asthma and also signal through the ITAM-containing adaptor FcRγ in mice.

Previously, our workgroup investigated the role of FcγR signaling in various neutrophil responses using a transgenic approach. Genetic deletion of the common FcRγ adaptor chain led to the abrogation of immune complex-induced spreading, degranulation and ROS production in murine neutrophils [50, 51]. While single lack of either FcγRs were dispensable for the activation of murine neutrophils by immobilized immune complexes, pharmacologic inhibition or genetic deficiency of both FcγRIII and FcγRIV receptors resulted in a complete defect in cellular responses [51]. In case of human neutrophils, FcγRIIA and FcγRIIIB had essential role on its own in immune complex signaling [51].

Our workgroup also elucidated the role of several downstream signaling components in cellular responses upon FcγR activation in vitro. Hck, Fgr and Lyn are the three relevant Src-family kinases expressed in neutrophils. They had essential, although redundant role in immune complex-mediated activation of neutrophils and macrophages in vitro. Complete abrogation of cellular responses occurred only, when all three kinases were deleted genetically from mice [8]. Regarding the Syk tyrosine kinase, both ROS production of neutrophils and phagocytosis of macrophages induced by antibody-opsonized particles were severely impaired in *Syk*$^{-/-}$ cells [52]. Other signaling components laying downstream of Src-family kinases and Syk include PLCγ2 (see in detail in section 1.3) and the caspase recruitment domain family member 9 (CARD9). Results of our workgroup implicated, that CARD9 is involved in FcγR-induced gene expression changes, but not in degranulation or ROS production of neutrophils [28]. It suggests, that downstream signal transduction splits into a CARD9-dependent and a CARD9-independent arm [28].

Taken together, FcγR signaling mediate various responses of innate immune cells in vitro. These include ROS production, cytoskeletal changes leading to phagocytosis and degranulation, as well as gene expression changes leading to the production of a variety of inflammatory mediators.

1.2.2. Signaling downstream of integrins

Integrins are heterodimeric adhesion molecules containing transmembrane α and β subunits. Besides their anchoring function to the extracellular matrix or adjacent cells,

they are also capable of inducing other signaling pathways (classical, so-called outside-in signaling) leading to leukocyte activation [53].

Leukocytes express the $\alpha_4\beta_1$ integrin (also called very late antigen-4, VLA-4) which binds to endothelial VCAM-1 (vascular cell adhesion molecule-1, member of the immunoglobulin superfamily) involved in the extravasation process mentioned before. Integrins containing the β_2 subunit (also called CD18) are also uniquely expressed by leukocytes. $\alpha_L\beta_2$ integrin (CD11a/CD18, also called lymphocyte function-associated antigen 1, LFA-1) is expressed by all leukocytes. It binds to ICAM ligands (intercellular adhesion molecule, members of the immunoglobulin superfamily) and is involved also in the extravasation process. $\alpha_M\beta_2$ integrin (CD11b/CD18, also called macrophage antigen 1, Mac-1) is considered the most prominent type of integrins on myeloid cells [54]. Various ligands were described to be able to activate signal transduction through Mac-1, including several extracellular matrix proteins like ICAMs, fibrinogen and the cleaved activated complement component iC3b (hence, Mac-1 is also known as complement receptor 3 or CR3) [54].

Integrins have distinct conformations affecting the affinity of ligand binding. In resting state, integrins are mostly present in a bent conformation with low ligand affinity. Upon cellular activation, they are upregulated at the cell surface through the exocytosis of secretory vesicles. Moreover, intracellular signaling leads to a conformational change of integrins (called inside-out signaling process) providing a high-affinity state for ligand binding. E-selectin, different chemokines, cytokines and lipid mediators have been described to initiate such conformational changes. The process possibly involves PLCγ enzymes and Rac GTPases, although the proper mechanism is not completely understood yet [55].

Classical outside-in signaling of integrins not only leads to cellular adhesion and migration, but to the activation of several effector functions of neutrophils, involving phagocytosis, degranulation and ROS production. Work from our laboratory described, that signaling downstream of β_2 integrins also utilized ITAM-dependent pathways [56-58]. ITAM-bearing transmembrane adaptors FcRγ and DAP12 were crucial to exert integrin-mediated cellular responses in vitro [56], as well as Src-family kinases and Syk [59]. Neutrophils and macrophages deficient in Hck and Fgr failed to undergo degranulation when plated onto fibrinogen-coated surfaces with additional

proinflammatory stimulus (for reaching the high affinity conformation of integrins) [58]. Similarly, neutrophils failed to undergo respiratory burst, degranulation, spreading and firm adhesion in the absence of Syk upon several activating stimuli of integrins [57]. Interestingly, however, migration of Src-family knock out or Syk deficient neutrophils were unaffected [57]. Therefore, it seems that there is a diverging signaling pathway downstream of β_2 integrins leading to a Src and Syk-dependent adherent activation and tyrosine kinase independent migration of neutrophils [57]. ITAM-independent activation of Syk has been also shown [59]. It may suggest a direct association between integrins and Syk, likely occurring parallel with ITAM-dependent processes [59]. Downstream signaling also involve Vav family members and PLCγ enzymes, leading to, among others, cytoskeleton reorganization and intracellular Ca^{2+} signal [55].

In line with the in vitro studies using murine cells, disruption of the human gene coding for the β_2 integrin chain causes a severe leukocyte adhesion deficiency syndrome. It is presented by recurrent bacterial infections due to impaired recruitment of leukocytes to the site of inflammation, showing the essential role of β_2 integrins in host defense [60].

1.2.3. Cytokine receptors

Various cytokine receptors signal through mechanisms utilizing Janus kinases (Jaks), as shown schematically in **Figure 4**. Ligand binding leads to the dimerization of their specific receptors, recruiting and activating usually two different Jaks. Jaks then phosphorylate the cytoplasmic tail of the receptor, recruiting signal transducer and activator of transcription (Stat) molecules. Stat phosphorylation leads to their dimerization and translocation to the nucleus where they influence gene expression and epigenetic modifications.

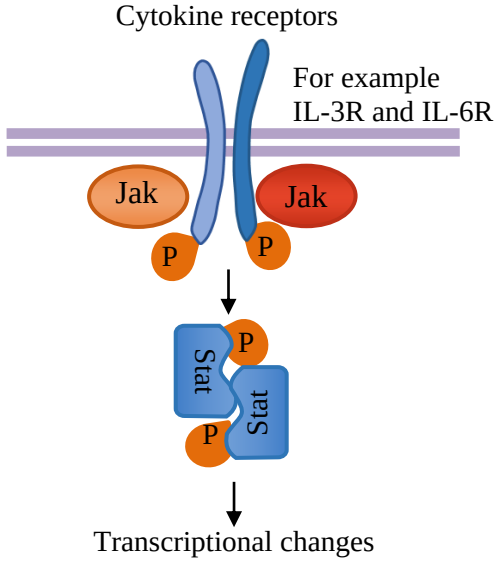

Figure 4. Jak-Stat signaling pathway
Cytokine receptors (e.g. receptors of IL-3 or IL-6) utilize Janus kinases for the initiation of downstream signaling. *Based on [1].*

Jak-coupled cytokine receptors are usually grouped into two major types, however, the classification criteria is not entirely clear. Type I receptors involve various receptors with different structure, specificity and function. Among them, there are receptors containing a common γ chain beside the specific ligand-binding chain (like IL-2, IL-4 and IL-9 receptors). These are mainly associated with activation and differentiation of lymphocytes. Receptors containing a shared gp130 subunit next to the ligand-specific chain (like IL-6R) are involved in acute inflammatory reactions. There are also growth hormone-like receptors forming homodimers (like G-CSF, erythropoietin or thrombopoietin receptors) basically important during hematopoiesis [61]. Type II cytokine receptors can bind to IFNα, IFNγ or IL-10 among others, exerting antiviral and immunomodulatory functions [62].

Regarding Janus kinases, there are four members of the Jak family: Jak1, Jak2, Jak3 and Tyk2. They are associated to certain cytokine receptors in a rather complicated pattern. Usually two different Jaks (acting as "heterodimers") are recruited to the receptor with a few exceptions. Jak1 is involved broadly in the signaling downstream of certain common γ chain-, shared gp130 subunit-containing and type II cytokine receptors. Based on genetic studies, it has an essential role during lymphoid development [63]. Jak2 is also involved downstream of certain common γ chain and type II cytokine receptors (besides Jak1). In addition, growth hormone-like receptor signaling utilizes exclusively Jak2 (acting as a "homodimer"). Its deficiency results in embryonic lethality in mice due to defective erythropoiesis [64]. Jak3 is uniquely expressed in the hematopoietic compartment acting through mainly common γ chain-containing receptors, therefore critically involved in lymphocyte function. Genetic deficiency leads to severe combined immunodeficiency in humans [65, 66] and defective lymphoid development in mice [67, 68]. Tyk2 has been described to be important in IFNα signaling [69]. Taken together, individual Jaks have often overlapping function since they usually act as "heterodimers". However, based on genetic studies, Jak1 and Jak3 are crucial in lymphoid development and function, and Jak2 is essential during erythropoiesis. Nevertheless, little is known about the role of Jaks in the function of myeloid cells such as neutrophils.

It is also important to mention, that other cytokines involved during acute inflammation (like IL-1β or TNFα) act through a different signaling machinery, mainly independent from tyrosine kinases.

1.2.4. Other tyrosine kinase-coupled signaling mechanisms

Selectins and selectin ligands are transmembrane glycoproteins involved in the rolling of leukocytes along the endothelial surface. The major selectin type on leukocytes is the P-selectin glycoprotein ligand 1 (PSGL-1) that has been also described to signal through Syk [70]. Here, PSGL-1 probably associates to receptors containing ITAM-bearing adapters, or to other proteins containing ITAM-like motifs [70, 71].

The majority of pattern recognition receptors (like toll like receptors of innate immune cells) act through a pathway that does not include tyrosine kinases. Certain pathogen recognition receptors, however, have been described to signal in a Syk-dependent manner. For instance, C-type lectins utilize ITAM-bearing adaptors or hemITAM (half of the ITAM) sequences in the cytoplasmic tail of the receptor itself [44]. Such a hemITAM-containing receptor is Dectin-1, which is involved in the recognition of fungal structures. Ligand binding initiates receptor dimerization resulting in the assembly of the whole ITAM motif. That recruits Syk, leading to gene expression changes through NF-κB, inflammasome activation and IL-1β production [44].

It is also important to mention that Syk has been shown not to participate in the signaling of G protein-coupled receptors in neutrophils and mast cells upon activation with LTB_4, MIP-2 or anaphylatoxin C5a [72].

Taken together, tyrosine kinase-coupled signaling mechanisms are involved in the recognition of diverse inflammatory signals ranging from pathogens to molecules involved in the communication between leukocytes and the environment. The two major tyrosine kinase pathways mainly involved in these processes are the ITAM-based signaling and the Jak-Stat pathway.

1.3. PLCγ ENZYMES

PLCγ enzymes are specifically activated by tyrosine kinases and are involved in ITAM-based signaling in leukocytes.

Phospholipase C (PLC) enzymes catalyze the hydrolysis of the phospholipid phosphatidylinositol 4,5-bisphosphate (PIP_2) to the second messengers inositol 1,4,5-trisphosphate (IP_3) and diacylglycerol (DAG). There are multiple isoforms of PLC enzymes classified into subfamilies based on similarities within their sequence and

specific regulation [73]. PLCβ and PLCγ represent the most important subfamilies, widely expressed in almost all mammalian cells. PLCβ is present in the signal transduction of G protein-coupled receptors and activated by $G_{q/11}$ heterotrimeric proteins. PLCγ is involved during the tyrosine kinase-coupled signaling process.

1.3.1. Structure, function and expression of PLCγ enzymes

PLCγ enzymes contain a conserved split catalytic domain, multiple Ca^{2+} binding domains and a pleckstrin homology (PH) domain, responsible for recruiting PLCγ to the membrane to its ligand by binding to phosphatidylinositol lipids [74] (**Figure 5A**). In addition, PLCγ enzymes uniquely contain additional binding sites for several scaffolding and adaptor proteins, namely SH2 and SH3 domains located between the split catalytic domain, through which they can bind to phosphorylated tyrosine residues and proline-rich motifs on other proteins, respectively [73]. These homology domain-containing regions also have important autoinhibitory functions. They prevent constitutive enzymatic activation and limit prolonged membrane interaction [75]. PLCγ isoforms are recruited to activated tyrosine kinase complexes by binding through their SH2 domain to phosphorylated tyrosine residues. Their activation is mediated through phosphorylation by tyrosine kinases (downstream of Syk and Btk), leading to a conformational change that exposes the catalytic site and relieves it from autoinhibition [76].

After PIP_2 cleavage, IP_3 will dissociate and diffuse into the cytosol, releasing Ca^{2+} from intracellular stores. The other product, DAG remains in the membrane and activates further downstream signaling through the activation of protein kinase C (**Figure 5B**).

The two isoforms of PLCγ enzymes are PLCγ1 and PLCγ2 [73]. PLCγ1 is expressed ubiquitously in all cells. It participates in the downstream signaling of various growth factor receptors, like epidermal growth factor EGF and vascular endothelial growth factor VEGF. Such receptors have intrinsic tyrosine kinase activity resulting in autophosphorylation upon ligand binding. PLCγ1 is recruited to autophosphorylated receptors via its SH2 domain and initiates downstream signaling. Genetic deficiency of PLCγ1 results in embryonic lethality of mice [77] with serious defects during erythropoiesis and vasculogenesis [78]. Regarding leukocytes, PLCγ1 is considered to be the major phospholipase downstream of the TCR. T cell-specific PLCγ1-deficient mice suffered from aberrant T cell development including defective negative selection, reduced

number of peripheral T cells and impaired TCR-mediated activation [79]. Moreover, some of these mice developed inflammatory-like symptoms including dermatitis and alopecia, which might be partly due to impaired development and function of regulatory T cell subsets [79].

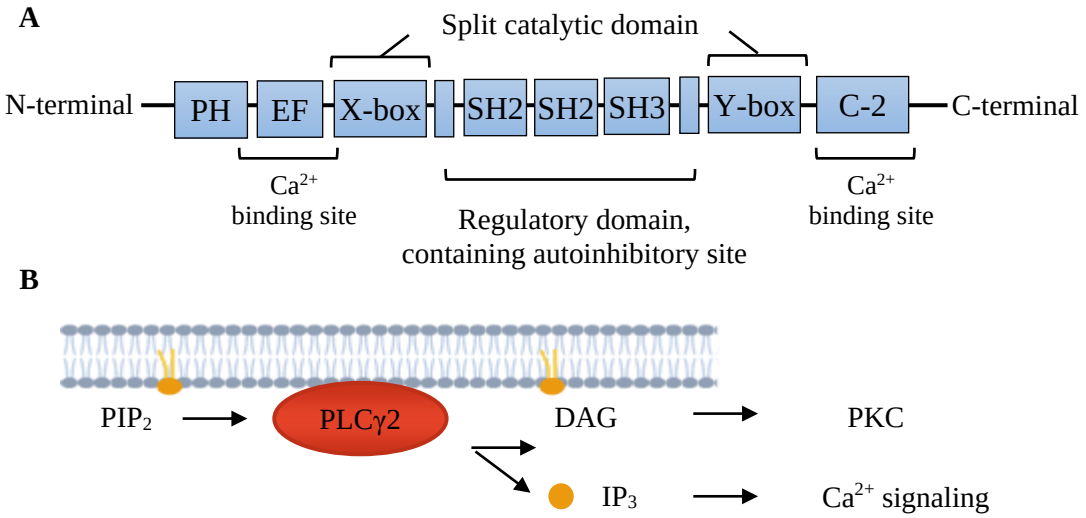

Figure 5. Structure and function of PLCγ

(**A**) Schematic structure of phospholipase Cγ (PLCγ) enzymes. Pleckstrin homology domain (PH) is responsible for membrane recruitment. EF hand and C-2 domain are both Ca^{2+} binding sites. Catalytic domain is split (to X-box and Y-box) by a complex regulatory domain containing Src homology domains (SH2 and SH3). The region responsible for autoinhibitory function is also located in the split. (**B**) Enzymatic function of PLCγ. After tyrosine kinase-mediated activation, PLCγ cleaves phosphatidylinositol 4,5-bisphosphate (PIP_2) and generate inositol 1,4,5-trisphosphate (IP_3) and membrane-bound diacylglycerol (DAG). These second messengers then induce Ca^{2+} signal and initiate protein kinase C (PKC)- dependent downstream signaling, respectively. *Based on [74].*

PLCγ2 is expressed mainly by cells of hematopoietic origin [73]. It is involved in immunoreceptor and integrin-mediated signaling, among others (see above). In vitro experimental data suggest that PLCγ2 is activated by tyrosine kinases involving Syk and Btk. It was shown by us and others that PLCγ2 phosphorylation and IP_3 production was abrogated upon Syk deficiency in B cells [80] and in myeloid cells [81]. Btk-deficient B cells showed only a small decrease in PLCγ2 phosphorylation but a drastic impairment in IP_3 production [82]. Furthermore, Rac GTPases have been also described to stimulate PLCγ2 [83]. Mouse strains, as well as patients with mutations in the *Plcg2* (mouse) or *PLCG2* (human) have largely contributed to the better understanding of the role of PLCγ2 in leukocyte function and in the pathogenesis of immune-mediated diseases.

1.3.2. Mutations in the *Plcg2* gene in mice

1.3.2.1. Loss-of-function mutations in the Plcg2 *gene*

Wang and colleagues generated *Plcg2*$^{-/-}$ mice by replacing the second exon of *Plcg2* gene with a *Neo* gene expression cassette [84]. Contrary to PLCγ1, disruption of PLCγ2 gene did not cause embryonic lethality. However, there was a decreased ratio of mature B cells, and an increased ratio of immature B cell population in the bone marrow, without any major alterations in other hematopoietic lineages. *Plcg2*$^{-/-}$ mice failed to develop antibodies upon immunization with T cell-independent antigens, however, normal antibody response was achieved using T cell-dependent antigens. T cell differentiation and function was unaffected [84]. Another group also confirmed the critical role of PLCγ2 in BCR signaling in mice with inducible disruption of *Plcg2* gene using the Cre-Lox system (detailed description of the Cre-Lox system is in Section 3.1.1) [85].

Besides B cells and BCR signaling, PLCγ2 expression was found to be critical in several other cell types and signaling pathways. *Plcg2*$^{-/-}$ mice presented reduced FcεR-dependent degranulation of mast cells [84, 86] and impaired FcγR-mediated cytotoxicity and IFNγ secretion of NK cells [84, 87, 88]. Integrin-mediated spreading and aggregation of platelets was also compromised upon PLCγ2-deficiency [84, 89]. Presence of PLCγ2 was also crucial during antifungal innate immune responses in dendritic cells and macrophages through C type lectin receptors [90-92] and during osteoclast development and function [93]. Moreover, PLCγ2 has been implicated in modulating even non-ITAM-related pathways like certain toll like receptor signaling in macrophages [94].

Our laboratory has also been working with this *Plcg2*$^{-/-}$ mouse strain and I also used these mice during my experiments. Previously, our laboratory showed, that *Plcg2*$^{-/-}$ neutrophils had defective responses upon activation of integrin-dependent, or FcγR signaling in vitro [81]. Integrin-dependent signaling was activated by plating neutrophils onto fibrinogen-coated wells in the presence of an additional proinflammatory stimulus (to achieve the high-affinity state of integrins). FcγR signaling was initiated by artificial immune complex surfaces, containing human serum albumin and anti-human serum albumin. Effector functions, such as superoxide release, degranulation and spreading were completely absent in the absence of PLCγ2. However, neutrophil migration and integrin- or FcR-independent functions remained intact [81]. These responses are in line with the responses seen in case of Src-family kinase- and Syk-deficient neutrophils

(mentioned in section 1.2), indicating that Src-family kinases, Syk and PLCγ2 act in the same signaling pathway, downstream of ITAM-coupled receptors. Furthermore, PLCγ2 may lie downstream of those kinases, since its phosphorylation disappeared if either Syk or Src-family kinases were absent in neutrophils [81].

A spontaneous loss-of-function mutation (due to early stop codon) in the *Plcg2* gene was identified by Ichise et al in mice [95]. They named the strain *Plcg2*^{al} (abnormal lymphatics). Mice with this mutation showed blood-filled lymphatic vessels mainly in the intestine and skin, indicating that PLCγ2 plays a role during the separation of blood and lymphatic vessels. Similarly, Wang et al. also reported a hemorrhaging-like phenotype in *Plcg2*$^{-/-}$ mice [84].

Taken together, *Plcg2*$^{-/-}$ mice are viable, showing macroscopic phenotype of blood-filled lymphatics due to inadequate lymphatic vessel separation. Knockout studies revealed that PLCγ2 plays a diverse role in B cell function and innate immunity, and becomes activated mainly in ITAM-coupled pathways.

1.3.2.2. Gain-of-function mutations

Known gain-of-function mutations in the murine *Plcg2* gene were chemically induced in mice by N-ethyl-N-nitrosourea (ENU) induced mutagenesis.

Plcg2^{Ali5} (abnormal limb 5) mice were discovered showing dominant inheritance of spontaneous inflammation of paws and skin in the first generation of offspring after ENU treatment [96]. The phenotype was caused by a single point mutation in the *Plcg2* gene leading to an amino acid substitution located in the catalytic domain. This point mutation removes a negative charge, therefore likely increases the interaction of mutated PLCγ2 with the negatively charged inner membrane, supposedly resulting in the enhanced or prolonged activation upon stimulation but not affecting resting conditions. Beside arthritis and dermatitis, *Plcg2*^{Ali5} mice often presented glomerulonephritis as well with intense inflammatory infiltration in the kidneys, joints and dermis. This inflammatory phenotype was also present in bone-marrow chimeras, or when the strain was crossed with Rag-deficient mice lacking B cells and T cells. It suggests, that the observed inflammatory phenotype is induced by bone marrow-derived leukocytes other than lymphocytes [96].

Another hypermorphic mutant strain was identified (called *Plcg2*^{Ali14} abnormal limb 14) on the basis of swollen footpads and rubor on the ears [97]. Histological analysis also

described severe inflammatory, mainly granulocytic infiltrate in the joints and ears. The *Ali14* mutation led to an amino acid substitution in the PH domain of the protein. It caused enhanced Ca^{2+}-entry upon stimulation, but did not affect basal enzymatic activity, nor the expression rate of the gene [97]. Interestingly, combining Ali5 and Ali14 mutations resulted in the increase in the basal PLCγ2 activity, as well [98].

1.3.3. *PLCG2* variants in humans

1.3.3.1. Inherited PLCG2 mutations

PLCγ2-associated antibody deficiency and immune dysregulation (PLAID) is a complex disorder presented with cold urticaria and variable immunological abnormalities involving hypogammaglobulinaemia, recurring infections, skin granulomas and the appearance of autoimmune diseases [99]. Laboratory findings include low serum IgA and IgM levels and low, but still substantial levels of circulatory and memory B cells. Other myeloid subsets and T cell numbers are usually not affected in those patients.

PLAID was originally described in 3 different families, caused by dominantly inherited heterozygous deletions in the autoinhibitory C-terminal SH2 domain of the *PLCG2* gene, located in-between the split catalytic domains [99]. This domain normally prevents constitutive activation of the enzyme, while mutated PLCγ2 showed normal expression but increased activity in both basal and stimulated cases in enzymatic assays. Therefore, these deletions are basically considered as gain-of-function mutations of PLCγ2. However, the functional consequences were much more complex.

Paradoxically, most PLCγ2-dependent downstream signaling pathways were impaired in B cells and NK cells isolated from PLAID patients or in cells transfected with mutant *PLCG2*, similarly to *Plcg2*$^{-/-}$ mice [99]. However, cytosolic Ca^{2+} levels in isolated B cells steadily increased with decreasing temperatures. In addition, mast cells also underwent spontaneous degranulation at room temperature if transfected with mutated *PLCG2*, suggesting a gain-of-function phenotype only in colder environments.

Loss of downstream signaling was hypothesized to occur as a consequence of chronic activated signaling, resulting in the depletion of PIP_2 (the substrate of PLCγ2), and/or the activation of negative feedback processes. Antibody deficiency and recurrent infections might be explained by this loss-of-function phenotype. Contrarily, cold urticaria may be elicited as a result of enhanced, even spontaneous leukocyte activation (supposedly mast

cell degranulation) at body parts exposed to colder temperatures [99]. Subsequent studies showed that neutrophils and monocytes from PLAID patients had an increased expression of the cell surface activation marker CD11b (the α-chain of the Mac-1 integrin) [100]. In addition, PLAID neutrophils showed elevated basal superoxide production compared to cells isolated from healthy controls, especially at lower temperatures, which could contribute to cold-induced inflammatory skin reactions and unhealing granulomas [100]. However, several aspects of the mechanism and regulation leading to this complex phenotype are still not clear.

Another syndrome was originally identified by Zhou and colleagues, which was caused by a Ser707Tyr substitution in the autoinhibitory SH2 domain of the PLCγ2 protein (the same domain affected in patients with PLAID) [101]. This mutation also led to immune dysregulation but, distinct from PLAID, tended to cause a more elaborated inflammatory phenotype, therefore named autoinflammation and PLAID (APLAID). APLAID was first described in two related individuals [101]. Both suffered from sterile inflammation present in several organs involving the skin, lungs, joints and intestine. Signs of immunodeficiency also occurred, like recurrent sinopulmonary infections, lower antibody numbers and almost complete absence of memory B cells. Skin manifestations presented as early as infancy with extensive epidermolysis bullosa-like eruptions, and often occurred also in adulthood as recurrent blistering lesions. Histologically, skin lesions usually showed massive inflammatory infiltrate containing neutrophils, eosinophils, histiocytes and lymphocytes [101].

Contrary to PLAID-associated mutations, the Ser707Tyr substitution observed in APLAID clearly led to increased downstream signaling events upon activation in a transfected human cell line, as well as in primary circulating mononuclear cells of the affected individuals [101]. The authors speculated that Ser707Tyr substitution may impair autoinhibition of PLCγ2, leading to increased function but not triggering negative feedback. It was even hypothesized that this mutation represents a new phosphorylation site that can render PLCγ2 to be activated more easily and efficiently [101].

More recently, several other missense *PLCG2* variants have been described in case reports leading to APLAID syndrome, causing increased activation of PLCγ2 [102-108].

The clinical phenotype of APLAID cases generally show severe spontaneous inflammation of the skin and joints among others, along with increased PLCγ2 signaling

events in circulating mononuclear cells. It closely resembles the phenotype and cellular functions seen in mice with gain-of-function mutations of *Plcg2* (*Ali5* and *Ali14*).

Interestingly, all patients with syndromes caused by *PLCG2* mutations developed cutaneous manifestations [99-108]. PLAID patients usually presented urticaria and skin granulomas in cold-sensitive regions, probably due to increased PLCγ2-mediated degranulation of mast cells and probably superoxide production of neutrophils. In APLAID, various polymorphic skin manifestations were described. Typically, patients developed vesicular-bullous eruptions with neonatal onset, sometimes even referred to as epidermolysis bullosa-like eruptions. Later, they often suffered from recurrent blisters and granulomas with neutrophil-rich dermal infiltration, suggesting a role for PLCγ2 in inflammatory and blistering skin diseases.

1.3.3.2. Acquired PLCG2 mutations in malignancies

The central role of PLCγ2 in B cell development and function suggests that PLCγ2 may also participate in B cell malignancies like chronic lymphocytic leukemia (CLL). CLL patients demonstrated high response rate to the Btk inhibitor ibrutinib, leading to long remission [109]. However, part of the patients developed resistance to ibrutinib treatment. Somatic *PLCG2* mutations associated with ibrutinib resistance have been described in CLL [110]. Interestingly, a somatic mutation causing the Ser707Tyr substitution (which leads to APLAID if germline mutation occurs) was also described in CLL patients with ibrutinib resistance. This mutation probably increases the basal activity of PLCγ2 and augments responsiveness to stimuli other than Btk [111].

1.3.3.3. PLCG2 *variants in neurodegeneration*

Excitingly, a protective variant of *PLCG2* was described in a genome-wide association study, associated with a decreased risk of Alzheimer's disease and associated with longevity and cognitive health [112].

PLCγ2 is primarily expressed by microglia cells in the brain and implicated in lipid metabolism, phagocytosis and clearance of myelin debris [113, 114]. The protective *PLCG2* variant (a missense amino acid substitution) acted as a small functional hypermorph based on enzyme activity and associated functional studies in transfected cell lines [113, 114]. Knock-in mice containing the protecting variant of PLCγ2 also showed mild activation of microglia in vivo, suspecting a more effective response against neurodegeneration [114].

1.3.4. Role of PLCγ2 in autoimmune and inflammatory diseases

The observed aberrant immune function in PLAID patients proposes a role for PLCγ2 during the pathogenesis of autoimmune diseases, as well. However, due to the controversial functional consequence of *PLCG2* mutations occurring in PLAID (complex mix of gain- and loss-of-functions), it is difficult to assess whether PLCγ2 activation promotes or counteracts autoimmunity. APLAID patients (as well as mice with gain-of-function mutations in *Plcg2*) show a more definite inflammatory phenotype in several organs, associated with a more clearly increased activation of the mutant form of PLCγ2. However, antibody deficiency and decreased memory B cells also occur in most of the APLAID cases (supposedly as a consequence of the increased activation-induced cell death), which still complicates the picture.

Our laboratory and others showed that *Plcg2*$^{-/-}$ mice were completely protected from autoantibody-induced arthritis [81, 115], which mimics the effector phase of the human autoimmune disease rheumatoid arthritis. While wild-type mice developed a severe arthritic phenotype with red, swollen and functionally impaired ankles, *Plcg2*$^{-/-}$ mice did not show any signs of joint inflammation after arthritogenic serum treatment [81].

PLCγ2 was described to be crucial in another animal model of rheumatoid arthritis, as well [116]. Here, mice were immunized with bovine serum albumin and local joint inflammation was elicited by the intraarticular injection of the same antigen. Therefore, mechanisms occurring in the immunization phase were also involved in this study. *Plcg2*$^{-/-}$ mice were also protected from disease development. Adoptive transfer of wild-type B cells could not restore disease. On the other hand, PLCγ2 turned out to be important in influencing the function of dendritic cells and their interaction with T cells and osteoclasts during the disease [116].

Getting closer to human pathology, the upregulation of *PLCG2* gene was also found in rheumatoid arthritis patients using quantitative PCR [117]. Further studies also implicated the role of PLCγ2 in the pathogenesis of other inflammatory conditions like cytokine storm syndrome [118], atherosclerosis [119] and dermatomyositis [120].

The above described cutaneous manifestations in APLAID patients (section 1.3.3.1, and similarly in mice, described in section 1.3.2.2) suggest a role for PLCγ2 during autoimmune and inflammatory skin diseases. There is increasing evidence that Janus kinases and tyrosine kinases in ITAM-coupled signaling are critical drivers of disease

pathology in several autoimmune and inflammatory skin disorders [1]. The latter pathway supposedly utilizes PLCγ2 in the downstream signaling process, underlying the relevance for the investigation of PLCγ2, as well. However, there are no studies elucidating the contribution of PLCγ2 in the development of such dermatological pathologies.

1.4. TYROSINE KINASES IN AUTOIMMUNE AND INFLAMMATORY SKIN DISEASES

Recently, I had the opportunity to collect literature data and write a review [1] about tyrosine kinases in autoimmune and inflammatory skin diseases. Multiple aspects of this wide topic are closely related to my research interest during my PhD studies. Therefore, in the following section, I would like to highlight some literature data reviewed in [1], that I find relevant to this thesis in a broader perspective.

1.4.1. Atopic dermatitis

Atopic dermatitis is the most prevalent inflammatory skin disease driven mainly by a T_H2 type immune response. Impaired barrier function of the skin is thought to be a key factor leading to the generation of keratinocyte-derived cytokines [121]. Cytokines then can activate different leukocytes, epithelial cells and sensory neurons utilizing the Jak-Stat pathway in humans [122]. Indeed, T_H2 cytokine-initiated signaling acting through mainly Jaks seems to be a crucial element of the pathogenesis of atopic dermatitis, promoting inflammation, itch sensation, and worsening barrier disruption [123-126]. The pivotal role of Janus kinases was further supported by the observation that mice with gain-of-function mutation in Jak1 spontaneously developed inflammatory dermatitis [127].

In line with the above observations, pharmacological inhibition of Janus kinases successfully reduced inflammation, scratching behavior, and improved barrier function in several dermatitis models in mice, as well as in multiple phase II and III trials in atopic dermatitis patients [1, 128-130]. At the end of 2020, the Jak1 and Jak2 inhibitor baricitinib was approved by the European Medical Agency (EMA) for the treatment of moderate-to-severe atopic dermatitis in adults [131]. Additionally, topical ruxolitinib treatment (inhibiting also mainly Jak1 and Jak2) gained FDA approval, as well [132, 133].

Besides cytokine signaling, B cells and mast cells have also been proposed as contributors to disease development during atopic dermatitis. It was supported by the

observation that elevated levels of IgE in the serum and upregulation of FcεRI in the skin are often present in patients [134]. Since both BCR and FcεRI signaling act through Src-family kinases and Syk, it raises the possibility that ITAM-coupled tyrosine kinases also have a pathogenic role during atopic dermatitis. However, direct experimental evidence for this possibility is still lacking.

1.4.2. Psoriasis

Psoriasis is another common inflammatory skin disease, presented by red scaling papules and plaques. Microscopically, epidermal hyperplasia, parakeratosis and dermal infiltration of different leukocytes occur in psoriasis patients. Pathogenesis is driven by IL-23, which induces the differentiation and activation of T_H17 cells and possibly resident γδ T cells. IL-23 acts through Jak-mediated downstream signaling, resulting in IL-17 and IL-22 production [135, 136]. IL-17 receptors are present on various immune cells, as well as on keratinocytes leading directly to keratinocyte hyperplasia, parakeratosis and the production of several proinflammatory mediators. The latter will then promote the further recruitment of immune cells such as neutrophils, worsening dermal inflammation [137].

Genetic deficiency of the Janus kinase Tyk2, as well as Jak inhibitors hampered T_H17 differentiation and reduced clinical signs of disease in experimental models of psoriasis [138-140]. Evidence from several human randomized clinical trials also showed promising efficacy of Jak inhibitors in psoriasis, applied orally or topically. However, there are currently no Jak inhibitors approved for the treatment of psoriasis [1, 141].

There is only limited data in the literature regarding the role of tyrosine kinases other than Jaks in psoriasis. In dendritic cells, activation of the fungal antigen receptor Dectin-1 has been implicated to promote the differentiation of T_H17 cells. Dectin-1 also induced their IL-17 production in vitro in a Syk- and CARD9-dependent manner [142]. Resident γδ T cells are considered to be a substantial source of IL-17 in psoriatic skin lesions besides conventional T_H17 cells. γδ T cells signal through Syk downstream of their T cell receptors (whereas classical αβ TCR utilizes mainly the ZAP-70 kinase). Disruption of γδ TCR-Syk signaling resulted in the amelioration of skin inflammation in an imiquimod-induced psoriasis model in mice [143]. These results also support the contribution of Syk in the development of psoriasis.

1.4.3. Alopecia areata and vitiligo

Alopecia areata and vitiligo are autoreactive cytotoxic T cell-mediated diseases, damaging hair follicles and melanocytes of the skin, respectively. Upregulation of T_H1-type cytokines, like IFNγ has been detected in the lesional skin. Many of these cytokines initiate Jak-Stat-driven signaling. Accordingly, Jak inhibition showed promising effects in some clinical trials both in patients with alopecia areata and vitiligo [1].

1.4.4. Systemic lupus erythematosus

Another autoimmune disease, systemic lupus erythematosus (SLE) often shows skin manifestations, as well. Cutaneous lupus can even represent a distinct disease entity. Interestingly, SLE patients can also develop bullous eruptions with autoantibody deposition along the dermal-epidermal junction (DEJ). Interestingly, deposited autoantibodies were shown to recognize not only nuclear antigens (characteristic for SLE), but also DEJ components in some cases, like in classical autoimmune bullous skin diseases [144]. Pathogenesis is thought to be driven by autoreactive B cells, suggesting a role for BCR-associated Src-family kinases, Syk and Btk in the development of the disease. In line with that, inhibition of Syk or Btk was able to attenuate cutaneous manifestations in lupus-prone mice [145, 146]. Moreover, increased production of proinflammatory cytokines acting through Jaks are also considered important in the development of the cutaneous manifestations, and Jak inhibition by ruxolitinib successfully prevented skin lesions in mouse models of SLE [147].

1.4.5. Neutrophilic dermatoses

Neutrophilic dermatoses represent a heterogeneous group of diseases. They are characterized by massive neutrophilic infiltration of the skin without evidence of infection. Loss-of-function mutation of the protein phosphatase SHP-1 (involved in ITAM-coupled signaling, limiting Syk-mediated downstream activation) caused severe skin inflammation in mice resembling neutrophilic dermatoses [148]. Another study further implied that overactivation of Syk-mediated processes is crucial to the development of neutrophil-mediated dermatoses [149].

Autoimmune blistering skin diseases represent an additional group of inflammatory skin diseases that involve tyrosine kinases in their pathogenesis. In the next chapter, I will

to summarize the clinical features and experimental approaches of these diseases. I will also present our current understanding of the pathomechanism and the underlying experimental evidence.

1.5. AUTOIMMUNE BLISTERING SKIN DISEASES

Autoimmune blistering skin diseases are prototypical autoantibody-mediated organ-specific diseases, consisting of two phases in their pathogenesis. First, during the immunization phase, adaptive immune players lose tolerance and form autoantibodies against certain structural proteins of the epidermis or against the DEJ (schematically shown in **Figure 6**), initiating pemphigus and pemphigoid diseases, respectively [150].

During the effector phase of the disease, pemphigus patients develop flaccid superficial blisters in the skin and mucosae due to mechanisms involving steric hindrance and keratinocyte signaling. These processes are thought to be initiated by the direct binding of antibodies without any secondary inflammation. On the other hand, the effector phase of pemphigoid diseases often involves inflammation which leads to the formation of tense blisters, finally developing into erosions and crusts. [151]. Detection of circulating autoantibodies and their deposition in the skin serves as a hallmark of diagnosis. There are several variants of pemphigoid diseases, identified based on their clinical presentation and specific target antigens summarized in **Table 2.**

In the following sections, I will describe our current understanding of pemphigoid diseases, focusing mainly on bullous pemphigoid (BP) and the inflammatory form of epidermolysis bullosa acquisita (EBA). The reason behind this choice is that BP is the most prevalent pemphigoid variant, whereas our experimental models mimic the inflammatory form of EBA.

1.5.1. General characterization of pemphigoid diseases

1.5.1.1. Incidence and target antigens

Pemphigoid diseases can affect both sexes equally. BP typically develops in elderly patients around the age of 70 or older. Its incidence is around 10-43 per million annually. Interestingly, it shows and increasing tendency, probably due to more efficient diagnosis, the aging of the overall population, and the increased use of drugs considered to elicit BP

[144, 152, 153]. EBA, however, has a bimodal peak affecting people in the 2nd and 7th decade, with 0.2-0.5 new cases per million people annually. It represents a rare but severe variant of subepidermal autoimmune diseases [152].

During BP, autoantibodies are formed against BP180 and or BP230. BP180 (also called collagen type XVII) is a transmembrane anchoring component of the hemidesmosome, connecting basal keratinocytes to the superficial part of the basement membrane (**Figure 6**).

In most cases, autoantibodies recognize the extracellular noncollagenous domain NC16A located close to the transmembrane region of the molecule. BP230 is an intracellular protein of the plakin family, anchoring keratin filaments to the hemidesmosome in basal keratinocytes (**Figure 6**) [152].

In EBA patients, collagen type VII (C7) is the autoantigen. C7 is a crucial anchoring protein located in the lower part of the DEJ (**Figure 6**). It is composed of three identical α subunits containing a central helical collagenous domain and two non-collagenous domains at the N- and C-terminal end (NC1 and NC2, respectively, also shown in **Figure 7**). Two C7 molecules form a tail-to-tail dimer, which is stabilized by disulfide bridges close to the NC2 domain [154]. In the majority of patients, the immunodominant regions in EBA are considered to be within the NC1 domain (**Figure 7**) [154].

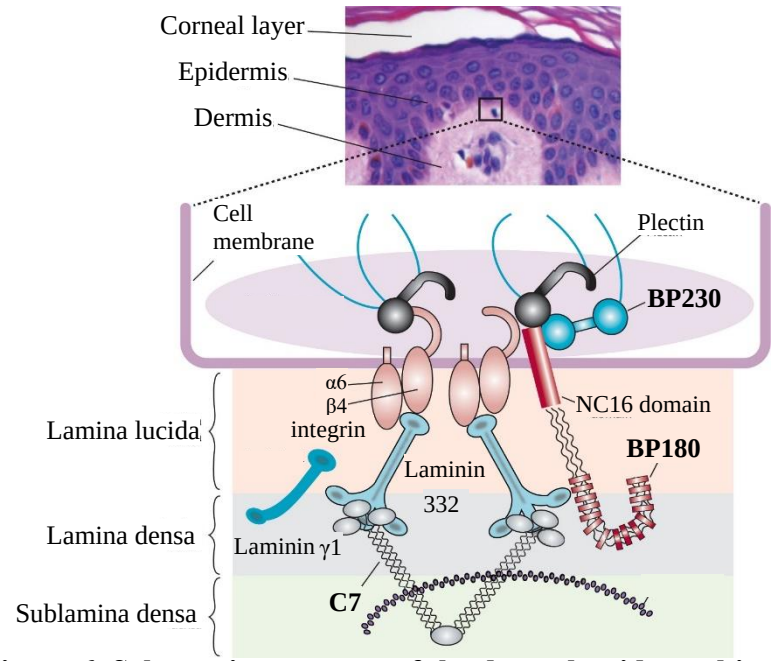

Figure 6. Schematic structure of the dermal-epidermal junction.
From Schmidt and Zillikens, Lancet, 2013 [154]

Table 2. Properties of subepidermal autoimmune blistering skin diseases [144].

Disease	Antigen	Antibody isotype	Inflammatory infiltrate	Clinical presentation
Bullous pemphigoid (BP)	BP180, BP230	IgG, IgE	eosinophil-rich	tense bullae and erosions on normal or inflamed skin; pruritic urticarial plaques; ~20% can be nonbullous; abdomen, flexor surfaces
Epidermolysis bullosa acquisita (EBA)	type VII collagen (C7)	IgG and/or IgM, IgA, IgE	neutrophil-rich	tense bullae and erosions mechanobullous form: trauma prone extensor surfaces inflammatory form: general
Pemphigoid gestationis	BP180	IgG	eosinophil-rich	pruritic urticarial plaques and or blistering on the abdomen
Lichen planus pemphigoides	BP180	IgG	lymphocytes, eosinophils	polygonal papules and tense bullae on flexor surfaces
Mucous membrane pemphigoid	variable	IgG and/or IgA	variable	erosions and ulceration of oral mucosa and conjunctiva; heal with scarring
Linear IgA bullous dermatosis	BP180 ectodomain	IgA	neutrophil-rich	pruritic, grouped papules and/or bullae on trunk, buttocks and extensor surfaces; mucous membrane is often involved
Dermatitis herpetiformis	epidermal trans-glutaminase	IgA	neutrophil-rich	pruritic, clustered erosions symmetrically in elbows, knees, scalp and buttocks; appear upon gluten exposure

1.5.1.2. Clinical presentation and associated diseases

Clinical presentation of BP typically involves tense blisters on normal or erythematous skin. Blisters usually evolve into erosions and often associated with severe pruritus. However, BP can be also presented by various non-classical symptoms, like erythematous

plaques and even non-bullous forms can occur [144].

Two major types of EBA have been described; the mechanobullous and inflammatory forms. During the mechanobullous form, bullous skin lesions are formed predominantly on trauma-prone, extensor surfaces, healing with significant scarring and milia formation. Nail dystrophy, scarring alopecia and mucosal involvement can also occur. In the inflammatory form of EBA, pruritic, bullous skin lesions develop, usually on inflamed skin similar to BP [155].

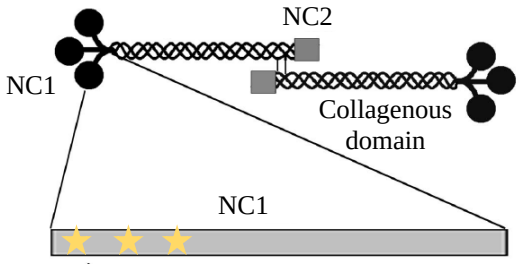

Figure 7. Structure of the type VII collagen. Immunogenic epitopes are located at the NC1 domain in most cases (marked by asterisks). *Adapted from [158].*

Interestingly, BP is highly associated with multiple neurological disorders, probably since BP180 and BP230 are also expressed in the central nervous system [150]. C7 is also expressed in the gut mucosa, which may explain why EBA has also been found to be associated with chronic inflammatory bowel diseases [156].

1.5.1.3. Diagnosis

The gold standard of the diagnosis of pemphigoid diseases is the detection of antibody deposition in the perilesional skin, using direct immunofluorescence.

The detection of circulating autoantibodies in the patient's serum by indirect immunofluorescence is also useful. Here, autoantibody deposition is studied in healthy skin sections incubated with the patient's serum [157]. Differential diagnosis between BP and EBA can be evaluated using salt-split skin. Incubation of normal skin samples with 1 M NaCl solution leads to the separation of the epidermis from the dermis. In this setting, autoantibodies in BP are deposited to the roof of the split, while autoantibodies of EBA patients attach to the dermal part.

Commercially available ELISA kits are used to test the antigen specificity of circulating autoantibodies. Specificity of these assays has been reported to be excellent, however, their diagnostic sensitivity can be variable (54-95%) [144, 157].

Taken together, definitive diagnosis of pemphigoid diseases relies on multiple aspects: clinical presentation, histopathological findings and direct immunofluorescent results

accompanied by detection of circulating autoantibodies by indirect immunofluorescence using salt-split skin or ELISA [158].

1.5.2. Experimental models of pemphigoid diseases

There are multiple experimental tools to investigate the various aspects of autoimmune skin blistering. There are in vitro cellular assays and more complex ex vivo experimental systems, which can utilize either human or murine cells and/or tissues. In addition, several in vivo animal models of pemphigoid diseases have been developed, recapitulating pathogenic events in a more complex manner. In the following sections, I will describe the available model systems for BP and EBA.

1.5.2.1. In vitro cellular assays

Activation of different innate immune cells can be studied in vitro by plating them onto immobilized immune complex surfaces consisting of dermal-epidermal antigens (such as the immunogenic epitope of C7) and the corresponding autoantibodies (i.e., anti-C7). Immune complex stimulation of leukocytes mimics the situation at the DEJ after autoantibody deposition. Polyclonal autoantibodies produced by immunization of laboratory animals can be used, providing an accessible and large amount of antibodies. Autoantibodies obtained from pemphigoid patients can also be used. Application of leukocytes obtained from experimental animals gives the opportunity to analyze certain molecular pathways using a clear transgenic approach. Alternatively, human leukocytes can also be applied, as well as autoantibodies obtained from pemphigoid patients, making it more similar to actual human pathology.

This approach is useful for the investigation of several effector functions of innate immune cells triggered directly by immune complex stimuli. Such readouts can be cellular adhesion, spreading, ROS production. Gene expression and release of proinflammatory mediators and proteolytic enzymes can also be measured.

Keratinocyte function can also be investigated in vitro upon their incubation with autoantibodies. In this way, one can test direct effects of autoantibody deposition without the contribution of inflammatory responses [159]. Of course, these experiments can be applied only in case of keratinocyte-expressed autoantigens, such as BP180 in BP. In case of EBA, autoantigens are extracellular, therefore autoantibody deposition supposedly does not affect keratinocyte function directly.

Taken together, in vitro assays are useful to analyze the effector phase of skin blistering. They provide the ability to directly analyze distinct signal transduction pathways, without the disturbing effects of other mechanisms. On the other hand, mechanisms occurring in this simple experimental setting can be altered by other complex processes in vivo, making it harder to extrapolate in vitro findings to the actual human disease.

1.5.2.2. Ex vivo models

Properly speaking, ex vivo experimental approaches belong to in vitro models. However, ex vivo methods utilize not only cellular components but tissues, as well, making the experimental setup more complex. These assays are one step more similar to the actual disease than simple cellular activation assays. Therefore, I will discuss them separately.

In the ex vivo skin separation assay, neutrophil-mediated dermal-epidermal (D-E) separation can be investigated in autoantibody-treated skin sections. Usually, cryosections of healthy human skin is used. Samples are pretreated with pathologic autoantibodies derived either from immunized animals or from pemphigoid patients. After that, dermal-epidermal separation is induced by the addition of leukocytes, mainly freshly isolated neutrophils. Human plasma is usually also added as a source of complement. The first description of this assay utilized serum of BP patients as a source of autoantibodies [160]. Serum of EBA patients could also initiate skin separation [161]. It has been shown that serum of EBA patients can cross-react with the murine C7 antigen. Skin separation could be induced in a hybrid system, using murine skin sections treated with pathogenic human serum and human neutrophils [162]. Vice versa, anti-C7 antibodies obtained from immunized rabbits recognizing immunogenic epitopes of the murine C7 protein could induce dermal-epidermal separation of human skin upon incubation with human neutrophils. We used this latter approach in our studies [3].

This method is also useful to investigate the effector phase of skin blistering. More specifically, neutrophil-mediated mechanisms of tissue damage and blister formation can be examined. Since autoantibodies and effector immune cells are added directly to the skin, leukocyte recruitment cannot be tested with this approach. The other advantage of this model is that human tissues and cells can be used, giving us direct information about the human pathology.

1.5.2.3. Autoantibody-induced in vivo models

In vivo animal models of pemphigoid diseases provide the opportunity to investigate disease development in a living animal, mimicking complex pathologic events of the human disease. There are basically two approaches. The autoantibody-induced models are induced by the direct administration of pathogenic antibodies, mimicking only the effector phase of the disease. On the other hand, active immunization-induced models recapitulate events involving both the immunization and effector phase of skin blistering.

It was first reported by Liu et al that passive transfer of antibodies against murine BP180 can induce skin blistering in mice [163]. In this model, polyclonal antibodies recognizing the NC14A domain of murine BP180 (corresponding to the immunogenic NC16A domain in human BP) were produced in rabbits. Antibodies were injected intraperitoneally or intradermally into neonatal BALB/c mice which presented epidermal detachment upon friction after 24 hours of treatment. There are multiple limitations of this early model. It has a relatively short time course compared to the human diseases or other antibody-induced animal models. The skin of the used neonatal mice is structurally rather different from the adult skin. Moreover, transiently appearing skin lesions usually did not develop spontaneously, only upon some mechanical stress. Other mouse strains are unfortunately not as susceptible, which limits the use of transgenic animals, since the majority of the latter are on the C57Bl/6 background.

Passive transfer of sera from BP patients were unable to generate skin blistering in mice. This is probably due to the limited cross-reactivity between the human autoantibodies and the mouse antigen. Humanization of the whole BP180 protein (or only the immunogenic domain) in mice made neonatal puppets susceptible to pathogenic IgG isolated from BP patients [164, 165]. However, adult mice containing such humanized BP180 were still unsusceptible [164, 165].

For long, there was no good adult model for BP. In 2012, Oswald and colleagues presented successful development of skin blistering in adult mice upon administration of rabbit anti-BP180 antibodies [166]. However, a pre-immunization with rabbit IgG was necessary to develop disease. In this case, immune complexes consisting of rabbit IgG and mouse anti-rabbit IgG were probably necessary to initiate tissue destruction in the skin. Schulze and colleagues were able to induce skin blistering resembling BP even in adult C57Bl/6 mice with repeated injections of polyclonal IgG recognizing the NC15A

epitope of mouse BP180 [167].

Regarding EBA, Sitaru et al established the first animal model for the inflammatory form of this disease [154]. Polyclonal anti-C7 antibodies were generated by the immunization of rabbits with the immunogenic epitope of mouse C7. Repeated subcutaneous injections of anti-C7 resulted in the appearance of erosions, erythema and crust formation in adult mice at multiple sites of their body after 2-4 days from the first injection. Disease severity reliably correlated with the applied antibody doses. Mice with multiple genetic background presented symptoms, although with different susceptibility. This model became a frequently used, well established model of autoantibody-induced skin blistering.

Parallel to Sitaru and colleagues, another workgroup also described an adult mouse model resembling EBA [168]. Here, disease was induced in nude immunocompetent mice by the injection of rabbit antibodies also recognizing the NC1 epitope of human C7. Moreover, direct transfer of affinity purified autoantibodies from EBA patients were also able to induce skin blistering in the same nude mouse strain [169]. However, widespread use of this model did not happen, probably due to its dependence on a unique mouse strain. Humanized mice containing human C7 have also been described to develop blisters upon injection with anti-human C7 [170].

It is also important to mention, that in some studies, anti-C7 antibodies were administered intradermally, instead of systemically. In such cases, blister formation occurred locally, usually within a relatively short time period of 24-48 hours.

The use of antibody-transfer models are important tools directly investigating the effector phase of pemphigoid diseases, excluding the immunization stage. The developing microscopic findings closely resemble the ones occurring in human diseases, like complement deposition, development of the inflammatory infiltrate and separation of the DEJ. In the majority of the models described above, the most prevalent cell types in the inflammatory infiltrate are neutrophils. This is characteristic for human EBA, but not for BP, where usually eosinophils dominate.

Overall, the passive transfer model of EBA is used more widely than BP models, potentially due to its excellent reproducibility, applicability for multiple mouse strains, and more similar disease characteristics to the human disease. In BP models, antibodies may have less disease-inducing potential probably due to the less interspecies similarity

between BP antigens and/or the weaker accessibility of such antigens within the DEJ.

Excluding pathogenic events during the immunization phase is, however, a substantial limitation of these models. This emphasizes the need for careful translation of experimental findings to human pathology.

1.5.2.4. Active immunization-induced in vivo models

Active immunization-induced or simply “active” mouse models are more complex approaches than passive transfer models. Disease is initiated by the administration of antigens which break the immune tolerance within the experimental mice. These models are useful to investigate adaptive immune mechanisms behind loss-of-tolerance and autoantibody-production, among others.

In the active immunization-induced model of BP, recombinant polypeptides of the murine NC14A domain are used [171]. It initiates the production of anti-BP180 antibodies in several mouse strains. However, only female mice on the SJL/J genetic background were susceptible to disease development with blistering skin lesions. First lesions occurred several weeks after the first immunization, and symptoms were usually less severe compared to the autoantibody-induced phenotype.

Another, more complicated model of BP was also described [172]. In this model, disease development takes place in two different animals. Loss of tolerance was achieved by grafting wild-type mice with human BP180-expressing skin tissue. Then, splenocytes were isolated from these ‘first’ mice and administered into BP180-humanized *Rag2*$^{-/-}$ ‘second’ mice lacking mature endogenous T- and B cells. The ‘second’ mice developed skin lesions resembling BP, making this model suitable to study the role of different adaptive immune players during the immunization phase. However, the immunocompromised nature of ‘second’ mice also hinders the translation of the mechanisms observed in the effector phase [172].

Regarding active models mimicking EBA, immunization with recombinant fragments of NC1 domain of murine C7 reliably induced the production of autoantibodies in mice [173, 174]. However, similarly to active BP models, clinical manifestation depended on the genetic background. Only certain strains were susceptible to blister formation, showing the pathogenic relevance of genetic factors in disease development. Disease persisted for several weeks in affected animals, making these models also suitable for long-term evaluation of potential therapeutic interventions.

Compared to the previously described passive approaches, active immunization-induced models of pemphigoid diseases are uniquely suitable to study the mechanisms involved in the immunization phase. Moreover, feasible pathogenic factors identified in simpler assays, can also be investigated in this more complex setting, making these models more closely resembling the actual mechanisms occurring in the human diseases.

1.5.2.5. Spontaneous development of pemphigoid diseases in mice

Interestingly, mice lacking the immunogenic NC14A domain of murine BP180 has been shown to produce autoantibodies against BP180. Moreover, they develop erosions, scratching behavior and severe dermal eosinophilic infiltration resembling BP [175]. This model may also be useful to test mechanisms leading to the spontaneous breakage of tolerance.

Taken together, all these in vitro and in vivo approaches represent extremely useful tools to study distinct pathologic processes of pemphigoid diseases and identify new possible therapeutic targets. However, their substantial limitations should also be kept in mind. Translation of findings from murine to human system always needs to be done carefully, since several aspects can be different between these species.

1.5.3. Pathogenesis of pemphigoid diseases

Our understanding about the development of subepidermal blistering skin diseases has been extended in the last decades, in large part due to the widespread use of the above described valuable experimental models. The main steps of the pathogenesis is schematically summarized in **Figure 8**.

1.5.3.1. The immunization phase

The exact factors initiating the break of tolerance are not known. Association of certain MHC loci with the susceptibility to EBA and BP has been described in patients and also in experimental mice, underlining the role of genetic predisposition [171, 176].

Regarding environmental factors, dipeptidyl-peptidase 4 inhibitors and checkpoint inhibitor treatment were implicated to induce BP [153]. Burn, irradiation or other skin trauma have also been suggested as a pathogenic element, possibly through liberating DEJ antigens and activating tissue resident leukocytes [150]. This may contribute to the enriched presentation of DEJ antigens and the generation of autoreactive T cells .

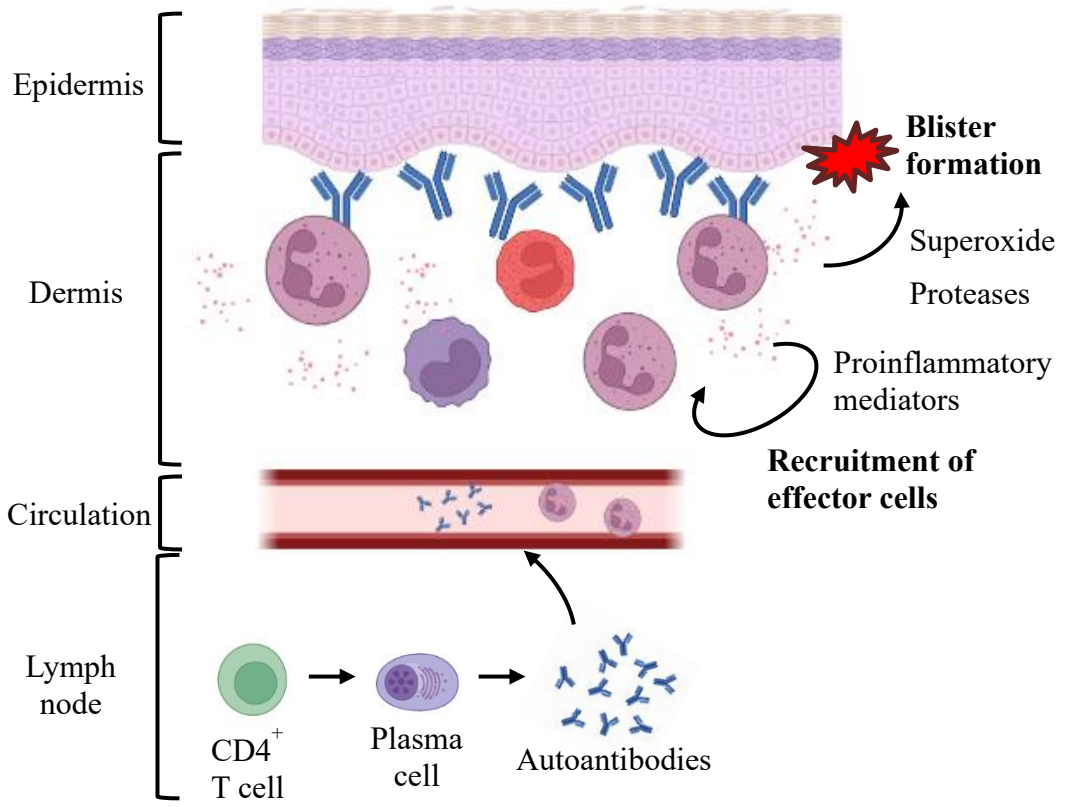

Figure 8. Pathogenesis of pemphigoid diseases.
Immunization phase begins with the loss of tolerance against antigens of the dermal-epidermal junction. Autoreactive T cells activate B cells which then differentiate into plasma cells producing autoantibodies. Autoantibodies are deposited along the basement membrane followed by complement deposition and the recruitment of effector cells (mainly eosinophils in BP and neutrophils in the inflammatory form of EBA). Effector cells then release superoxide, proteases and several proinflammatory mediators, which will lead to blister formation and further recruitment of leukocytes. *Created in BioRender.*

$CD4^+$ T cells have been shown to be crucial in the pathogenesis of active immunization-induced BP and EBA [172, 174, 177]. This indicates that $CD4^+$ T cells are important for the induction of skin blistering possibly through initiating B cell activation and autoantibody production.

The isotype of autoantibodies differs between variants (summarized in **Table 2)**. IgG is usually present in patients with BP. In addition, high IgE levels are often detected in the serum, as well [178]. During EBA, multiple antibody isoforms can be found, but IgG is usually present [144]. Besides their essential diagnostic value, serum autoantibody titers are also associated with the severity of the disease [154].

The half-life of circulating autoantibodies is controlled by the neonatal Fc receptor

(FcRn) expressed by endothelial cells. FcRn-deficient mice developed a milder anti-C7-induced skin blistering disease phenotype [179]. Furthermore, anti-FcRn treatment was able to reduce symptoms in active immunization-induced EBA, as well [180].

Circulating autoantibodies are deposited along the DEJ. The pathogenic importance of autoantibodies is clearly confirmed by their ability to induce skin blistering upon passive administration in mice. It has been shown that the Fc portion is crucial, since autoantibodies containing only the antigen-specific $F(ab')_2$ region are insufficient to induce skin blistering in ex vivo and in vivo models of EBA [154, 161].

1.5.3.2. Importance of complement components

Complement components are deposited along the DEJ in pemphigoid diseases. C5-deficient mice were completely protected from skin blistering in autoantibody-induced EBA [154], and partially protected from autoantibody-induced BP [181].

It seems, however, that the role of distinct complement activation pathways upon antibody deposition is not obvious. In the neonatal antibody-induced model of BP, complement components of the classical activation route were crucial to induce blister formation [182]. Contrarily, in anti-C7-induced EBA, mice lacking C1q (which is involved in the classical pathway) showed only a partial reduction in skin blistering [183]. On the other hand, Factor B-deficient mice were more protected from anti-C7 induced disease [183], indicating that the alternative pathway may have an essential augmenting effect in this model.

The activation of the complement cascade finally leads to the assembly of the membrane attack complex (including the complement component C6) and the production of different inflammatory cleavage products (for example C5a). During the anti-C7-induced mouse model of EBA, the impact of these two aspects was investigated [184]. While $C6^{-/-}$ mice developed severe skin blistering similar to wild-type animals, C5aR1-deficient mice presented significantly less severe disease [184]. This suggests that complement activation is linked to tissue damage through C5a-mediated events, rather than the assembly of the membrane attack complex.

C5a has been shown to be able to induce the recruitment of myeloid cells, as well as to activate their effector functions in various autoantibody-induced models [185]. In vitro migration of neutrophils towards C5a was dependent on C5aR1, but BP180/anti-BP180 immune complex-induced ROS production was not [181]. This indicates that C5a may be

mainly important in the recruitment of leukocytes, rather than in the activation of their effector functions in pemphigoid diseases.

1.5.3.3. Recruitment of effector cells

The infiltration of different myeloid cells after autoantibody deposition is characteristic for BP and the inflammatory form of EBA (**Figure 8**). Complement degradation products can serve as ligands for the β_2 integrin Mac-1, among others (see in section 1.1.1). β_2 integrin-mediated migration and activation of myeloid cells was found to be crucial in other autoantibody-mediated disease models [186].

Neonatal mice lacking CD11b (the α chain of Mac-1) were resistant to autoantibody-induced BP after 24h [187]. Skin blistering was restored upon intradermal injection of CD11b-deficient neutrophils [187]. This indicates that CD11b-mediated signaling is essential during the recruitment of neutrophils but dispensable during tissue destruction. Unexpectedly, CD11b-deficient adult mice showed a more severe skin blistering in the anti-C7-induced disease model at the later phases of the disease [188]. However, this latter observation was based on a small study without any deep mechanistic examinations.

Mice lacking CD18 (the β_2 chain) were protected from anti-C7-induced skin blistering [189]. Moreover, blocking β_2 integrin signaling resulted in the inhibition of immune complex-induced adhesion of human neutrophils but did not affect ROS production in vitro [190]. The ex vivo separation of anti-C7-treated mouse skin was also severely impaired upon CD18-inhibition [190]. This suggests that β_2-dependent adhesion of neutrophils may be a prerequisite to tissue damage during pemphigoid diseases.

Multiple proinflammatory mediators are proposed to induce the extravasation and recruitment of leukocytes into the dermis. Besides C5a mentioned above, chemoattractants like IL-8 and LTB_4 have also been suggested in this process.

IL-8 is a potent neutrophil (and eosinophil) chemoattractant. Increased concentration of IL-8 was detected in blister fluid of BP patients [191]. Keratinocytes produced IL-8 upon anti-BP180 treatment [159] and activated inflammatory cells may also release it further augmenting leukocyte recruitment.

LTB_4 is a potent chemoattractant and activating mediator of myeloid cells through the BLT1 receptor. Concentration of LTB_4 in blister fluid and expression of BLT1 was also increased in perilesional skin of BP patients [192, 193]. In addition, mice lacking either 5-lipoxigenase (a key enzyme of LTB_4 biosynthesis) or BLT1 were protected from anti-

C7-induced recruitment of leukocytes and development of skin blistering [194]. However, BLT1-deficient neutrophils were capable of ROS production upon immune complex activation in vitro and were able to induce blister formation when injected directly into the ears of anti-C7-treated mice [194]. This indicates, that LTB_4 /BLT1 axis may be crucial for the recruitment of neutrophils, but not directly for tissue destruction.

1.5.3.4. Fc receptor signaling

The Fc portions of autoantibodies have been shown to be crucial for blister formation in pemphigoid diseases. This strongly assumes that Fc receptor signaling in infiltrating leukocytes also contributes to the pathogenesis of pemphigoid diseases.

The absence of the common FcRγ chain protected mice in the anti-C7-induced EBA model [195]. FcγRIV-deficient mice remained completely protected from anti-C7-induced skin disease, while the lack of FcγRI and FcγRIII did not change the disease course [195]. Moreover, this and another study (using immunization-induced EBA) showed that FcγRIIB deficient mice developed an aggravated disease phenotype [195, 196]. and soluble FcγRIIB treatment decreased disease development in active immunization-induced EBA [197]. These results suggest that FcγRIV is essential for blister formation, while the inhibitory FcγRIIB-mediated signaling processes may exert a protective role in the anti-C7-induced EBA model.

In an antibody-induced adult BP model, FcRγ chain-deficient mice were protected, whereas FcγRIIB deficiency worsened skin blistering, similar to the anti-C7-induced EBA model [167]. However, disease phenotype were strongly reduced in both $Fc\gamma RIII^{-/-}$ and $Fc\gamma RIV^{-/-}$ mice, while the lack of FcγRI did not affect blister formation [167]. Neonatal mice lacking FcγRIII were also resistant to antibody-induced BP [198].

Taken together, it seems that activating FcγRs were crucial in the development of skin blistering in mice regardless of the used model. However, the particular involvement of distinct FcγR subsets may be different in different mouse models.

As I mentioned in section 1.2.1, mouse and human Fcγ receptors are not entirely correspond with each other. This makes translating the above mentioned findings difficult. In a human ex vivo skin separation model, inhibition of FcγRII (which is similar to mouse FcγRIII), as well as FcγRIII (similar to mouse FcγRIV) resulted in the almost complete abrogation of neutrophil-induced D-E separation [199]. These results support that FcγR-driven processes are important in the development of the human disease, too.

Our laboratory have investigated different signaling components downstream of FcγRs in diverse in vitro and in vivo inflammatory conditions [44]. In the context of autoimmune skin blistering, our group showed that in vitro activation of murine neutrophils on immobilized C7/anti-C7 immune complexes induced spreading and respiratory burst [9]. Such effector functions were dependent on Src-family kinases and Syk [9].

Importantly, our laboratory also showed that both *Syk*$^{-/-}$ and Src-family-deficient mice were completely protected from anti-C7-induced skin blistering [8, 9]. Another workgroup also investigated the role of Syk in this model [200]. They used conditional knockout mice and showed that Syk expression is essential in the myeloid, but not in the lymphoid compartment to develop anti-C7-dependent skin blistering. They also demonstrated that a Syk inhibitor (BAY61-3606) dose-dependently inhibited immune complex-induced ROS release of neutrophils in vitro and D-E separation ex vivo [200].

Our laboratory also described that PLCγ2 was essential in FcγR signaling, using aspecific HSA (human serum albumin)/anti-HSA immune complexes in vitro. Moreover, they implicated that PLCγ2 may lay downstream of Src-family kinases and Syk. They also found PLCγ2 indispensable in an antibody-induced arthritis model in vivo [81] (see also in section 1.3.4). Importantly, however, the role of PLCγ2 in the context of antibody-induced skin blistering is not known.

Our group also found, that immune complex-initiated signaling cascade divides into CARD9-dependent gene expression changes and CARD9-independent short-term functions like ROS release, degranulation and LTB_4 release [28]. CARD9-deficient mice were partially protected from anti-C7-induced skin blistering [28].

PI3K enzymes are responsible for the generation of PIP_2 and PIP_3, that are needed for the recruitment of PH-domain containing molecules such as Btk and PLCγ2. PI3Kβ was found to be essential in C7/anti-C7 immune complex-induced ROS production of neutrophils in vitro and in anti-C7-induced blister formation in vivo [201]. Pharmacologic inhibition of the PI3Kδ isoform led to similar reduced disease phenotype in mice [202].

Taken together, multiple lines of evidence support the crucial role of FcγRs and associated tyrosine kinases in the effector phase of skin blistering.

Fcε receptors may also contribute to the development of skin blistering in cases when pathogenic IgE is present. In a study, IgE antibodies against human BP180 were injected into neonatal mice containing humanized BP180 [203]. IgE antibodies were deposited at

the DEJ, but did not induce blister formation, nor leukocyte infiltration [203]. When FcεRI was also humanized, mice developed local skin blistering with eosinophilic infiltration [203]. This suggests a role for FcεRI signaling in this complex experimental setup, but more studies are needed to find out its exact relevance.

1.5.3.5. Neutrophils

Infiltration of neutrophils is characteristic for EBA. In case of BP, eosinophils are the predominant cell type in lesional skin. Although, neutrophils were also found abundant in lesional skin and blister fluid in BP patients [204]. Moreover, neutrophil-rich infiltration occurs in the majority of the animal models of BP and EBA too. Therefore, neutrophils are the mostly used cell type to induce split formation in autoantibody-treated cryosections, as well [160, 161].

Antibody-induced skin blistering was examined in multiple neutropenic mouse strains. Neutrophil depletion by antibodies against Gr-1 (recognizing Ly6G and Ly6C surface markers) or against the more specific Ly6G prevented mice from autoantibody-induced blister formation [164, 189, 194]. More recently, another genetic neutropenic mouse strain was developed in our laboratory which showed also complete protection from anti-C7-induced skin blistering [205].

Furthermore, anti-Ly6G treatment reduced circulating anti-C7 levels during the active immunization-induced model of EBA [206]. This suggests that neutrophils may also participate in the immunization phase possibly by promoting autoantibody production.

The recruitment of neutrophils supposedly involves β_2 integrin-mediated processes induced by chemokines such as C5a, IL-8 or LTB_4, as mentioned before. Then, based on the previous results of our laboratory, murine neutrophils can get activated through C7/ anti-C7 immune complexes in a Src-family kinase- and Syk-dependent manner [9]. Activation of neutrophil effector functions may also occur through other pathways such as integrins, cytokine and chemokine receptors. Activated neutrophils has also been shown to release proinflammatory mediators like IL-8 and LTB_4, creating a positive feedback loop, further amplifying neutrophil recruitment to the dermis [194].

Multiple lines of evidence supports the role of neutrophil-derived substances during tissue damage. Neutrophil-derived proteases and ROS were found elevated in the blister fluid of BP patients [207, 208]. Mice lacking gelatinase B, neutrophil elastase or functional NADPH oxidase (responsible for superoxide anion production) were all

protected from autoantibody-induced skin disease [189, 209, 210]. Importantly, skin blistering was rescued by the intradermal injection of wild-type neutrophils [209, 210]. This suggests that neutrophil-derived proteases and ROS are crucial for tissue destruction after effector cells have recruited to the dermis.

Neutrophil elastase has been shown to directly cleave BP180 protein in human skin in vitro [211]. Moreover, pharmacological inhibition of proteases or the NADPH oxidase complex was able to reduce neutrophil-mediated split formation of autoantibody-treated human skin ex vivo [189, 212], underlining the human relevance of the above studies.

1.5.3.6. Eosinophils and mast cells

Peripheral blood eosinophilia and eosinophil-rich dermal infiltrate are considered as a hallmark of BP. Eosinophil chemoattractants (like IL-5 and eotaxin), as well as eosinophil cationic protein (ECP) were also found elevated in blister fluid [207, 213, 214]. In addition, eosinophils express FcεRI that may be important in BP patients with elevated serum IgE levels. Still, it is unclear why eosinophils are predominant in BP and how they contribute to the pathogenesis.

Eosinophils were investigated in ex vivo skin separation models. Using a human cell-line differentiated towards eosinophils, treatment of skin sections with pathogenic IgG, but not with IgE resulted in the accumulation of eosinophils at the DEJ. Nevertheless, D-E separation did not occur [215]. In another study, primary eosinophils induced D-E separation in the presence of BP serum, when they were preactivated with IL-5 [216].

Eosinophil-deficient ΔdblGATA mice remained protected from skin blistering in an anti-BP180 IgE-induced, double-humanized local BP model (using mice expressing humanized BP180 domain and humanized FcεRI) [203]. Importantly, mice injected with anti-BP180 IgG developed skin blistering with the infiltration of neutrophils but not eosinophils in wild-type mice [203]. In contrast, the same eosinophil-deficient mice developed severe skin blistering in the anti-C7 IgG-induced model of EBA [194].

Mast cells are also present in the skin of pemphigoid patients and proposed to be involved in the beginning of the effector phase of skin blistering [217]. In BP patients, $CD117^{+}$ mast cells colocalized with IgE in immunostained sections of the skin, probably binding them through FcεRs [178]. Mast cell-deficient strains ($Mgf^{Sl}/Mgf^{Sl\text{-}d}$ and $Kit^{w}/Kit^{w\text{-}v}$) were protected in the neonatal BP model [218]. However, mast cell deficiency did not affect blister formation in anti-C7-induced EBA using any of the known mast cell-

deficient mouse strains [219]. It suggests that mast cells might be activated during EBA, but their role generating tissue damage is dispensable.

1.5.3.7. Jak-Stat signaling

There are several proinflammatory cytokines which were found in increased concentrations in blister fluids of pemphigoid patients [220]. Many of those signal through the Jak-Stat pathway, suggesting a role for them in the pathogenesis. It was mentioned in a review that Jak inhibition impaired disease development both in autoantibody-induced and immunization-induced EBA in mice [155]. However, only a conference paper was cited with the title available. According to my knowledge, results regarding Jak inhibitors in experimental skin blistering have not been published yet.

1.5.4. Therapeutic opportunities and prognosis

The therapeutic repertoire is rather limited in pemphigoid diseases. In case of mild BP, topical corticosteroids are the first choice. In moderate-to-severe BP, systemic corticosteroid treatment is often needed with or without other immunomodulatory drugs, however, evidence-based recommendations are limited [158]. This regimen is highly associated with severe adverse effects. The multiple comorbidity and polypharmacy in the affected elderly population further complicates the picture.

Treatment of EBA, unfortunately, still lack proper international guidelines. Skin lesions in EBA patients are often severe and typically difficult to treat. Systemic corticosteroids represent usually first line treatment. Additional immunosuppressive drugs are frequently applied with considerable side effects [221].

Currently, there is no biological therapy approved in pemphigoid diseases. Case reports and a small retrospective study suggested that depletion of B cells with anti-CD20 antibody can be beneficial in BP [222, 223]. Case reports showed promising clinical benefit of anti-IgE antibody treatment in patients with high IgE [222].

Regarding biological therapies against proinflammatory mediators, monoclonal antibodies against IL-4Rα has been tested in BP patients demonstrating promising response [224, 225]. Controversial effects were described upon blocking IL-12 and IL-23, as well as using anti-TNF treatment [226, 227]. Anti-eotaxin-1 treatment effectively reduced symptoms in BP patients [228]. However, anti-IL-5 antibody failed to improve BP as an additive therapy compared to oral corticosteroids alone [229].

A lot of cytokines signal through the Jak-Stat pathway. Despite the increasing use of Jak inhibitors in systemic autoimmune diseases and inflammatory skin diseases, clinical application is still awaited in pemphigoid diseases. I only found a case report describing improvement of dermatitis herpetiformis after tofacitinib treatment [230].

There are other approaches that interfere with autoantibody levels. Intravenous immunoglobulin therapy leads to the increased degradation of circulating autoantibodies likely through the saturation of FcRn molecules. Direct removal of pathogenic autoantibodies can also be achieved by plasmapheresis or immunoadsorption [231].

1.5.4.1. Prognosis

Pemphigoid diseases are considered as severe disorders that have significant impact on the quality of life. Discontinuation of treatment often leads to a relapse even in responding patients. As a consequence, usually long-time treatment regimens occur with the accumulating risk of serious side effects. This is especially true for the elderly population. One-year mortality for BP patients is around 20-40%, which is about 2-3 times higher than the age- and sex-matched control population [150].

Taken together, there is an unmet need for more effective and more specific therapeutic options in pemphigoid diseases. There is increasing knowledge about the pathogenesis of these disorders. However, several aspects of the exact cellular and molecular mechanisms are still not clear. Multiple components of Fc receptor signaling have revealed to be important in the effector phase of pemphigoid diseases. However, exact events downstream of ITAM-coupled tyrosine kinases are incompletely understood. PLCγ2 is an important component of Fc receptor and integrin signaling, lying downstream of Src-family kinases and Syk. PLCγ2 was found essential in autoantibody-induced arthritis models. Moreover, severe inflammatory skin lesions and epidermolysis bullosa-like phenotype were described in gain-of-function mutations of PLCγ2 in mice and humans. These observations prompted us to the characterize role of PLCγ2 in the pathogenesis of autoimmune skin blistering in well-established mouse and human models of EBA.

In addition, there are practically no experimental evidence published about the effect of Jak inhibition in pemphigoid diseases. Therefore, we also intended to test the effect of tofacitinib treatment in autoantibody-induced skin blistering in mice.

2. OBJECTIVES

During my PhD studies, we aimed to analyze the molecular mechanisms during the effector phase of autoimmune skin blistering, utilizing *in vitro*, *ex vivo* and *in vivo* models of EBA. More specifically, we intended to investigate the role of PLCγ2, and in less detail Janus kinases according to the following objectives:

1. General characterization of *Plcg2*$^{-/-}$ mice. Survival analysis and measurement of PLCγ2 expression in circulating leukocyte subsets. Comparison of circulating leukocyte counts and the expression of critical cell surface markers on myeloid cells.

2. Investigating the role of PLCγ2 in the development of an antibody-induced skin blistering in intact mice and bone-marrow chimeras.

3. Checking *in vitro* functional responses of murine *Plcg2*$^{-/-}$ neutrophils to chemotactic- and immune complex stimuli.

4. Lineage-specific analysis of PLCγ2 function. Examining the effect of neutrophil-specific PLCγ2 expression during antibody-induced skin blistering.

5. Studying the effect of PLC inhibition in a neutrophil-dependent, autoantibody-induced human *ex vivo* skin separation assay.

6. Investigating the impact of Jak inhibition in the development of autoimmune skin blistering in mice.

3. METHODS

3.1. EXPERIMENTAL ANIMALS

Generally, mice were kept and bred in sterile individually ventilated cages (Tecniplast) under specific pathogen-free conditions. For experiments, animals were transferred to a conventional facility at approximately 2-6 months of age. All animal experiments were approved by the Animal Experimentation Review Board of Semmelweis University (ethical approval ID: PE/EA/1967-7/2017) or of University of Pécs (ethical approval ID: BA02/2000-8/2020).

3.1.1. Utilized mouse strains

Mice carrying the *Plcg2*^{tm1Jni} (referred to as *Plcg2*$^{-}$) mutation inactivating the PLCγ2-encoding gene [84] were obtained from James Ihle (St. Jude Children's Research Hospital, Memphis, TN). Due to the reported infertility of male *Plcg2*$^{-/-}$ mice [232] and the limited availability of *Plcg2*$^{-/-}$ females, the strain was maintained by heterozygous breeding to obtain *Plcg2*$^{-/-}$ animals. Age- and gender-matched *Plcg2*$^{+/+}$ littermates or wild-type C57BL/6 mice were used as controls in our experiments. The latter was purchased from the Jackson Laboratory.

Neutrophil-specific deletion of the *Plcg2* gene was accomplished utilizing the Cre-Lox transgenic approach. Transgenic mice expressing Cre recombinase driven by the neutrophil-specific myeloid-related protein 8 (MRP8) promoter (MRP8-*Cre* mice) were obtained from Emmanuelle Passegue (Stanford University, Stanford, CA) [233]. Animals carrying floxed *Plcg2* allele (*Plcg2*^{tm1Kuro}, referred to as *Plcg2*^{flox}) were obtained from Tomihiro Kurosaki (Kansai Medical University, Moriguchi, Japan) [85]. Crossing these two strains allowed us to obtain MRP8-*Cre*$^{+}$*Plcg2*$^{flox/flox}$ animals (referred to as *Plcg2*$^{\Delta PMN}$). In our experiments, we used age- and gender-matched MRP8-*Cre*$^{-}$ *Plcg2*$^{flox/flox}$ littermates or wild-type C57BL/6 mice as controls. Genotyping was performed in every case by allele-specific PCR from tail DNA. All transgenic strains were on C57BL/6 genetic background, expressing the CD45.2 allele on leukocytes. In experiments using pharmacologic inhibition, wild-type C57BL/6 mice were used.

3.1.2. Generation of bone-marrow chimeras

To isolate bone marrow cells, wild-type or *Plcg2*$^{-/-}$ donor mice from C57BL/6 genetic background were sacrificed. The tibiae and femurs were removed and cleaned. Bone marrow cavity was opened by cutting both ends and bone marrow cells were flushed out with HBSS medium (Hank's Balanced Salt Solution) supplemented with 20 mM HEPES (abbreviated to HBSS/H), using a fine needle. During preparation, we always used HBSS/H that was free from Ca^{2+} and Mg^{2+}, in order to avoid preactivation of leukocytes. Cell suspension was filtered through a 70 μm cell strainer in order to get rid of large contaminants such as scattered bone fractions or other tissue remnants.

Recipient wild-type mice were from the B6.SJL-*Ptprc*^{a} congenic strain (referred to as BoyJ mice). They express the CD45.1 allele on the C57BL/6 genetic background, and were purchased from the Jackson Laboratory. BoyJ mice were lethally irradiated with 11 Gy from a ^{137}Cs source using a Gamma-Service Medical D1 irradiator. Then, the suspension of unfractionated donor bone marrow cells were injected into the retroorbital venous plexus of the recipient mice. Usually 7-9 chimeras were generated from the bone marrow of one donor.

4 weeks after transplantation, we assessed the repopulation of the bone marrow in the chimeras. The donor origin of circulating leukocytes was checked by measuring the expression of the CD45.2 marker by flow cytometry. We considered the transplantation successful (and most of the time it was the case), if circulating leukocytes (explained in detail in section 3.4) were at least 95% of donor origin (expressing CD45.2).

3.1.2.1. Generation of mixed bone-marrow chimeras

In some experiments, we generated mixed bone-marrow chimeras. Here, we transplanted wild-type (BoyJ) recipient mice with a mixture of bone marrow cells from donors of different genotypes as shown in **Figure 9**.

Namely, we mixed suspensions of bone marrow cells isolated from wild-type (BoyJ) and *Plcg2*$^{-/-}$ donors in varying ratios (usually 2:3 and 3:2) in order to get WT: *Plcg2*$^{-/-}$ mixed chimeras. In these chimeras, we could identify the genotype of the circulating leukocytes based on their different CD45 allelic expression. Leukocytes originated from wild-type (BoyJ) donors expressed CD45.1, while cells from *Plcg2*$^{-/-}$ mice expressed CD45.2. As control, we also generated WT:WT mixed chimeras, where mixture of CD45.1-expressing wild-type (BoyJ) and CD45.2-expressing wild-type (C57BL/6) bone

marrow cells were transplanted into irradiated recipients. Notably, we transplanted not only CD45.2 but also CD45.1-expressing cells into CD45.1-expressing recipients in case of mixed chimeras. Therefore, we could not determine the efficacy of transplantation as easily as in case of a simple bone-marrow transplantation. Yet, we could indirectly monitor the efficacy by comparing the ratio of cells with different genotypes injected at transplantation with the ratio of cells with different genotypes in the circulation 4 weeks after the transplantation. Upon successful bone marrow repopulation, the two ratios did not differ substantially.

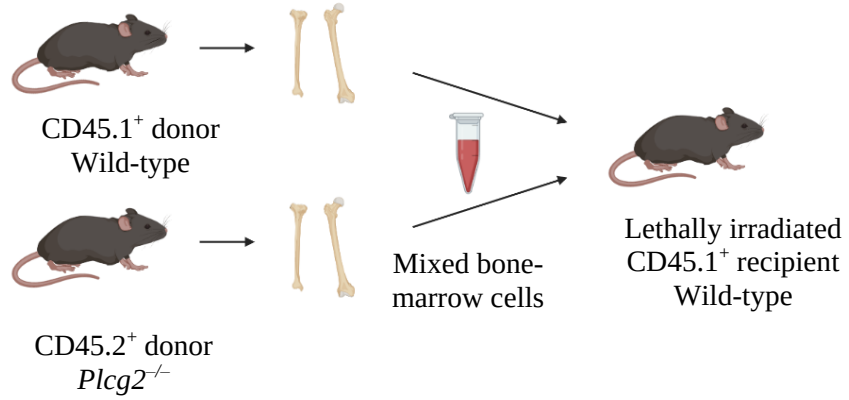

Figure 9. Generation of WT:*Plcg2*$^{-/-}$ mixed bone-marrow chimeras.
Created in BioRender.

3.2. ANALYSIS OF THE SURVIVAL RATE OF MICE

All mice born in our animal facility get an individual identifier. Their most important parameters are recorded in our online database, including genotype, date of birth, date and cause of death. Survival data of all *Plcg2*$^{+/+}$, *Plcg2*$^{+/-}$ and *Plcg2*$^{-/-}$ mice born in our facility were obtained from this database and analyzed by the Kaplan-Meier method.

3.3. ANALYSIS OF PLCγ2 EXPRESSION WITH WESTERN BLOT

We analyzed PLCγ2 expression on the protein level in unfractionated bone marrow cells. Bone marrow cells were retrieved as described in section 3.1.2. Then, cells were lysed in 100 mM NaCl, 30 mM HEPES, 20 mM NaF, 1 mM Na-EGTA, 1% Triton X-100, and 1 mM benzamidine, freshly supplemented with 0.1 U/ml Aprotinin, 1:100 Mammalian Protease Inhibitor Cocktail, 1:100 Phosphatase Inhibitor Cocktail 2, and 1 mM phenylmethylsulphonyl fluoride (PMSF). After the removal of insoluble fraction,

whole cell lysates were boiled in reducing SDS (sodium dodecyl sulphate) sample buffer. Samples were run using SDS-polyacrylamide gel electrophoresis (PAGE) and immunoblotted with antibodies against PLCγ2 (Q20, Santa Cruz Biotechnology) or β-actin (clone AC-74; Sigma-Aldrich), followed by horseradish-peroxidase- (HRP-) labeled secondary antibodies (Cytiva). Signal was developed using enhanced chemiluminescence and exposed to X-ray films.

3.4. FLOW CYTOMETRY MEASUREMENTS OF CIRCULATING LEUKOCYTE SUBSETS

3.4.1. Sample preparation

10 µl peripheral blood was sampled from tail vein incisions with heparinized pipette tips into ice cold phosphate buffered saline (PBS) supplemented with 5% fetal calf serum (FCS) and 2% heparin. Samples were then mixed on ice with fluorophore-conjugated antibodies against cell surface markers for 40-60 minutes, washed and resuspended with 500 µl FACS Lysing Solution (BD Biosciences) to lyse red blood cells and fix samples.

The following antibodies were used for cell surface marker staining, all purchased from BD Biosciences: B220 (clone RA3-6B2), CD11a (M17/4), CD11b (M1/70), CD18 (C71/16), CD3 (17A2), CD45 (30-F11), CD45.2 (104), FcγRII/III (2.4G2), FcγRIV (9E9), Ly6C (AL-21), Ly6G (1A8), Siglec F (E50-2440).

In case of intracellular PLCγ2 staining, cells were fixed and permeabilized (Thermo Fischer Fixation & Permeabilization Buffer Set) after cell-surface labeling and incubated with anti-PLCγ2 antibodies (Q20) followed by fluorophore-conjugated anti-rabbit secondary antibodies.

3.4.2. Flow cytometry and gating strategy

Flow cytometry was performed using a FACS Calibur flow cytometer (BD Biosciences) and analyzed by FCS Express 6 (De Novo Software). Specified volumes were used throughout sample preparation. We performed each measurement for a defined time and with known sampling velocity in order to precisely determine absolute cell counts. The different leukocyte populations were identified based on their typical distribution on the forward and scatter-side scatter diagram, and their specific cell surface

marker expression according to the followings (**Figure 10**):

- neutrophils: medium sized, quite granulated, $CD11b^{+}Ly6G^{+}Siglec\text{-}F^{-}$,
- eosinophils: medium sized, highly granulated, $CD11b^{+}Ly6G^{-}Siglec\text{-}F^{+}$,
- monocytes: bigger, not granulated, $CD11b^{+}Ly6G^{-}Siglec\text{-}F^{-}$,
- T cells: small, not granulated, $CD3^{+}$ and
- B cells: small, not granulated $B220^{+}$ cells.

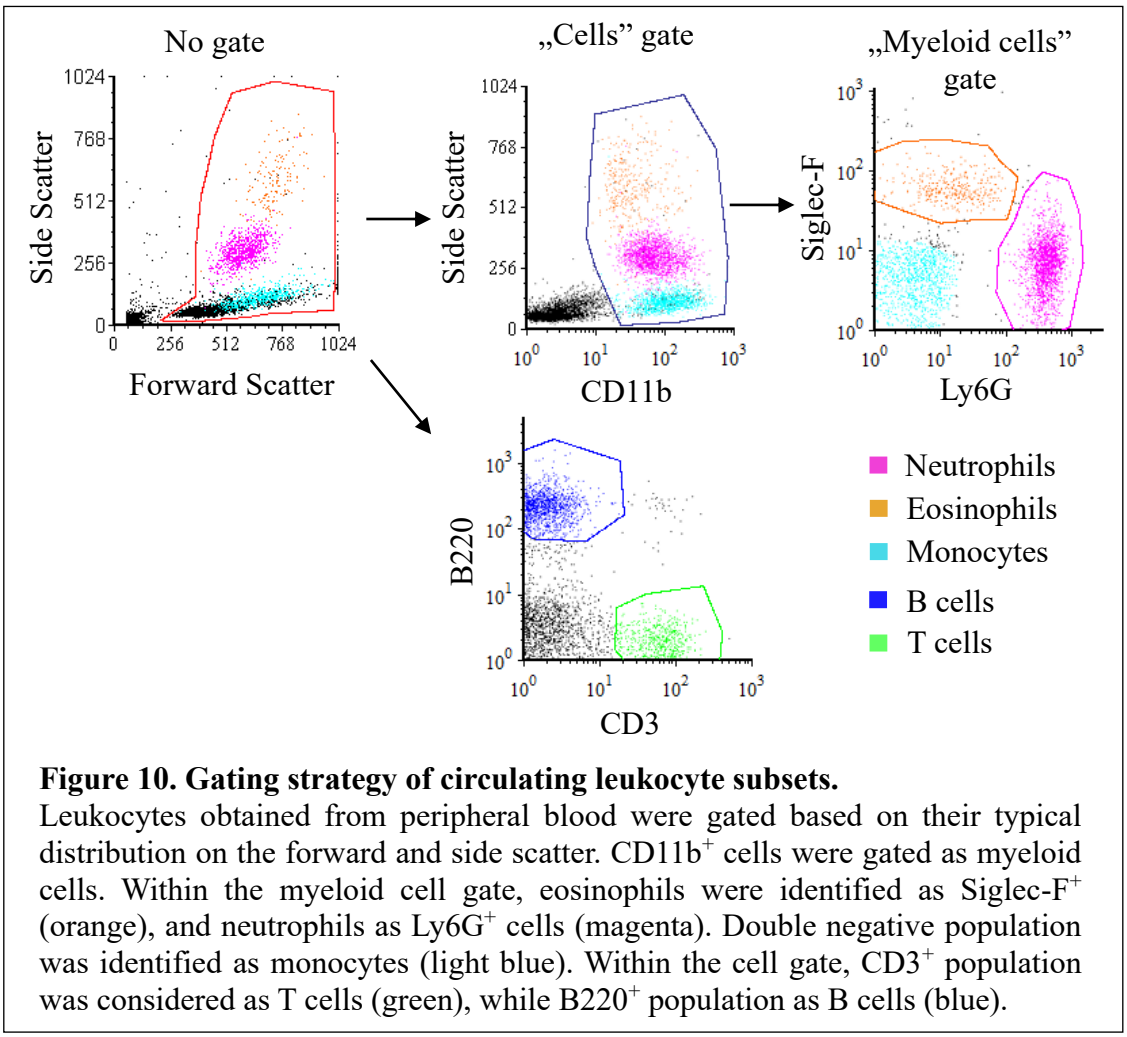

Figure 10. Gating strategy of circulating leukocyte subsets.
Leukocytes obtained from peripheral blood were gated based on their typical distribution on the forward and side scatter. $CD11b^{+}$ cells were gated as myeloid cells. Within the myeloid cell gate, eosinophils were identified as $Siglec\text{-}F^{+}$ (orange), and neutrophils as $Ly6G^{+}$ cells (magenta). Double negative population was identified as monocytes (light blue). Within the cell gate, $CD3^{+}$ population was considered as T cells (green), while $B220^{+}$ population as B cells (blue).

3.5. PRODUCTION OF TAGGED C7 FUSION PROTEINS

Plasmids coding a 698 bp long immunodominant fragment of murine C7 (mC7Cr) were obtained from Cassian Sitaru (Freiburg, Germany). Primer sequences used for PCR amplification of mC7Cr cDNA fragments were described in [162]. mC7Cr was expressed in E.coli either tagged with glutathione-S-transferase-(GST-) or with a 6xHis affinity tag in order to easily purify them from the bacteria. The use of two different tags was

necessary because of the following. We immunized rabbits against the GST-tagged fragment and we tested the presence of antibodies recognizing specifically the mC7Cr fragment in immunized rabbit sera by a custom-made ELISA, where His-tagged mC7Cr served as the capturing antigen. Thus, we could avoid measuring antibodies against GST.

3.5.1. Production of GST-C7 and C7

pGEX-mC7Cr recombinant vector was used to generate GST-C7 fragments. Plasmids were transformed into a BL21 Rosetta competent Escherichia coli strain with heat shock. Transformed bacteria were selected on agarose plates containing ampicillin. The presence of recombinant vectors were checked with Sanger sequencing (Eurofins Genomics).

Expression of the GST-C7 fusion protein was induced in BL21 Rosetta E. coli by isopropyl β-d-1-thiogalactopyranoside (IPTG). Bacterial cell lysis was performed by sonication with 40% capacity for 45 sec 3 times. The lysis buffer contained 50 mM Tris-Cl pH 7,6, 50 mM NaCl, 5 mM $MgCl_2$, 1 mM dithiothreitol and 1 mM EGTA, pH 7,4. It was also supplemented with the following protease inhibitors:2 μM pepstatin A, 10 μM leupeptin, 10 μg/ml aprotinin and 1 mM PMSF.

After high speed centrifugation, soluble fraction was preserved and GST-C7 fusion protein was purified by glutathione-based affinity chromatography. Namely, cell lysate was incubated for 30 min with Glutathione Superflow Agarose (Thermo Scientific) resin. After washing out unbound proteins with lysis buffer, resin-bound GST-C7 was eluted with soluble glutathione-containing buffer. Eluted GST-C7 was placed into Slide-A-Lyzer™ G2 Dialysis Cassette (Thermo Scientific) with 2 kDa molecule weight cut-off semi-permeable membrane and dialyzed overnight with PBS to remove glutathione and other possible salt contamination. Purity of the solution was checked with Coomassie staining after SDS-PAGE (single 50 kDa band appearing on the gel).

To retrieve C7 fragment alone without any tags, GST-C7 fusion protein was cleaved using PreScission protease (Cytiva). Here, GST-C7 protein bound to glutathione-containing resin was incubated with PreScission Protease at 4°C in a cleavage buffer containing 50 mM Tris-HCl pH 7.0, 150 mM NaCl, 1 mM EDTA and 1 mM dithiothreitol. Following incubation, the GST moiety of the tagged protein and the PreScission Protease remained bound to the glutathione-containing beads, while C7 fragment eluted to the supernatant.

3.5.2. His-C7 production

In order to produce His-tagged C7 fragment, we started working with the pQE41-mC7Cr plasmid coding C7 fragment with a 6xHis affinity tag (obtained from Cassian Sitaru). Since we could not express His-C7 efficiently enough, we cloned C7 fragment into a pLATE31 vector using the aLICator Ligation Independent Cloning and Expression Kit (Thermo Scientific).

pLATE31-mC7Cr was transformed into BL21 Rosetta E.coli. Induction of His-C7 expression and bacterial lysis was achieved with the same method as described in 3.5.1.

Purification of His-C7 was performed with immobilized metal affinity chromatography using HisPur Ni-NTA Superflow Agarose (Thermo Scientific). Bacterial cell lysate solution was first incubated with nitrilotriacetic acid (NTA) chelator-activated agarose resin charged with divalent nickel (Ni^{2+}) ions in an equilibration buffer (pH 8) containing 20 mM NaH_2PO_4, 300 mM NaCl and 10 mM of imidazole. This low imidazole concentration was sufficient for the binding of His-tagged protein with high affinity to the resin, but still interfered with the possible weak binding of other proteins. After washing out unbound proteins, resin was resuspended with a buffer containing high concentration of (300 mM) imidazole. It led to the elution of His-C7 by competing for the binding to the Ni^{2+}-charged resin. Eluted fraction was then dialyzed overnight. Purity was checked using SDS-PAGE (a single 25 kDa band appearing on the gel). Protein concentration was measured with NanoDrop (Thermo Scientific).

3.6. PRODUCTION OF ANTI-C7 ANTIBODIES

Polyclonal anti-C7 antibodies were produced by immunizing New Zealand white rabbits with GST- C7 at the Hungarian National Agricultural Innovation Center, Gödöllő, Hungary. A classical immunization protocol was applied with the subcutaneous injection of 200 μg purified GST-C7 together with complete Freund adjuvant (1:1). After 2 and 4 weeks, 2 booster injections were applied in incomplete Freund adjuvant. Blood samples were taken from marginal veins of ears before every injection to monitor antibody-production. After 6 and 10 weeks from the first shot, approximately 40 ml of blood were taken. We always paid attention not to withdraw more than 1% of the total body weight of the rabbits due to ethical reasons. Final bleeding occurred usually 14 weeks from start.

Sera were obtained by centrifugation after blood clotting.

Anti-C7 titer of immunized rabbit sera was checked using our custom-made ELISA. 1 μg/ml His-C7 was bound to the bottom of Nunc Maxisorp 96-well plates (Thermo Fischer) serving as antigen. Thus, we were able to exclude measuring anti-GST antibodies. After blocking non-specific binding with 10% FCS in PBS, preimmune and immunized sera were applied to the wells in a dilution series. Then, HRP-labeled secondary antibodies against rabbit IgG were added. Signal was developed using the HRP-substrate o-phenylenediamine dissolved in a citric acid and H_2O_2 containing buffer (pH 5). Optical density of a yellow product was measured photometrically at 492 nm by a plate reader.

Total IgG was purified from those immunized rabbit sera that had high anti-C7 titer (usually more than 1:100 000). Agarose beads containing recombinant form of the streptococcal IgG binding protein G (Thermo Scientific) were incubated with rabbit sera diluted in commercially available Binding Buffer (Thermo Scientific) for 4 hours. After washing out unbound serum components, IgG was eluted utilizing low pH (Elution Buffer, commercially available, Thermo Scientific). The neutral pH of the elute was immediately restored using 1 M Tris-Cl (pH 8). Eluted IgG solution was concentrated by centrifugation and stored in -20°C until use. I will use the term “anti-C7 antibodies” in the followings to such purified total IgG solution obtained from immunized rabbit sera.

3.7. ANTI-C7-INDUCED SKIN BLISTERING IN MICE

We used a mouse model mimicking the effector phase of the inflammatory form of EBA first described by Sitaru et al (see in detail in section 1.5.2) [154]. Here, autoimmune skin blistering was induced by repeated subcutaneous injections of pathogenic anti-C7 antibodies recognizing the immunogenic epitope of murine collagen type VII (C7).

3.7.1. Disease induction

In experiments using wild-type and *Plcg2*$^{-/-}$ mice (section 4.2 and 4.3), 12 mg anti-C7 antibodies were injected subcutaneously under isoflurane anesthesia every second day from Day 0 to Day 8 (5 injections in total, 60 mg anti-C7). Control group received normal rabbit IgG or PBS. Since it was shown that lower antibody-concentrations can also reliably induce disease and its severity correlates with the amount of anti-C7 antibodies

injected [154], in experiments conducted later on (sections 4.5 and 4.7) we used 10 mg anti-C7 per injection with the same regimen to a total of 50 mg anti-C7 per mice. This slightly reduced amount was still capable of consistently generating a robust skin blistering phenotype in wild-type mice. Titer of circulating anti-C7 antibodies in mice were checked on Day 0, Day 8 and Day 14 by custom-made ELISA described in section 3.6.

In experiments using inhibitors, wild-type C57BL/6 mice were treated with 0.4 or 1 mg tofacitinib (Selleck Chemicals) twice daily (bid) from Day –1 (one day before the first anti-C7 injection) until Day 13. Since the body weight of the mice were around 25 g, this amount served as 16 and 50 mg/kg of bodyweight, respectively. Inhibitor was dissolved in tap water containing 0,05% methylcellulose and administered by intragastric gavage. Control mice were treated similarly with vehicle (0,05% methylcellulose in tap water).

3.7.2. Evaluation

Disease onset and progression was followed every second day for 2 weeks by assessing the following parameters macroscopically:

Table 3. Percentage of individual skin areas

Body part	Total body surface (%)
Ear	2.5
Eye	0.5
Snout	5
Forelimb	5
Hind limb	10
Head	10
Neck	9
Trunk and tail	40

– Size of total affected skin area

We evaluated the whole body surface of mice divided to smaller regions shown in **Table 3**. The ratio of affected areas in every region were assessed and then added together.

– Severity score

Here, we took into consideration both the extent and the severity of lesions. The following symptoms developed usually (but not necessarily) in the order of increasing severity: alopecia, scaling, induration, erosion and crust formation. These symptoms received a score from 0.1, 0.2 and so on to 0.5, respectively. Scores of all symptoms present were summed in a given region (maximal value was set to 1). Then it was weighted by the extent. Thus, maximal severity score (100) theoretically could be reached when 100% of the surface is affected in every region with multiple severe lesions.

However, due to ethical reasons, in order to avoid unnecessary suffering, animals would be euthanized if reached a severity score of 60 (importantly, it has not happened in any of the mice we used).

– Size of erosions alone

Erosion is the most direct sign of blister eruptions without the masking effect of other, more severe secondary elementary lesions. We were not able to detect blisters in particular in most of the cases, presumably due to the massive scratching behavior of mice. Therefore, we measured the extent of erosions alone in every region and then summed.

– Ear thickness

As a more objective parameter, ear thickness was measured by a spring-loaded caliper.

3.8. HISTOLOGICAL ANALYSIS OF THE EAR TISSUE

Control and anti-C7-treated mice were sacrificed on Day 8, at the peak of acute lesions. Ear tissue was removed, fixed in 4% paraformaldehyde, dehydrated in uprising ethyl-alcohol series (50, 70, 95 and 100%) and embedded in paraffin using a Leica EG1150H embedding station. 6-8 μm sections were made with a microtome (HM340E, Thermo Scientific). Sections were either stained with hematoxylin and eosin (H&E) or underwent immunostaining. In the latter case, we blocked non-specific binding with 10% goat-serum in PBS 0.5% Tween 20, then incubated samples with anti-Ly6G antibodies (diluted 1:50) overnight at 4°C. Finally, Alexa Fluor 488-labelled secondary antibodies were added (1:250) and incubated for 1 hour at room temperature. Sections were coated with 4′,6-Diamidino-2-phenylidole (DAPI)-containing mounting medium to visualize nuclei.

For assessing anti-C7 deposition in the skin, mice were injected once with 4 mg anti-C7 or normal rabbit IgG as control. Mice were sacrificed after 24 hours, ears were removed and frozen in optimal cutting temperature compound (Tissue-Tek). 5 μm cryosections were made using Epredia^{TM} Cryotome. Samples were blocked and immunostained with Alexa Fluor 488-conjugated anti-rabbit IgG or irrelevant anti-rat IgG as control. Sections were coated with DAPI-containing mounting medium.

Microscopic images were taken and evaluated by an ECLIPSE Ni-U microscope (Nikon Instruments) connected to Nikon DS-Ri2 camera using NIS-Elements Imaging Software (Nikon, version BR 4.60.00).

3.9. ANALYSIS OF LEUKOCYTE INFILTRATION AND INFLAMMATORY MEDIATORS

Control and anti-C7-treated mice were sacrificed on Day 8. Ear tissues were digested with 200 μg/ml Liberase Thermolysin Medium enzyme mixture (containing highly purified collagenase I and II, obtained from Roche) in HBSS/H containing Ca^{2+} and Mg^{2+} for 1 hour at 37°C with continuous stirring in a shaker. Single cell suspension was obtained by filtering digested samples through a 70 μm cell strainer. Cell suspension was then washed and resuspended in PBS 5% FCS. Samples were diluted and fluorescently labeled for flow cytometric analysis using antibodies against CD11b, CD45.2, Ly6G and Siglec F. Samples were measured and analyzed as described in section 3.4.2.

Cell free supernatant of digested ear tissue was used to test the concentration of different proinflammatory mediators using a mouse cytokine antibody array kit (Panel A) or commercial IL-1β, MIP-2 and LTB_4 ELISA kits (all from R&D Systems) according to manufacturer's instructions.

3.10. COMPETITIVE IN VIVO MIGRATION ASSAY

We assessed intrinsic migrating capacity of myeloid cells in vivo in mixed bone-marrow chimeras. Generation of such chimeras was described in section 3.1.2.1. WT:WT and WT: *Plcg2*$^{-/-}$ chimeras were treated with repeated injections of anti-C7. Usually all mice developed skin blistering, since wild-type leukocytes were present in every mouse.

On Day 8, blood samples were obtained, mice were sacrificed and ear tissue was digested as described above. Next, we prepared the blood and ear samples for flow cytometric analysis using antibodies against CD45.2, CD11b, Ly6G and Siglec F. After gating the major myeloid-cell populations (neutrophils, eosinophils and monocytes/macrophages), the percentage of CD45.2-expressing cells were calculated in blood and ears. Those $CD45.2^+$ cells were wild-type in WT:WT and *Plcg2*$^{-/-}$ in WT: *Plcg2*$^{-/-}$ chimeras.

Relative migration of $CD45.2^+$ neutrophils, eosinophils and monocytes/macrophages were calculated according to the following formula:

$$relative\ migration = \frac{\left(\frac{\%\ of\ CD45.2^{+}cells\ in\ ears}{\%\ of\ CD45.2^{+}cells\ in\ blood}\right)}{\left(\frac{\%\ of\ CD45.2^{-}cells\ in\ ears}{\%\ of\ CD45.2^{-}cells\ in\ blood}\right)}$$

3.11. IN VIVO CHEMILUMINESCENCE ASSAY

In vivo myeloperoxidase (MPO) activity was detected using a chemiluminescence assay at the Small Animal Imaging Core Facility of the Szentágothai Research Centre of the University of Pécs with the kind help of Ádám I. Horváth [234].

Control and anti-C7-treated chimeras were injected intraperitoneally with 150 mg/kg luminol sodium salt (Gold Biotechnology) on Day 8. Luminescence images were captured 10 minutes after injection by IVIS Lumina II imaging system (PerkinElmer, 120 sec acquisition, Binning=8, F/Stop=1) under 120/6 mg/kg intraperitoneal ketamine-xylazine anesthesia. For quantitative analysis, total radiance values (total photon flux/sec) were used from standardized regions of interest of the ears using the Living Image software (PerkinElmer).

3.12. IN VITRO EXPERIMENTS USING MURINE NEUTROPHILS

3.12.1. Isolation of murine neutrophils

To isolate mouse neutrophils, wild-type and *Plcg2*$^{-/-}$ mice were sacrificed and femurs and tibias were taken. Bone marrow was opened and flushed as described in 3.1.2.

Bone marrow cell suspension was centrifuged and pellet were reconstituted with hypotonic (0.2%) NaCl solution in order to lyse red blood cells. After 40 sec, osmotic conditions were set back to physiological with equal volume of 1.6% NaCl.

After a wash step, cell suspension in HBSS/H was pipetted onto 62% Percoll gradient (GE Healthcare) and centrifugated with 2500 rpm for 30 min with slow acceleration and deceleration. After gradient centrifugation, mononuclear cells (such as lymphocytes and monocytes) appeared on the border of the two solution phases, while neutrophils were able to sediment, creating a cloudy pellet at the bottom of the falcon. Therefore, we could obtain neutrophil suspension of more than 90% purity based on our previous results [57].

After some washing steps, cells were counted in Boyden chambers and immediately used in the following experiments. Cells were kept at room temperature in media lacking any Ca^{2+} and Mg^{2+} throughout the preparation period in order to avoid preactivation.

3.12.2. In vitro Transwell migration assay

Transwell inserts (Corning) containing a polycarbonate membrane with 5 μm pore size at the bottom were precoated with 10 μg/ml fibrinogen for 1 hour. After washing with HBSS/H, they were filled with isolated neutrophils in 10^6/ml concentration in HBSS/H supplemented with Ca^{2+} and Mg^{2+} immediately before start. Transwell inserts were then placed into wells of a 24-well plate filled with media containing 100 ng/ml MIP-2 (PeproTech GmbH), 50 ng/ml LTB_4 (Santa Cruz Biotechnology) or media alone and incubated for 1 hour at 37°C. Migration was stopped on ice, plates were centrifuged and ratio of cells that migrated out from the inserts were determined using an acid phosphatase assay. Cells were lysed in an acid-phosphatase buffer (pH 5) containing 10 μM p-nitrophenyl phosphate (pNPP) for 10 min on ice. Lysates were transferred to a new 96-well plate and incubated further for 90 min at 37°C. Reaction was stopped with 5 N NaOH and yellow color was determined photometrically at 405 nm in a plate reader. To calculate the amount of cells transmigrated, a calibration curve was set using the data of known amount of neutrophils (100%, 50%, 25%, 12.5% and 0%).

3.12.3. In vitro immune complex-induced proinflammatory mediator release

For the in vitro mimicking of immune complex formation during anti-C7-induced skin blistering, we created immobilized C7/ anti-C7 immune complex surfaces on Nunc MaxiSorp 96-well plates. Namely, 20 μg/ml C7 in carbonate buffer was bound to the bottom of wells, blocked in 10% FCS in PBS and then treated with 300 μg/ml anti-C7 in 10% FCS in PBS. Control wells were treated with C7 alone.

Isolated neutrophils were diluted to $3x10^6$/ml. For the analysis of MIP-2 production, cells were plated onto the wells in Ca^{2+} and Mg^{2+} supplemented HBSS/H and incubated for 4 hours at 37°C. For testing LTB_4 release, cells were suspended in RPMI medium and incubated on immune complex surfaces for 1 hour. Reaction was stopped on ice and supernatant was stored at -20°C. Concentration of MIP-2 or LTB_4 in the supernatants were measured by commercial ELISA kits.

3.13. EXPERIMENTS USING HUMAN CELLS AND TISSUE

All experiments on human samples were approved by the Scientific and Research Ethics Committee of the Medical Research Council of Hungary (Ethical approval ID: IV/3052-1/2021/EKU). All human subjects provided their written informed consent.

3.13.1. Isolation of human neutrophils

Human neutrophils were isolated from the peripheral blood of healthy volunteers. Blood was taken into a falcon containing PBS with 5% heparin with a 18 gauge needle. It was important to prevent physical distress, like vacuum that would activate neutrophils. Sedimentation of red blood cells was increased by the addition of 0.4% dextran. After 20 min, leukocyte-rich supernatant was centrifuged and pellet was resuspended in HBSS/H. The supernatant was also used as fresh human plasma as a source of complement components later in our experiments.

Human neutrophils were separated by gradient centrifugation using Ficoll gradient (GE Healthcare). Residual red blood cell contamination was removed by hypotonic lysis.

Isolated neutrophils were then counted and proceeded for experiments. Similarly to murine ones, human neutrophils were also handled carefully to avoid preliminary activation by using endotoxin, Ca^{2+} and Mg^{2+} free solutions at room temperature throughout the preparation.

3.13.2. Ex vivo human skin separation assay

Neutrophil-mediated dermal-epidermal separation of human skin was performed based on Gammon et al [160]. Schematic experimental setup is presented in **Figure 11**.

Healthy human skin samples were obtained from surgical interventions at the Department of Dermatology, Venereology and Dermatooncology, Semmelweis University. Samples were frozen in optimal cutting temperature compound by liquid nitrogen. 5 μm cryosections were made and incubated with 6 mg/ml anti-C7 or normal rabbit IgG as control for 1.5 hours at 37°C. PLC inhibitor U73122 (Selleck Chemicals) was dissolved in dimethylformamide (DMF). Isolated neutrophils were diluted to 10^7/ml in RPMI (Biosera) in the presence of fresh normal human plasma (1:4) as a source of complement proteins. Next, neutrophils were preincubated with either 10 μM U73122 or vehicle alone for 20 min at 37°C. Final samples contained 0.05% DMF.

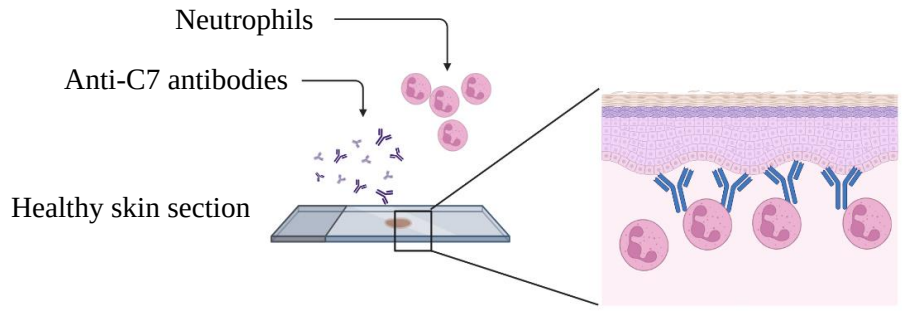

Figure 11. Ex vivo skin separation model. *Created in BioRender.*

Chambers were assembled above the anti-C7-treated cryosections and filled with approximately 500 µl of preincubated neutrophil suspension. Chambers were incubated for 1.5 hours at 37°C then washed, fixed in 4 % paraformaldehyde and stained with H&E.

Microscopic images were taken with ECLIPSE Ni-U microscope (Nikon Instruments) connected to Nikon DS-Ri2 camera. Dermal-epidermal separation was quantified using NIS-Elements Imaging Software (Nikon, version BR 4.60.00).

3.14. PRESENTATION OF THE DATA AND STATISTICAL ANALYSIS

Experiments were performed the indicated number of times discussed at figure legends. All macroscopic pictures and microscopic images are representative of the indicated number of independent experiments. Quantitative graphs and kinetic curves show mean and standard error of the mean (SEM) from all individual mice or samples from the indicated number of experiments.

Statistical analyses were carried out by the STATISTICA software using two-way (factorial) analysis of variance (ANOVA). Treatment and genotype were the two independent variables. One-way ANOVA was used to evaluate in vivo migration experiments. Area under the curve was used for statistical analysis in kinetic measurements. p values were indicated in figure legends and p below 0.05 were considered statistically significant.

4. RESULTS

4.1. GENERAL CHARACTERIZATION OF *Plcg2*$^{-/-}$ MICE

As a first step towards the detailed analysis of PLCγ2 deficiency during autoantibody-induced skin blistering, we carried out a general characterization of *Plcg2*$^{-/-}$ mice. *Plcg2*$^{-/-}$ transgenic animals were maintained by heterozygous breeding due to the reported male infertility of *Plcg2*$^{-/-}$ males [232], and limited availability of *Plcg2*$^{-/-}$ females. Offspring were genotyped at weaning (2-3 weeks of age) by allele-specific polymerase chain reaction (PCR). Namely, amplified products were run on an agarose gel to separate 340 base pair-long wild-type alleles (*Plcg2*$^{+}$) from 700 base pair-long *Plcg2*$^{-}$ knockout alleles (**Figure 12**).

We also calculated the distribution of genotypes at weaning age. Only 12% of the offspring were *Plcg2*$^{-/-}$, contrary to the expected 25% ratio from heterozygous breeding (**Figure 13A**). This suggests a survival defect in *Plcg2*$^{-/-}$ mice during embryonal development or newborn life. After weaning age, we found only a moderate deficit in the survival of adult *Plcg2*$^{-/-}$

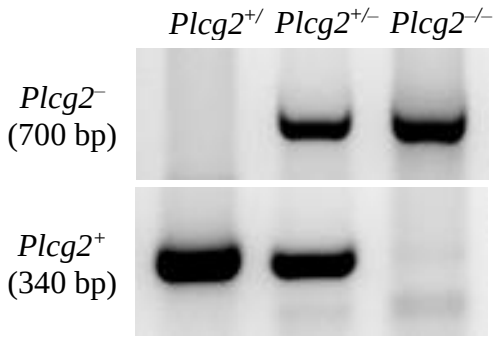

Figure 12. Genotyping of *Plcg2*$^{-/-}$ transgenic mice by allele-specific PCR.
Representative DNA gels of more than 3 independent experiments.

A

	% at weaning age	
	Expected	Found
Plcg2 $^{+/+}$	25	33
Plcg2 $^{+/-}$	50	55
Plcg2 $^{-/-}$	25	12

B

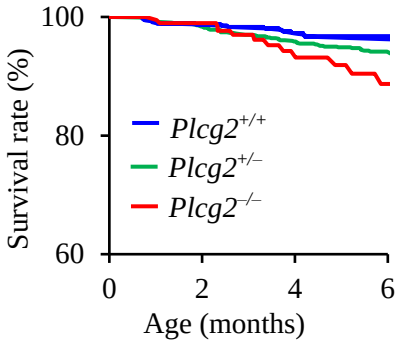

Figure 13. Survival rate of *Plcg2*$^{-/-}$ mice.
(**A**) Genotype distribution after heterozygous breeding at weaning age.
(**B**) Survival rate after weaning. Data show more than 200 mice per group.

mice compared to *Plcg2*$^{+/+}$ or *Plcg2*$^{+/-}$ animals until 6 months of age (**Figure 13B**).

In the following steps, we used *Plcg2*$^{-/-}$ offspring in our experiments. *Plcg2*$^{+/+}$ or C57BL/6 mice served as controls (collectively referred to as wild-type mice).

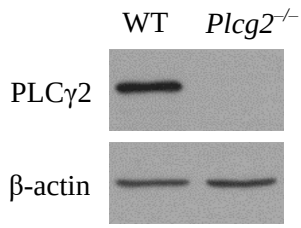

Figure 14. PLCγ2 expression in total bone-marrow cell lysates.
Representative blot from 3 independent experiments.

We analyzed the presence of PLCγ2 in hematopoietic cells. As a first approach, we measured the expression of PLCγ2 protein in unfractionated bone marrow cell lysates. Wild-type cell lysates but not *Plcg2*$^{-/-}$ samples showed signal in immunoblots (**Figure 14**). This confirms that PLCγ2 is expressed in the hematopoietic compartment. However, this bulk technique is not useful for analyzing the expression profile in different leukocyte lineages.

Therefore, we used flow cytometry to measure intracellular PLCγ2 expression in circulating leukocytes. We identified different leukocyte subsets based on their specific surface protein expression pattern. Wild-type neutrophils, eosinophils, monocytes and B cells showed higher PLCγ2 fluorescence intensity than cells obtained from *Plcg2*$^{-/-}$ mice (**Figure 15**). We found no difference regarding T cells (**Figure 15**). This indicates that PLCγ2 is expressed in all myeloid cells and B cells, but not in T cells.

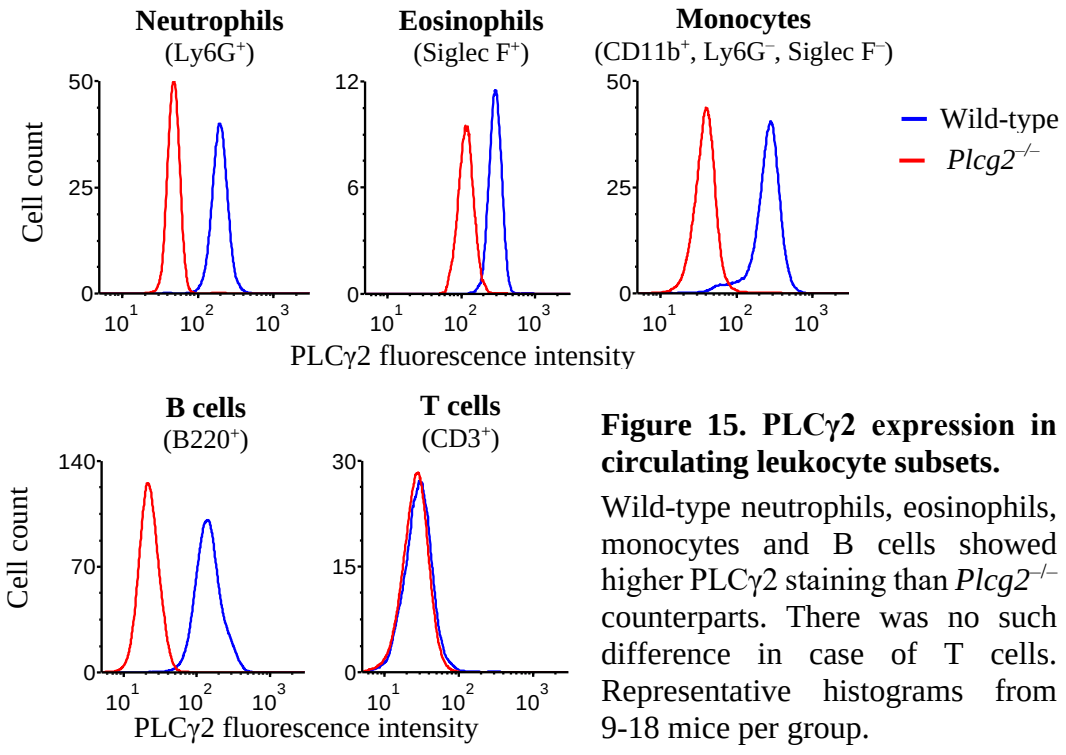

Figure 15. PLCγ2 expression in circulating leukocyte subsets.
Wild-type neutrophils, eosinophils, monocytes and B cells showed higher PLCγ2 staining than *Plcg2*$^{-/-}$ counterparts. There was no such difference in case of T cells. Representative histograms from 9-18 mice per group.

Next, we wanted to check the effect of PLCγ2 deficiency on the absolute number of circulating leukocytes and on the expression of different maturation and functional cell surface markers on myeloid cells. We found no substantial difference between cell counts of wild type and *Plcg2*$^{-/-}$ neutrophils, eosinophils, monocytes, B cells or T cells in the blood (**Figure 16**).

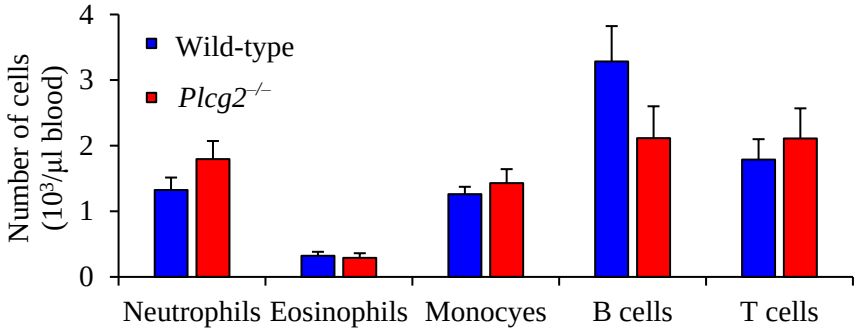

Figure 16. Number of leukocyte subsets in wild-type and *Plcg2*$^{-/-}$ mice.
Bar graphs show mean and SEM of 9-18 mice per group. p= 0.10-0.75

Regarding the expression profile of myeloid cells, the *Plcg2*$^{-/-}$ mutation had no effect on the expression of the major integrin chains (CD11a, CD11b, and CD18) or Fcγ receptors (FcγRII/III and FcγRIV) on circulating neutrophils, eosinophils and monocytes (**Figure 17**). FcγRIV expression on eosinophils could not be tested due to interference between available reagents. *Plcg2*$^{-/-}$ mice also showed normal expression of the Ly6G maturation marker on neutrophils and the Siglec F maturation marker on eosinophils, and normal distribution of the Ly6C polarization marker on monocytes (**Figure 17**).

Taken together, we found that PLCγ2 deficiency resulted in a survival defect in embryos and/or newborn pups. PLCγ2 was present in every major leukocyte subsets except T cells. Its absence neither caused significant reduction in circulating leukocyte numbers, nor affected the expression of maturation markers, integrins and FcγRs on myeloid cells.

4.2. SETTING UP THE ANTI-C7-INDUCED SKIN BLISTERING MODEL

We chose a widely used passive-transfer model of epidermolysis bullosa acquisita, initially described by Sitaru et al [154]. To this end, we injected polyclonal IgG obtained from rabbits immunized against the immunogenic epitope of murine type VII collagen (C7, see in detail in section 1.5.2).

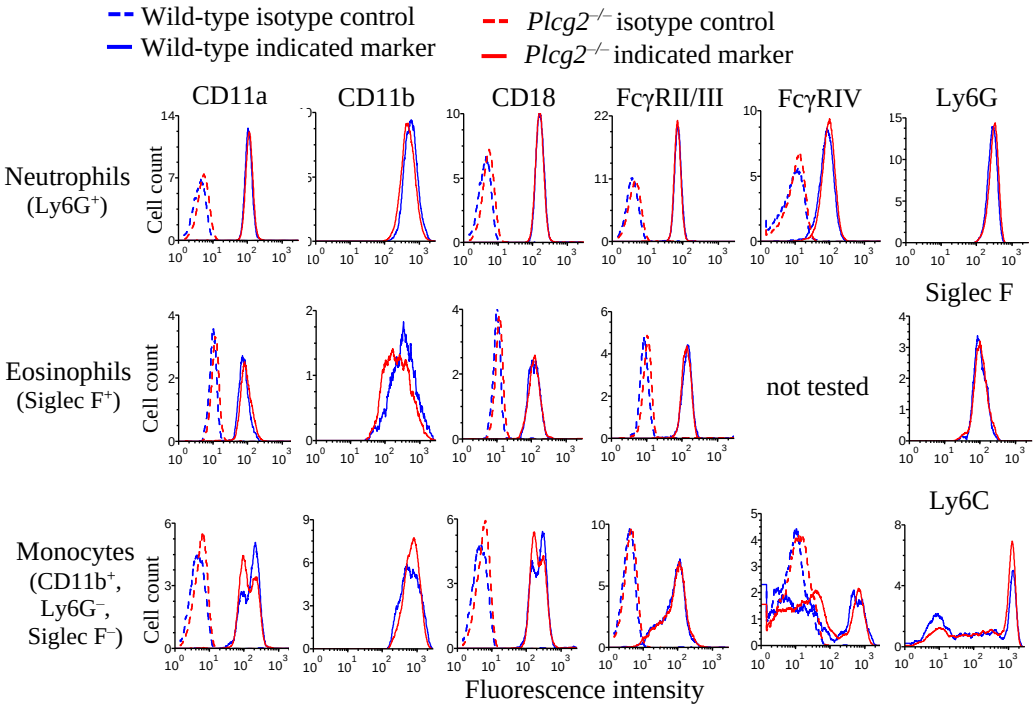

Figure 17. Cell surface marker expression profile of circulating myeloid cells. Expression of major integrin chains (CD11a, CD11b and CD18), Fcγ receptors and maturation markers (Ly6G on neutrophils, Siglec F on eosinophils and polarization marker Ly6C on monocytes) were measured in myeloid cells by flow cytometry. Histograms are representative of 3 independent experiments.

Our workgroup have used this model in collaboration with Cassian Sitaru before [8, 9, 28, 205]. However, multiple aspects were not completely elaborated in our hands. Here, I mention some main steps, describing how we fine-tuned the model mentioned above. A more general description of the method can be found in sections 3.5-3.7.

4.2.1. Purification of antigens and antibodies

First, we set up the expression and purification of GST-tagged and His-tagged fusion proteins of C7. We expressed fusion proteins in E. coli bacteria followed by affinity purification. We used glutathione-based or metal-based column chromatography in case of GST-C7 and His-C7, respectively. Purity of the antigen solutions were checked by running them on SDS-PAGE followed by Coomassie staining, shown in **Figure 18**. Sample "GST alone" was purified from lysed E. coli transformed with empty pGEX plasmid (expressing only GST upon induction). GST-C7 sample was purified from E. coli transformed with pGEX-mC7Cr recombinant vector. C7 samples were obtained after cleavage of gluthathione-bound GST-C7 with PreScission protease. GST and C7 both

have a molecular weight around 25 kDa, while GST-C7 fusion protein is around 50kDa.

Next, we produced polyclonal anti-C7 antibodies by immunizing rabbits against GST-C7 at the Hungarian University of Agriculture and Life Sciences, Gödöllő. We performed custom-made ELISA in order to test the reactivity of immunized rabbit sera (**Figure 19A**). We used His-C7 as capturing antigen to exclude anti-GST signals.

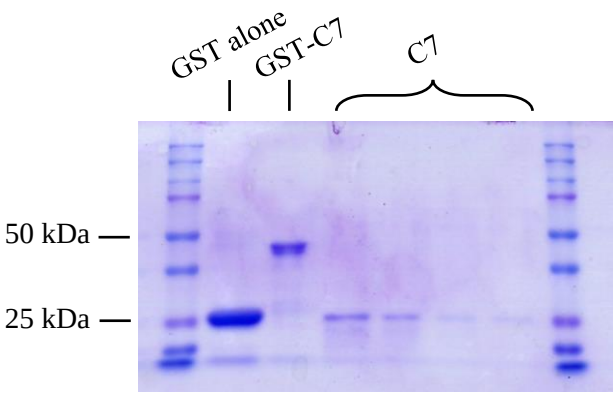

Figure 18. Purity of GST-C7 and C7 solutions.
Purified GST (~25 kDa), GST-C7 (~50 kDa) and C7 (~20 kDa) samples were run on SDS-PAGE followed by Coomassie staining. Representative gel from at least 3 independent experiment.

Compared to the preimmune serum, optical density of immunized sera already increased after 2 weeks of the first GST-C7 injection, which was maintained throughout the bleeding period (**Figure 19B**). This indicated the appearance of specific anti-C7 antibodies. Then, we purified total IgG from immunized rabbit sera by protein G-based affinity chromatography. Later on, I am referring to such purified total IgG as anti-C7.

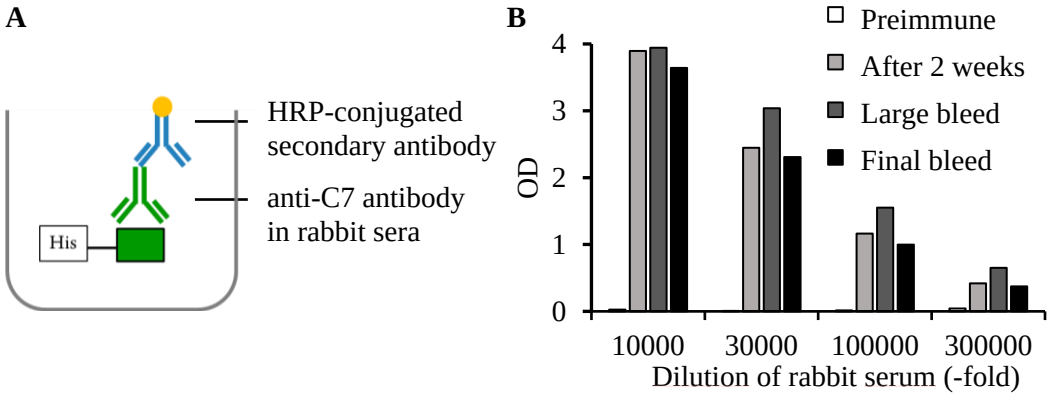

Figure 19. Reactivity of immunized rabbit sera.
A. Design of our custom-made ELISA. **B.** Optical density (OD) of immunized sera obtained from a representative rabbit. Serum samples were taken at the beginning (preimmune serum), 2 weeks, 6 weeks (large bleed) and 14 weeks (final bleed) after the first GST-C7 injection.

4.2.2. Disease induction

We induced skin blistering by the subcutaneous injections of 12 mg anti-C7 on Days 0, 2, 4, 6 and 8 (60 mg total IgG/mouse). The timeline is present in **Figure 20**.

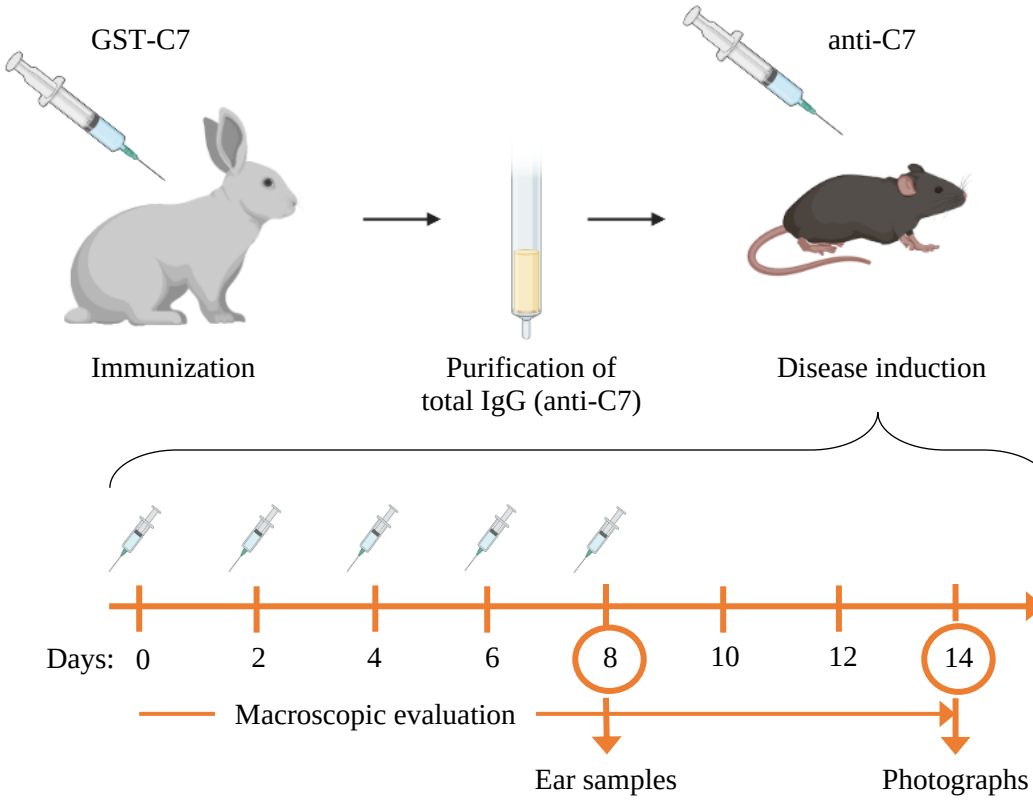

Figure 20. Timeline of anti-C7-induced skin blistering.
Disease was induced by the passive transfer of anti-C7 antibodies purified from immunized rabbit sera. 12 mg anti-C7 was injected subcutaneously on Days 0, 2, 4, 6 and 8 (60 mg/mouse). We evaluated macroscopic phenotype every second day for 2 weeks. Photographs were made on Day 14. In some cases, mice were terminated and ear samples were taken on Day 8. *Created in BioRender.*

In our first experiments, we used purified normal rabbit IgG as control treatment. As shown in **Figure 21**, repeated systemic injection of anti-C7 antibodies triggered a severe disease phenotype involving signs of alopecia, scaling, erosions, and crust formation in the skin of wild-type mice. Symptoms were most prominent on the ears, head and limb regions, but appeared at various areas on the neck and trunk, as well. Importantly, normal rabbit IgG induced no such changes in the skin of wild-type animals. We observed that the injected massive amount of systemic IgG induced a transient joint swelling irrespective of the specificity of the antibodies. Importantly, joint swelling disappeared 3-5 days from start and did not involve the skin.

Since preparation of normal rabbit IgG was quite time- and animal-consuming, after ruling out the skin blistering-causing effect of rabbit IgG itself, in our following experiments, we chose to use PBS as control treatment.

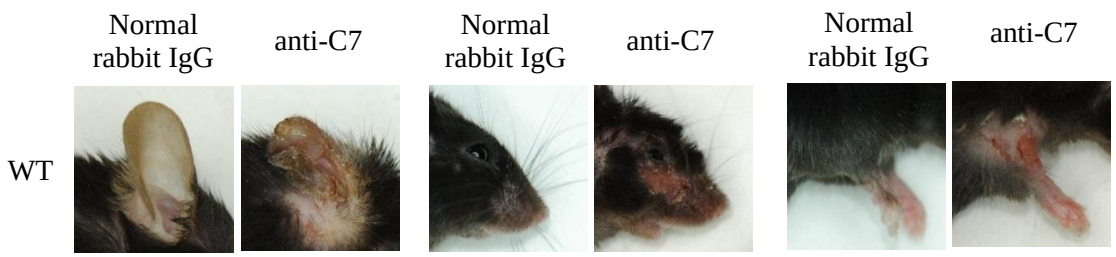

Figure 21. Autoantibody-induced skin blistering in wild-type mice.
Total IgG from immunized rabbit sera (anti-C7), but not normal rabbit IgG was able to induce autoimmune skin blistering in wild-type mice. Photographs are representative of 3-4 mice from 2 independent experiments.

4.3. THE ROLE OF PLCγ2 IN ANTIBODY-INDUCED SKIN BLISTERING

After we generally characterized the phenotype of *Plcg2*$^{-/-}$ mice and have been able to reproducibly induce skin blistering in mice, we started to include *Plcg2*$^{-/-}$ animals in this model. The majority of our following results were published in Szilveszter et al., J Invest Dermatol, 2021 [3], as indicated in the figure legends.

4.3.1. Anti-C7-induced skin blistering in intact *Plcg2*$^{-/-}$ mice

First, we repeatedly injected intact wild-type and *Plcg2*$^{-/-}$ mice (i.e non-transplanted, see below) with anti-C7 or with PBS as control. Similar to our initial experiments, wild-type mice developed severe skin disease upon anti-C7 treatment with erosions, crust formation and signs of cutaneous inflammation (**Figure 22A)**. Contrarily, *Plcg2*$^{-/-}$ mice showed no such signs of skin pathology after anti-C7 treatment. Representative pictures (presented in **Figure 22A**) were taken on the 14th day from the first anti-C7 injection.

We followed the time course of the disease for two weeks by measuring the extent of affected skin area (**Figure 22B**) and by calculating a severity score taking into account both the size and the severity of the lesions (**Figure 22C**). More specifically, alopecia, scaling, induration, erosion and crust formation were considered as increasingly severe lesions. We also quantified areas showing erosions as signs of blister eruption without any more severe secondary lesions (**Figure 22D**). Upon anti-C7 treatment, wild-type

mice showed a robust increase in the extent and severity of the lesions over time. The extent of erosions, in particular, also gradually increased after anti-C7 treatment. In contrast, *Plcg2*$^{-/-}$ mice failed to develop any signs of skin lesions during the entire investigation period (**Figure 22B-D**).

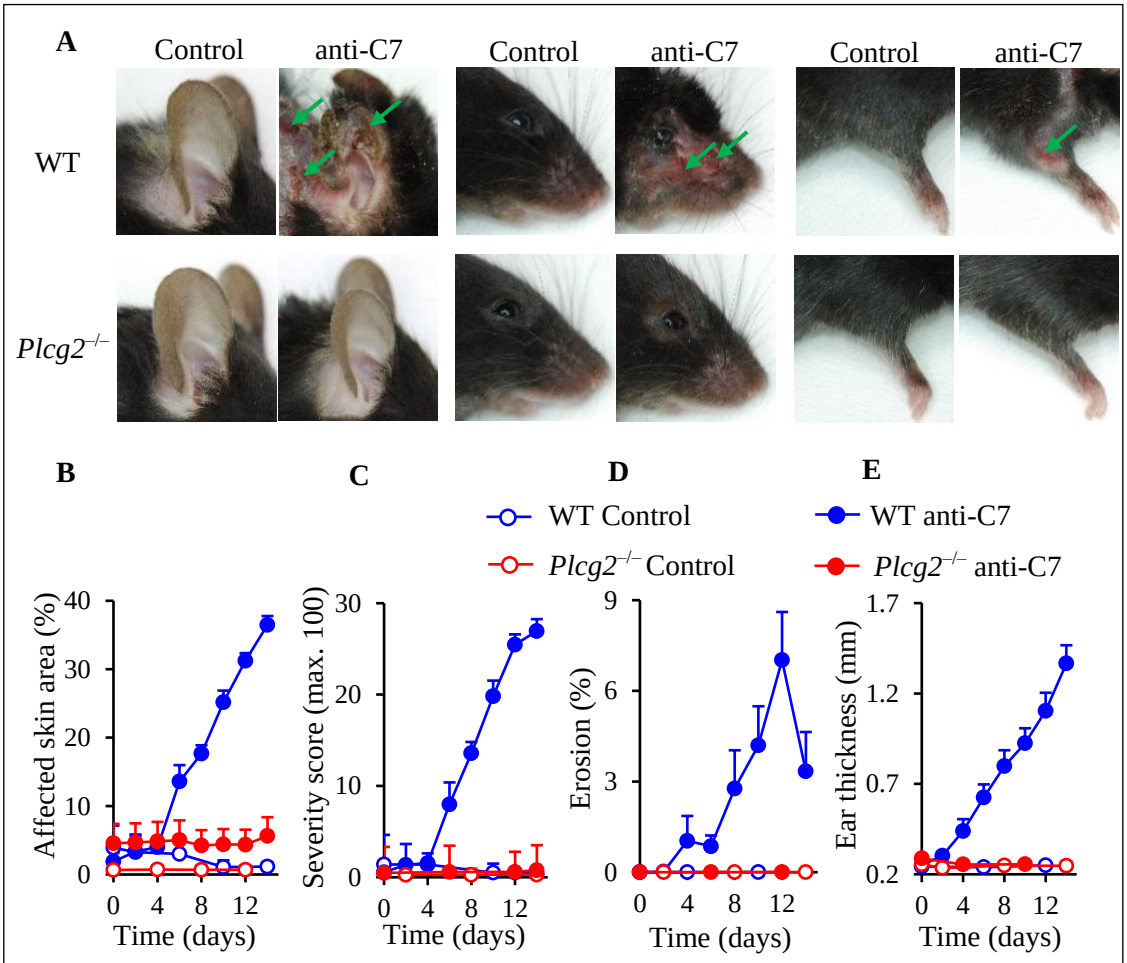

Figure 22. Autoantibody-induced skin blistering in wild-type and Plcg2$^{-/-}$ intact mice.

Skin blistering was induced by repeated injections of anti-C7 on Days 0, 2, 4, 6 and 8. (**A**) Macroscopic phenotype on Day 14. Green arrows indicate erosions. (**B**) Extent of affected skin area, p = 0.0011. (**C**) Severity score, p = 1.2×10^{-8}. (**D**) Percentage of erosions in particular, p= 0.042. (**E**) Evaluation of ear thickness, p = 5.2×10^{-5}. Representative photographs and quantitative data show mean and SEM from, 5-9 mice per group from 4-5 individual experiments except control-treated *Plcg2*$^{-/-}$ mice, where data of 3 mice from 2 experiments are shown due to the limited availability of *Plcg2*$^{-/-}$ animals. [3]

As a more objective parameter of disease development, ear thickness was also measured. Ears of wild-type mice robustly thickened from Days 2-4 until the end of the experiment, whereas *Plcg2*$^{-/-}$ mice completely failed to develop ear thickening upon anti-C7 treatment (**Figure 22E**). Taken together, *Plcg2*$^{-/-}$ mice remained completely protected

from the development of any clinical signs and quantitative measures of anti-C7-induced skin disease.

4.3.2. Anti-C7-induced skin blistering in *Plcg2*$^{-/-}$ bone-marrow chimeras

The limited number of *Plcg2*$^{-/-}$ mice (due to their survival defect and male infertility mentioned in Section 4.1) prompted us to generate bone-marrow chimeras with a *Plcg2*$^{-/-}$ hematopoietic system.

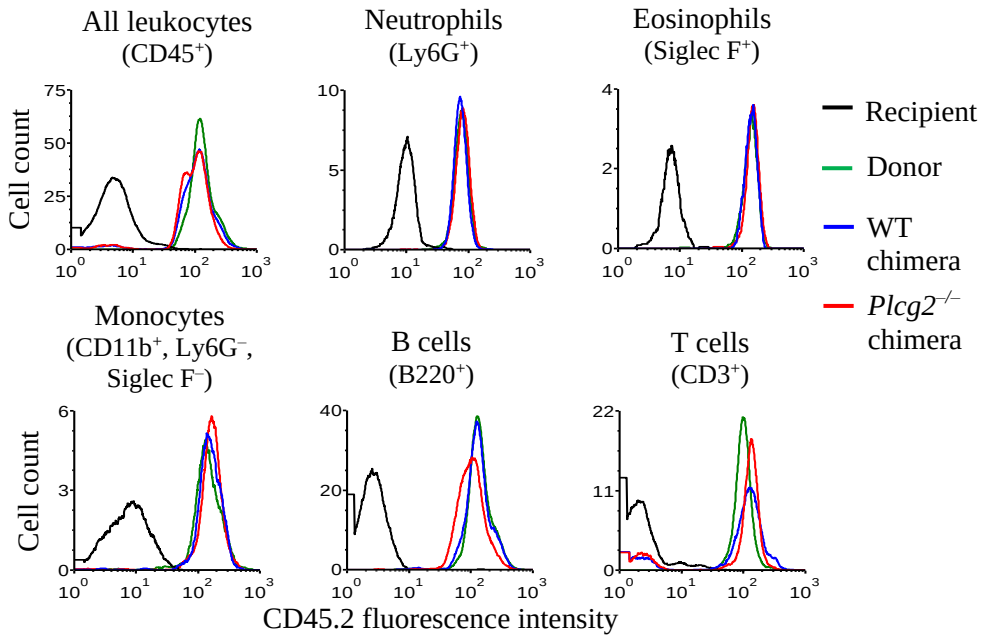

Figure 23. Checking the replacement of circulating leukocyte subsets in wild-type and *Plcg2*$^{-/-}$ bone-marrow chimeras 4 weeks after transplantation.
Recipient mice carrying CD45.1 leukocyte marker were transplanted with unfractionated bone marrow cells of wild-type or *Plcg2*$^{-/-}$ donors, expressing CD45.2. Histograms are representative of 2-3 individual experiments, involving 12-23 bone-marrow chimeras per group. Histograms showing neutrophils, eosinophils and monocytes are from [3].

Replacement of the hematopoietic compartment was tested by flow cytometry, based on the CD45.2 expression profile of circulating leukocytes. **Figure 23** shows representative histograms of cells obtained from a donor and a recipient mouse before transplantation (in green and black, respectively) along with leukocytes obtained from wild-type and *Plcg2*$^{-/-}$ bone-marrow chimeras (marked with blue and red). 4 weeks after transplantation, practically all circulating leukocytes (CD45$^+$ cells), were of donor origin expressing CD54.2, including all neutrophils, eosinophils, monocytes, B cells and the majority of T cells. This was irrespective of the presence of PLCγ2 (**Figure 23**).

Next, we subjected such bone-marrow chimeras to autoantibody-induced skin blistering. Repeated anti-C7 injections induced a massive, severe disease phenotype in wild-type chimeras with erosions, crust formation and dermal inflammation affecting significant areas of the skin involving the ears, cheeks and forelimbs (**Figure 24A-E**). In line with our findings with intact mice, *Plcg2*$^{-/-}$ bone-marrow chimeras were also completely protected from any macroscopic signs of disease development (**Figure 24A**) and quantitative measures of skin blistering during the entire investigation period, including the extent of affected skin surface, severity score, the extent of erosions, and ear thickening (**Figure 24B-E**).

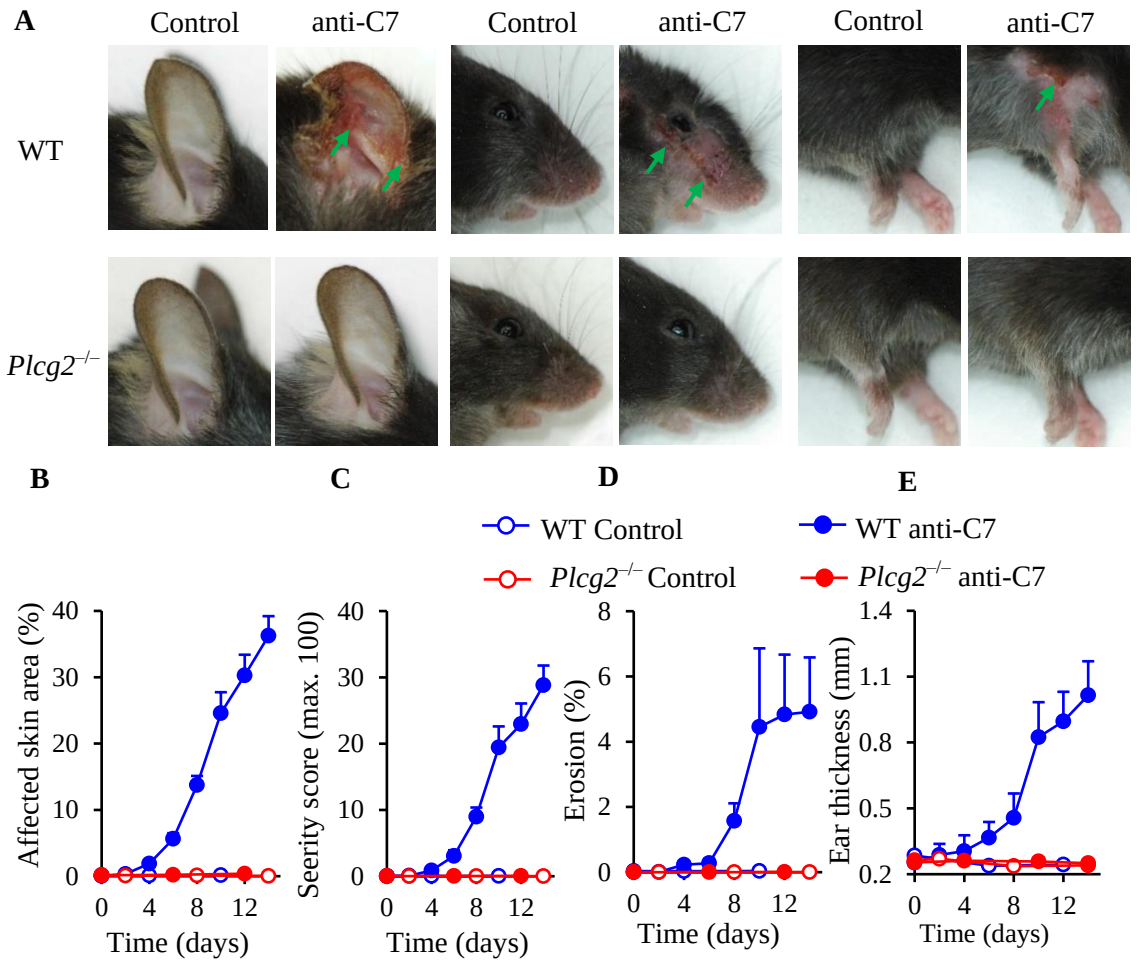

Figure 24. Autoantibody-induced skin blistering in wild-type and Plcg2$^{-/-}$ bone-marrow chimeras.

Skin blistering was induced by repeated injections of anti-C7 on Days 0, 2, 4, 6 and 8. (**A**) Macroscopic phenotype on Days 12-14. Green arrows indicate erosions. (**B**) Extent of affected skin area, $p = 6.9\times10^{-14}$. (**C**) Severity score, $p = 9.3\times10^{-11}$. (**D**) Percentage of erosions in particular, $p = 0.0061$. (**E**) Evaluation of ear thickness, $p = 0.0063$. Representative photographs and quantitative data show mean and SEM from, 5-12 mice per group from 3-5 individual experiments. [3]

Since we were able to generate a large number of *Plcg2*$^{-/-}$ chimeras in a reproducible manner, we performed the following experiments using *Plcg2*$^{-/-}$ bone-marrow chimeras.

First, we analyzed histological aspects of skin blistering and inflammation in ear samples obtained from wild-type and *Plcg2*$^{-/-}$ chimeras on Day 8 after disease induction. We chose this time point because acute inflammatory lesions and erosions peaked usually at this time point.

Anti-C7 treatment resulted in massive ear thickening in wild-type mice. This affected both the epidermal and dermal layers. We observed hyperplasia of keratinocytes and robust dermal infiltration of inflammatory cells (**Figure 25A**). We also found split formation in several places between the epidermal and dermal layers in H&E-stained sections of wild-type ear samples. Contrarily, ear samples obtained from anti-C7-treated *Plcg2*$^{-/-}$ chimeras showed normal microscopic structure similar to samples obtained from control-treated littermates (**Figure 25A**). Quantification revealed that significant dermal-epidermal separation occurred upon anti-C7 treatment in the ears of wild-type mice, indicating blister formation. Contrarily, this was completely absent in *Plcg2*$^{-/-}$ samples (**Figure 25B**).

Taken together, mice with a *Plcg2*$^{-/-}$ hematopoietic system are protected from macroscopic and microscopic development of anti-C7-induced skin disease, including macroscopic erosions, as well as histological separation along the DEJ.

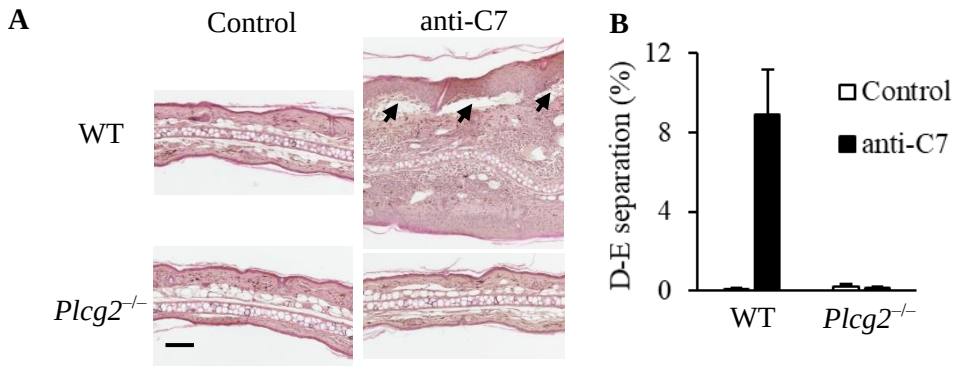

Figure 25. Microscopic analysis of anti-C7-induced skin blistering.
Ear samples were obtained from wild-type and *Plcg2*$^{-/-}$ chimeras 8 days after the first anti-C7 injection. (**A**) H&E stained paraffin-embedded sections. Black arrows indicate dermal-epidermal (D-E) separation. Scale bar: 100 μm. (**B**) Extent of D-E separation, p = 0,012. Histological images are representative of and data show mean and SEM from, 5-8 chimeras per group from 3 independent experiments. [3]

4.3.3. Circulating anti-C7 levels and antibody deposition

Next, we wanted to exclude the possibility that the *Plcg2*$^{-/-}$ mutation reduces the circulating amount and/or the skin deposition of injected anti-C7 antibodies. Therefore, we measured anti-C7 levels in the serum of animals by ELISA and investigated its deposition along the dermal-epidermal junction by immunostaining.

Serum anti-C7 levels increased both in wild-type and *Plcg2*$^{-/-}$ chimeras on Day 8 and showed a decreasing tendency at the end of the experiment on Day 14 (**Figure 26**). PLCγ2 deficiency even moderately increased the circulating levels of anti-C7 on Day 8 compared to the wild-type genotype. Anti-C7 level also remained higher on Day 14 in *Plcg2*$^{-/-}$ samples, possibly due to the reduced "consumption" of antibodies in the skin.

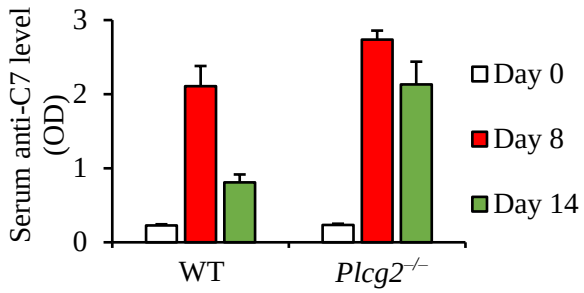

Figure 26. Circulating anti-C7 levels.
Serum anti-C7 level of wild-type and *Plcg2*$^{-/-}$ mice obtained on Days 0, 8 and 14 was measured by indirect ELISA. Bar graphs show mean and SEM from 8 mice per group from 3 independent experiments. [3]

We also analyzed frozen ear sections by immunostaining. Deposition of anti-C7 at the dermal-epidermal interface (**Figure 27**, green fluorescence signal) was present in both wild-type and *Plcg2*$^{-/-}$ ear samples after 24 hours of subcutaneous injection of 4 mg anti-C7. Importantly, we could not detect any specific fluorescence signal, when we injected mice with normal rabbit IgG instead of anti-C7, or when we used irrelevant secondary antibodies instead of anti-rabbit IgG (**Figure 27**).

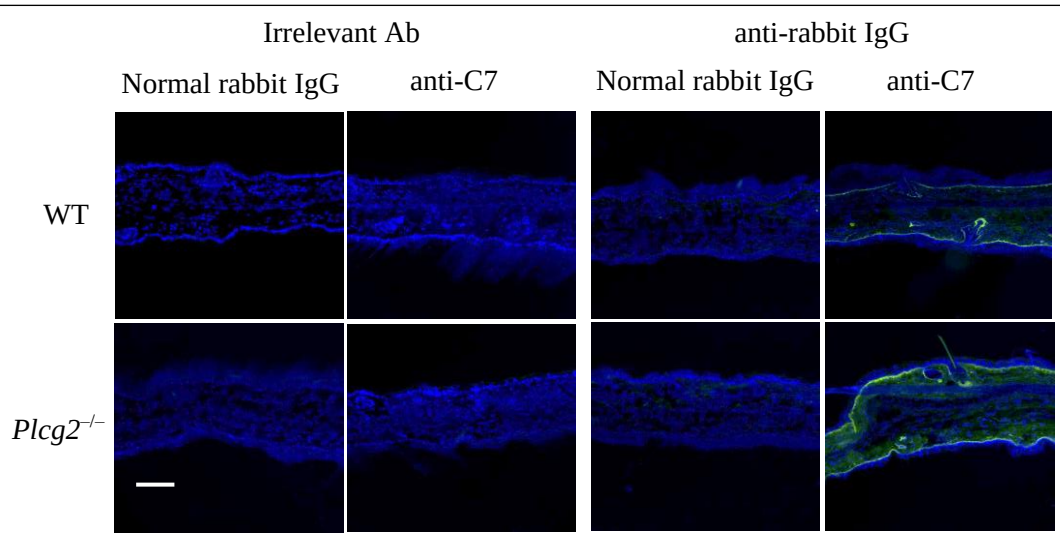

Figure 27. Anti-C7 deposition at the dermal-epidermal junction

Wild-type and *Plcg2*$^{-/-}$ chimeras were injected with 4 mg normal rabbit IgG or anti-C7. Immunostaining of rabbit antibodies was obtained on cryosections of ears after 24 hours. Histological images are representative of 3 independent experiments. Scale bar: 60 μm. [3]

4.3.4. Dermal infiltration of leukocytes

The defective dermal cellular infiltration found in histological sections of *Plcg2*$^{-/-}$ mice (**Figure 25A)** prompted us to analyze the tissue accumulation of different leukocyte populations after anti-C7 treatment.

As a first approach, we applied immunofluorescence staining on histological sections of the ears to detect neutrophils. To do so, we used antibodies against the neutrophil marker Ly6G, followed by fluorescently labeled secondary antibodies in ear sections obtained on Day 8. Specificity of green fluorescence signal was tested by applying secondary antibodies alone.

We did not find any Ly6G-positive cells in control-treated ear sections (**Figure 28**). In contrast, the dermis of anti-C7-treated wild-type sections were massively infiltrated with green fluorescent Ly6G-positive cells, representing neutrophils. Importantly, we did not find substantial green fluorescence signal in *Plcg2*$^{-/-}$ sections after anti-C7 treatment (**Figure 28**).

Next, we wanted to analyze infiltration of neutrophils and other immune cell populations that were previously implicated in the pathogenesis of autoantibody-induced skin blistering in a more quantitative manner.

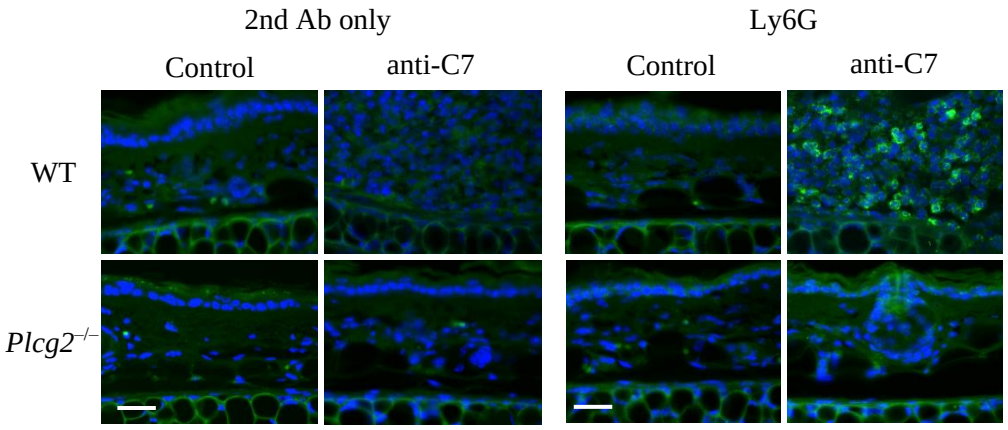

Figure 28. Accumulation of neutrophils in the skin

Skin blistering was induced in wild-type and *Plcg2*$^{-/-}$ chimeras. Ear sections were made on Day 8 and stained with anti-Ly6G antibodies, followed by Alexa Fluor 488-labeled secondary antibody or secondary antibody alone. Green fluorescence indicate Ly6G^{+} cells. DAPI shows nuclei in blue. Images are representative of 3-6 mice per group from 2 independent experiments. Scale bar: 30 μm. [3]

Therefore, we used flow cytometry on digested ear tissue samples obtained from Day 8. The total number of leukocytes increased dramatically after anti-C7 treatment in the ears of wild-type mice compared to the control **(Figure 29A**).

Neutrophils (**Figure 29B**) consisted almost the half of the measured leukocytes, but the absolute numbers of eosinophils (**Figure 29C**) and monocytes/macrophages (**Figure 29D**) also increased significantly upon disease induction in wild-type samples.

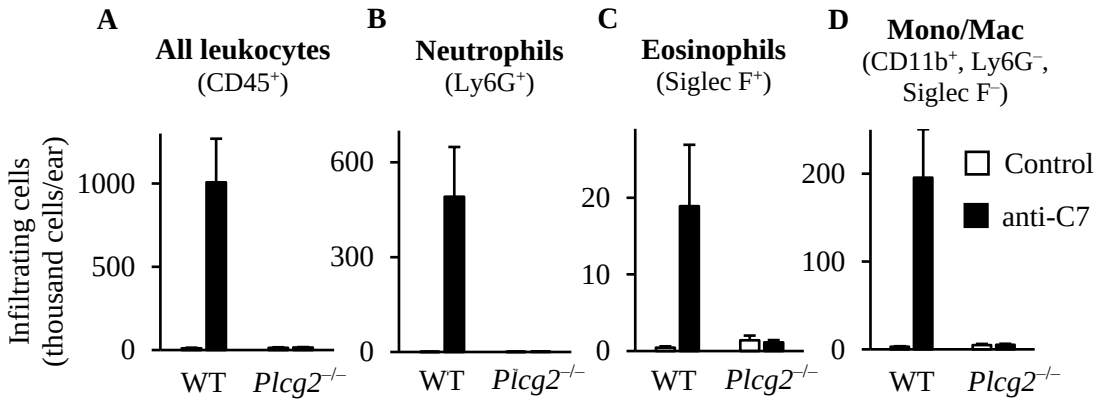

Figure 29. Quantitative analysis of infiltrating leukocyte subsets in the ears

Skin blistering was induced in wild-type and Plcg2$^{-/-}$ chimeras. Absolute number of CD45^{+} leukocytes (**A**, $p = 7.7\times10^{-6}$), Ly6G^{+} neutrophils (**B**, $p = 9.1\times10^{-4}$), Siglec F^{+} eosinophils (**C**, $p = 0.0097$) and CD11b^{+}, Ly6G^{-}, Siglec F^{-} monocytes/macrophages (**D**, $p = 0.0013$) was measured by flow cytometry in digested ear samples from Day 8. Data show mean and SEM from 3-10 mice per group from 2-4 independent experiments. [3]

Importantly, the infiltration of leukocytes and of all investigated myeloid subsets was completely abrogated in *Plcg2*$^{-/-}$ chimeras (**Figure 29**).

Taken together, PLCγ2 deficiency completely prevented the accumulation of several myeloid-cell populations at the site of antibody deposition in our model.

4.3.5. Intrinsic migratory capacity of leukocytes

Next, we wanted to test the mechanism of the infiltration defect upon PLCγ2 deficiency found above. Since PLCγ2 is involved in integrin-mediated signaling processes, our first hypothesis was that PLCγ2 might affect the intrinsic migratory capacity of leukocytes, therefore they might fail to migrate out from the circulation to the dermis. To measure the intrinsic migratory capacity of leukocytes in vivo, we generated mixed bone-marrow chimeras. We obtained bone marrow cells from wild-type and *Plcg2*$^{-/-}$ donor mice, mixed them together in a certain ratio and transplanted into lethally irradiated wild-type recipient mice. After transplantation, we could detect the genotype of the circulating donor-derived cells based on their different allelic expression of the common leukocyte marker CD45. Wild-type leukocytes expressed CD45.1 and *Plcg2*$^{-/-}$ cells expressed CD45.2.

Figure 30 shows the CD45.2 expression profile of circulating neutrophils obtained from a representative WT:*Plcg2*$^{-/-}$ mixed bone-marrow chimera. In this histogram, the left peak represents the CD45.2^{-} (CD45.1^{+}) WT neutrophils, while right peak illustrates CD45.2^{+} *Plcg2*$^{-/-}$ cells. This approach also provided us the benefit that we could investigate wild-type and *Plcg2*$^{-/-}$ leukocytes within the same animal.

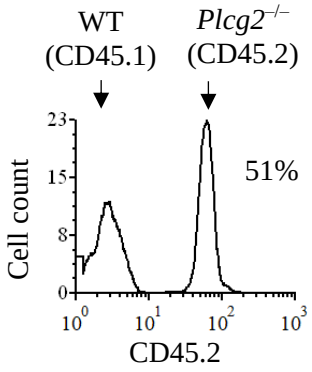

Figure 30. CD45.2 expression profile of circulating neutrophils in a WT:*Plcg2*$^{-/-}$ mixed bone-marrow chimera

Percentage indicates the ratio of CD45.2^{+} cells within the neutrophil gate. Representative histogram from 9 mice from 3 independent experiments [3].

We then subjected such WT:*Plcg2*$^{-/-}$ mixed bone-marrow chimeras to our anti-C7-induced skin blistering model. We used WT:WT mixed chimeras as control, where CD45.1^{+} wild-type (BoyJ) and CD45.2^{+} wild-type (C57BL/6) hematopoietic cells were transplanted into BoyJ recipients. All mice developed signs of skin blistering (data not shown), presumably due to the presence of wild-type cells. As we investigated wild-type and *Plcg2*$^{-/-}$ hematopoietic cells within the same animal, cells of both genotypes were subjected to the same chemotactic stimuli developing in the skin. This provided the opportunity to investigate the cell-autonomous migratory capacity of leukocytes without any other major influencing factors. To do so, we determined the ratio of CD45.1^{+} and CD45.2^{+} cells in the blood and in the digested ear samples on Day 8.

Figure 31A-B show representative histograms of neutrophils. As expected, percentage of CD45.2-expressing wild-type neutrophils in WT:WT chimeras was comparable both in the blood and the ear tissues (**Figure 31A**). This suggests that CD45.2^{+} cells can freely migrate out from the circulation to the ear tissue. The observed decrease in the ear sample compared to the blood was modest and possibly due to some technical issues.

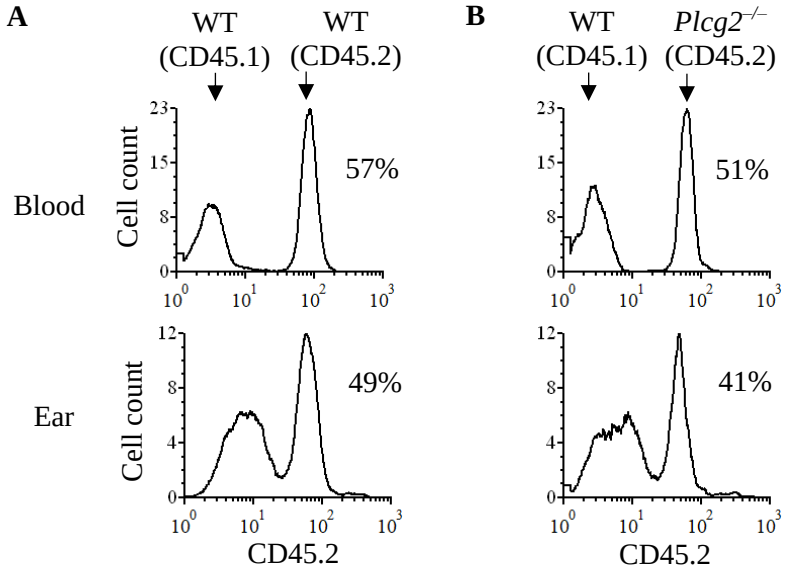

Figure 31. Migration of wild-type and *Plcg2*$^{-/-}$ neutrophils from the blood to the ears in mixed bone-marrow chimeras.

Skin blistering was induced in WT:WT and WT:*Plcg2*$^{-/-}$ mixed bone-marrow chimeras. CD45.2 expression of neutrophils in WT:WT (**A**) and WT:*Plcg2*$^{-/-}$ mixed chimeras (**B**) were analyzed in blood and digested ear samples from Day 8. Percentages indicate ratio of CD45.2^{+} cells within the neutrophil gate. Histograms are representative of 3 independent experiments using 7-8 mice per group. [3]

Surprisingly, CD45.2-expressing PLCγ2-deficient neutrophils definitely appeared in the skin of WT:*Plcg2*$^{-/-}$ mixed bone-marrow chimeras at a similar ratio as in the blood (**Figure 31B**). This indicates that *Plcg2*$^{-/-}$ neutrophils are capable of migrating from the circulation to the dermis similarly to wild-type cells. This finding was sharply in contrast to our previous result when all hematopoietic cells were *Plcg2*$^{-/-}$ (**Figure 29**).

We also plotted the average percentage of different CD45.2^{+} leukocyte subtypes in the ears and blood of anti-C7-treated mixed bone-marrow chimeras, as shown schematically in **Figure 32**. If the percentage of CD45.2^{+} cells in the blood and in the ear sample was similar, the dots were aligning the 45° line on the graph colored in yellow. This would suggest that such CD45.2^{+} myeloid cells can freely migrate into the inflamed tissue from the blood, in other words, their endogenous migrating capability is maintained.

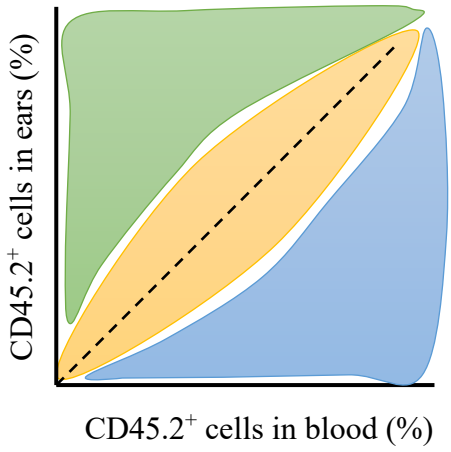

Figure 32. Evaluation of intrinsic migratory capacity of leukocytes in vivo. For detailed explanation, see main text.

This approach is suitable to detect higher or lower intrinsic migrating capacity of a given cell population according to the following way: Theoretically, if the percentage of CD45.2^{+} cells in the blood was higher than its ratio in ears, the dots would appear in the blue colored areas on the graph in **Figure 32**. This would implicate that CD45.2^{+} cells have trouble migrating towards the inflamed tissue compared to CD45.1^{+} wild-type cells within the same animal. Since they probably received the same chemotactic stimulus from the tissue, this scenario would implicate impaired intrinsic migratory capacity of CD45.2^{+} cells compared to CD45.1^{+} WT cells. If the ratio of CD45.2^{+} cells was reduced in the blood compared to the ears (appearing in the green area in **Figure 32**), this would imply that CD45.2^{+} cells could migrate more readily than CD45.1^{+} wild-type cells under the same circumstances, suggesting increased migratory capacity.

Going back to our initial experiment, we measured the percentage of different CD45.2^{+} leukocyte subtypes in the ears and blood of anti-C7-treated mixed bone marrow chimeras

on Day 8. **Figure 33A** shows the ratio of CD45.2$^+$ neutrophils in all conducted experiments. Each dot represents the average ratio of CD45.2$^+$ neutrophils in one individual mouse. Black dots of WT:WT chimeras distributed along the 45° oblique line, indicating equal ratios of CD45.2$^+$ cells in the blood and the inflamed ear tissue. Similarly, red dots of WT:*Plcg2*$^{-/-}$ chimeras aligned nicely along the 45° dashed line. This indicates that intrinsic migratory capacity is not different between WT and *Plcg2*$^{-/-}$ neutrophils.

Eosinophils and monocytes/macrophages of such mixed chimeras were also tested in a similar manner. We found no differences in the ratios of wild-type and *Plcg2*$^{-/-}$ eosinophils or monocytes/macrophages in the blood and ear tissues, since black and red dots also tended to distribute along the 45° line (**Figure 33B-C**).

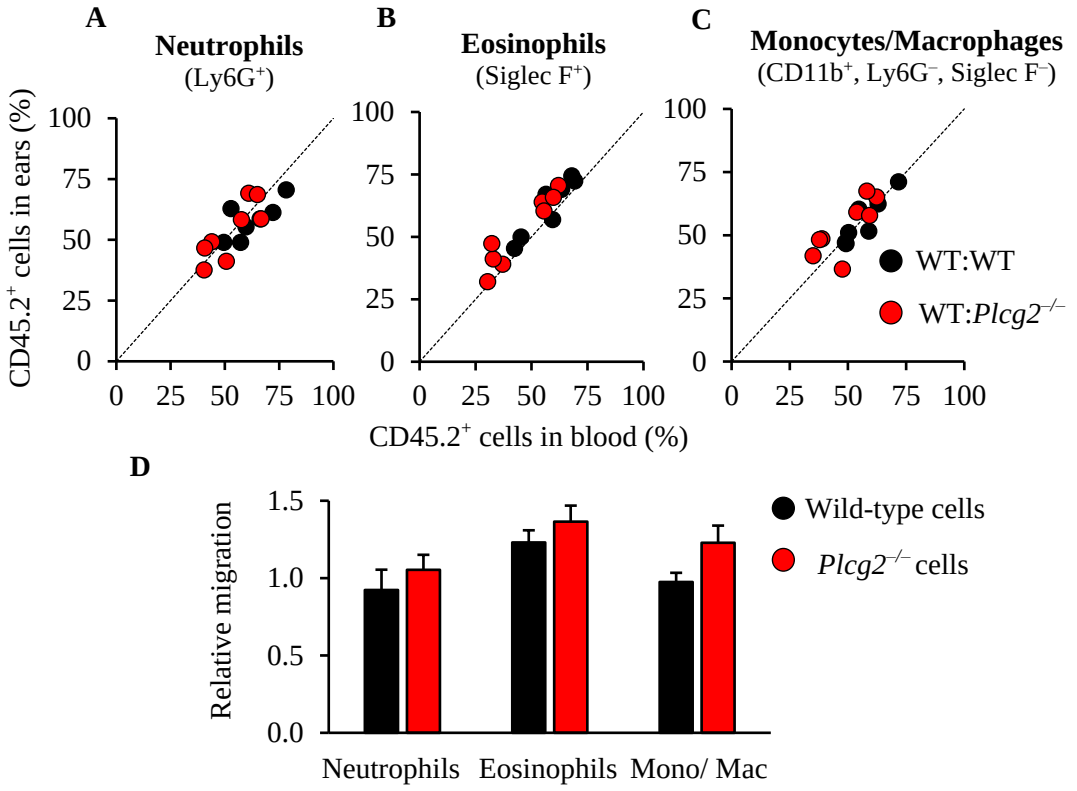

Figure 33. Intrinsic migratory capacity of wild-type and *Plcg2*$^{-/-}$ leukocytes in mixed bone-marrow chimeras

Skin blistering was induced in WT:WT and WT:*Plcg2*$^{-/-}$ mixed bone-marrow chimeras. CD45.2 expression of different myeloid subsets were analyzed in blood and digested ear samples from Day 8. Ratio of CD45.2$^+$ neutrophils (**A**), eosinophils (**B**) and monocytes/macrophages (**C**) in blood and in ears, with each dot representing one mixed chimera. Panel **D** shows calculated relative migration of CD45.2$^+$ wild-type or *Plcg2*$^{-/-}$ cells compared to CD45.2$^-$ wild-type cells within the same animal. Data shows mean and SEM from 7-8 mixed chimeras per group from 3 independent experiments. Panel **D** is from [3].

We also quantified the relative migration of CD45.2$^+$ wild-type and *Plcg2*$^{-/-}$ cells compared to CD45.1$^+$ wild-type cells within the same animal. The precise formula is presented in Section 3.10. We found that intrinsic migratory capacity of both wild-type and *Plcg2*$^{-/-}$ neutrophils, eosinophils and monocytes/macrophages were around 1 in all cases (**Figure 33D**). This means that such CD45.2$^+$ cells can migrate similar to CD45.1$^+$ wild-type cells, so their intrinsic migratory capacity is maintained, so PLCγ2 deficiency did not impair the intrinsic migratory capacity of the investigated myeloid cells (if the relative migration would be below 1, it would implicate impaired endogenous migrating capacity of CD45.2$^+$ cells).

Taken together, the observed protection against skin blistering and defective leukocyte accumulation in total *Plcg2*$^{-/-}$ chimeras is presumably not due to a cell-autonomus migration defect of myeloid cells.

4.3.6. Development of the proinflammatory microenvironment in vivo

An alternative explanation for the defective leukocyte accumulation in the absence of PLCγ2 might be related to the development of the inflammatory microenvironment upon anti-C7 deposition in the skin. To test this, we measured the concentration of different proinflammatory mediators in the ear tissue of wild-type and *Plcg2*$^{-/-}$ chimeras on Day 8 after the induction of skin blistering.

First, a wide variety of different chemokines and cytokines was measured by a semiquantitative approach, using a commercial cytokine array kit. Following anti-C7 treatment, a robust signal emerged in a large number of mediators in those membranes that were incubated with supernatant of digested ear samples of wild-type animals (**Figure 34A**).

The array map is shown in **Figure 34B**. On the other hand, there was no difference between samples obtained from anti-C7-treated and control-treated *Plcg2*$^{-/-}$ chimeras. We also quantified these data by densitometry and confirmed that the concentration of several chemokines and cytokines increased in the ears of wild-type but not *Plcg2*$^{-/-}$ mice after anti-C7 treatment. **Figure 34C** shows mediators with at least 5-fold increase in anti-C7-treated wild-type samples compared to wild-type control samples. It included complement component C5/C5a; well-known proinflammatory cytokines like IL-1β and TNF-α; and neutrophil chemoattractants like keratinocyte-derived chemokine (KC),

monocyte chemoattractant protein 1 and 5 (MCP-1, MCP-5), and macrophage-inflammatory protein 1α and 2 (MIP-1α and MIP-2). **Table 4** shows normalized data of all measured mediators.

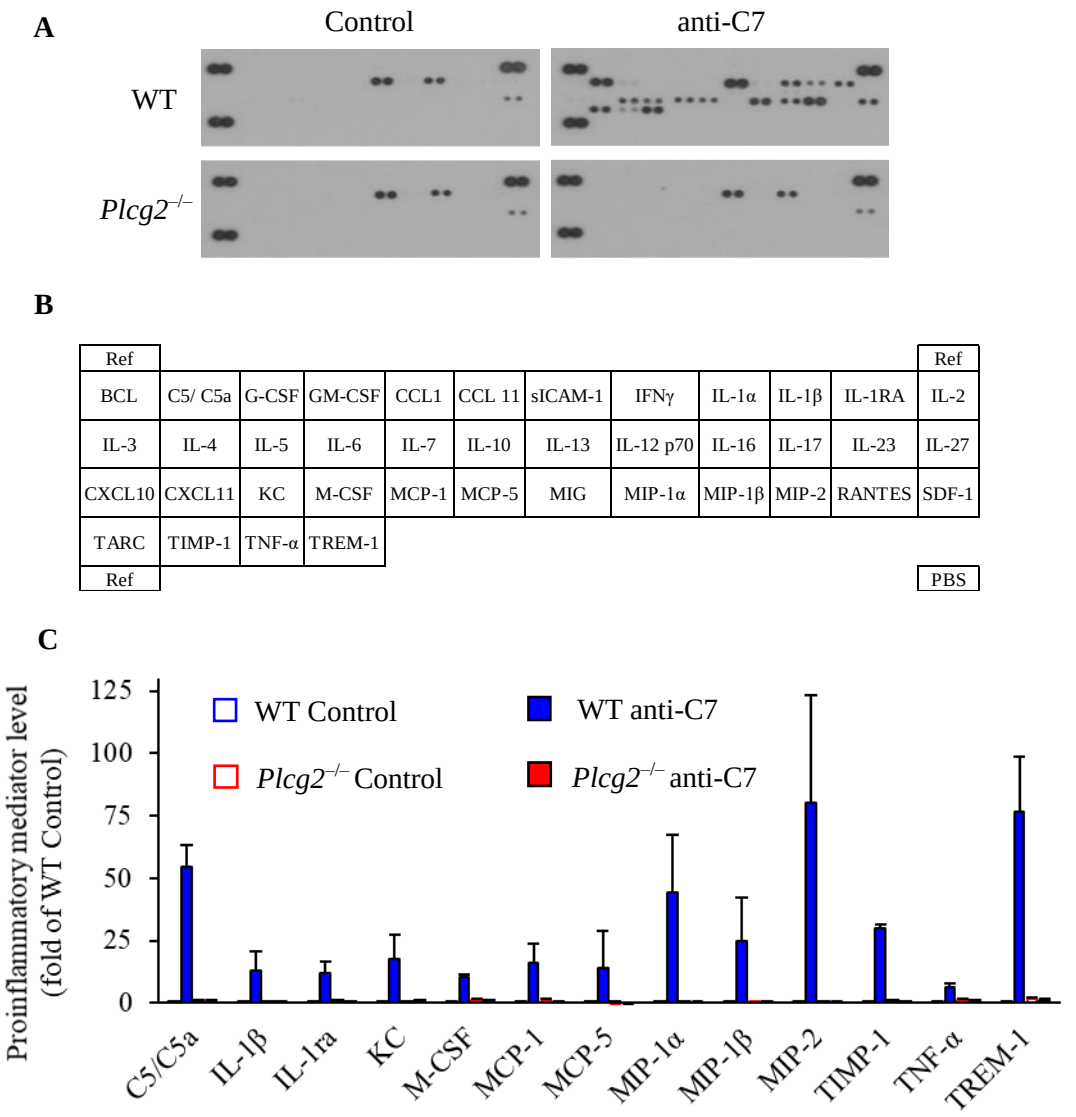

Figure 34. Presence of different chemokines and cytokines in ears during autoantibody-induced skin blistering.

Cell-free supernatants of digested ear samples of wild-type and *Plcg2*$^{-/-}$ bone-marrow chimeras were analyzed by cytokine array kit. Samples were obtained 8 days after disease induction. (**A**) Representative images of developed cytokine array membranes. (**B**) Layout of analytes. (**C**) Integrated densitometry values of mediators with at least 5-fold change normalized to wild-type control samples. Data show mean + SEM from 2 independent experiments. [3]

Table 4. Integrated densities of all mediators measured in the ears.
Cell-free supernatants of digested ear samples of wild-type and *Plcg2*$^{-/-}$ bone-marrow chimeras was analyzed by cytokine array kit. Samples were obtained 8 days after disease induction. Table show mean and SEM from 2 independent experiments. Mediators highlighted in bold have at least 5-fold change in anti-C7-treated WT samples compared to control-treated WT samples (also shown in **Figure 34C**).

	Integrated density									
	Wild type					*Plcg2* $^{-/-}$				
	Control		Anti-C7			Control		Anti-C7		
	Mean	SEM	Mean	SEM	Fold change	Mean	SEM	Mean	SEM	Fold change
BLC	5,7	0,5	6,9	1,8	1,2	4,9	1,4	2,6	0,5	0,5
C5/C5a	**3,0**	**0,6**	**150,0**	**9,6**	**50,6**	**3,3**	**0,3**	**2,7**	**0,2**	**0,8**
CCL1	2,4	0,2	3,1	3,1	1,3	2,3	0,4	1,8	0,2	0,8
CCL11	2,6	0,5	2,8	0,2	1,1	2,0	0,2	1,6	0,2	0,8
CXCL11	4,0	0,8	6,7	0,6	1,7	3,3	0,3	2,6	0,3	0,8
G-CSF	3,4	0,6	9,0	0,3	2,7	2,0	0,1	2,1	0,2	1,1
GM-CSF	2,3	19,4	3,3	5,3	1,4	2,5	12,3	1,4	25,9	0,6
IFNγ	32,1	16,9	9,2	2,7	0,3	4,5	0,1	3,2	1,3	0,7
IL-10	1,8	20,2	2,8	15,2	1,6	1,8	0,5	1,3	1,6	0,7
IL-12p70	2,9	0,7	4,8	14,7	1,7	1,9	0,4	1,1	0,3	0,6
IL-13	5,5	0,4	12,2	25,3	2,2	3,9	0,6	4,3	1,6	1,1
IL-16	4,8	0,4	7,3	1,2	1,5	3,4	0,2	1,8	2,5	0,5
IL-17	3,0	0,2	7,3	0,4	2,5	1,8	0,3	1,1	0,5	0,6
IL-1RA	**4,5**	**0,2**	**58,0**	**0,9**	**13,0**	**4,2**	**0,0**	**2,7**	**0,3**	**0,6**
IL-1α	86,8	0,1	86,9	0,1	1,0	106,5	0,4	104,8	0,3	1,0
IL-1β	**3,2**	**0,7**	**32,3**	**0,2**	**10,0**	**2,3**	**0,1**	**1,5**	**0,0**	**0,6**
IL-2	3,4	0,8	3,4	0,8	1,0	3,9	0,4	5,4	0,2	1,4
IL-23	2,2	0,6	2,7	0,2	1,2	2,0	0,1	0,6	0,3	0,3
IL-27	1,1	1,1	2,5	3,4	2,2	2,3	0,2	1,2	1,5	0,5
IL-3	3,3	0,5	3,7	1,1	1,1	2,5	0,6	1,9	0,3	0,8
IL-4	2,8	0,1	7,9	3,5	2,8	2,7	0,7	2,2	0,5	0,8
IL-5	2,7	0,7	4,3	2,9	1,6	1,8	0,4	2,2	0,2	1,3
IL-6	1,9	0,8	4,2	1,3	2,2	2,2	0,7	1,8	0,4	0,8
IL-7	1,7	0,2	3,7	1,1	2,2	2,3	0,4	1,6	0,5	0,7
IP-10	3,3	0,2	5,9	2,3	1,8	2,6	0,3	2,2	0,5	0,9
KC	**2,2**	**0,7**	**45,9**	**1,9**	**20,8**	**1,9**	**0,1**	**2,1**	**0,3**	**1,1**
MCP-1	**2,0**	**0,4**	**42,6**	**28,9**	**21,2**	**2,0**	**0,5**	**1,1**	**0,1**	**0,5**
MCP-5	**0,3**	**1,5**	**38,3**	**19,9**	**116,3**	**1,6**	**0,0**	**1,3**	**0,1**	**0,8**
M-CSF	**4,0**	**0,7**	**45,0**	**25,8**	**11,3**	**3,5**	**0,3**	**3,2**	**0,1**	**0,9**
MIG	2,7	1,1	4,5	21,1	1,7	2,3	0,1	1,9	0,1	0,8
MIP-1α	**2,6**	**0,4**	**89,1**	**1,3**	**33,7**	**1,6**	**0,2**	**0,4**	**0,3**	**0,3**
MIP-1β	**2,8**	**0,6**	**47,6**	**33,6**	**17,0**	**1,0**	**0,5**	**0,9**	**0,2**	**0,9**
MIP-2	**2,3**	**0,6**	**113,2**	**32,1**	**48,8**	**1,4**	**0,3**	**0,6**	**0,2**	**0,5**
RANTES	1,8	0,9	2,7	30,9	1,5	1,1	0,5	0,5	0,1	0,4
SDF-1	33,9	0,8	56,4	1,3	1,7	33,6	0,8	31,3	0,4	0,9
sICAM-1	124,3	9,7	166,9	29,2	1,3	126,2	10,5	116,6	11,4	0,9
TARC	4,7	0,3	5,3	1,2	1,1	4,8	0,8	4,9	0,9	1,0
TIMP-1	**3,2**	**0,4**	**96,1**	**18,3**	**30,4**	**3,5**	**0,2**	**2,3**	**0,2**	**0,7**
TNFα	**2,8**	**1,0**	**20,7**	**10,9**	**7,5**	**2,9**	**0,1**	**2,5**	**0,3**	**0,9**
TREM-1	**1,1**	**0,8**	**120,9**	**14,8**	**112,4**	**2,1**	**0,2**	**1,7**	**0,2**	**0,8**

In addition, we quantified more precisely the accumulation of some mediators using ELISA technique. More specifically, we measured a well-known proinflammatory cytokine IL- 1β, the neutrophil chemokine MIP-2 (which is thought to be the murine analog of human IL-8) and the lipid mediator LTB_4. All of these proinflammatory mediators have been implicated in the pathogenesis of pemphigoid diseases [191, 193, 194, 235]. Accordingly, we found high concentrations of all three substances in the ears of anti-C7-treated wild-type mice compared to the control. In sharp contrast, accumulation of these mediators were completely abrogated in *Plcg2*$^{-/-}$ chimeras (**Figure 35**).

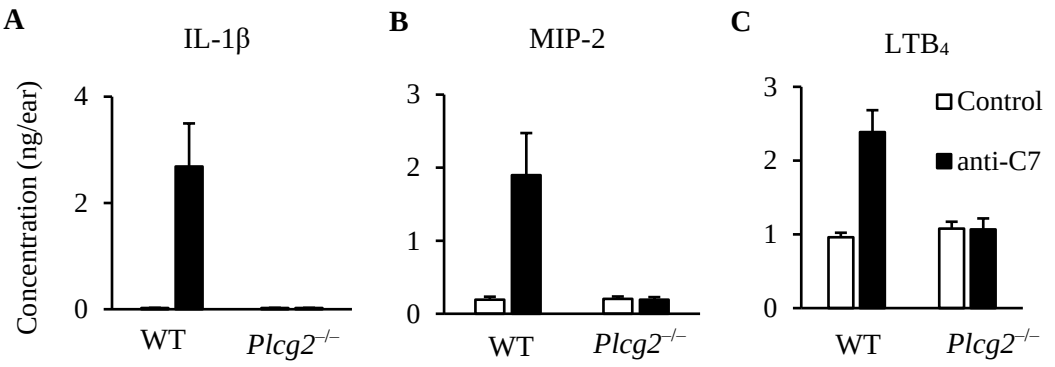

Figure 35. Concentration of proinflammatory mediators in the ears.
Cell-free supernatant of digested ears from wild-type and *Plcg2*$^{-/-}$ chimeras were analyzed by ELISA on Day 8. Concentration of IL-1β (**A**), MIP-2 (**B**) and LTB_4 (**C**) were measured. Data show mean and SEM from 5-6 chimeras per group from 3 independent experiments. p = 0.044 (**A**), 0.0046 (**B**), 1.1×10^{-4} (**C**). [3]

Besides of cytokines, chemokines and lipid mediators, reactive oxygen species (ROS) have also been described to participate in autoantibody-induced skin pathology [189]. Therefore, we also tested in vivo ROS production in mice 8 days after disease induction. Namely, we measured MPO activity with a chemiluminescence-based in vivo imaging method. As shown in **Figure 36A**, anti-C7 treatment led to a significant increase in MPO activity in wild-type mice. Increased MPO activity was visible mostly in regions of ears, shoulder region and paws. This was in sharp contrast to *Plcg2*$^{-/-}$ chimeras, whose MPO activity was consequently below the detection limit. We also quantified MPO activity in defined regions of the ears. This further confirmed that production of reactive oxygen species was increased in wild-type but completely abrogated in *Plcg2*$^{-/-}$ mice during skin blistering in our model (**Figure 36B**).

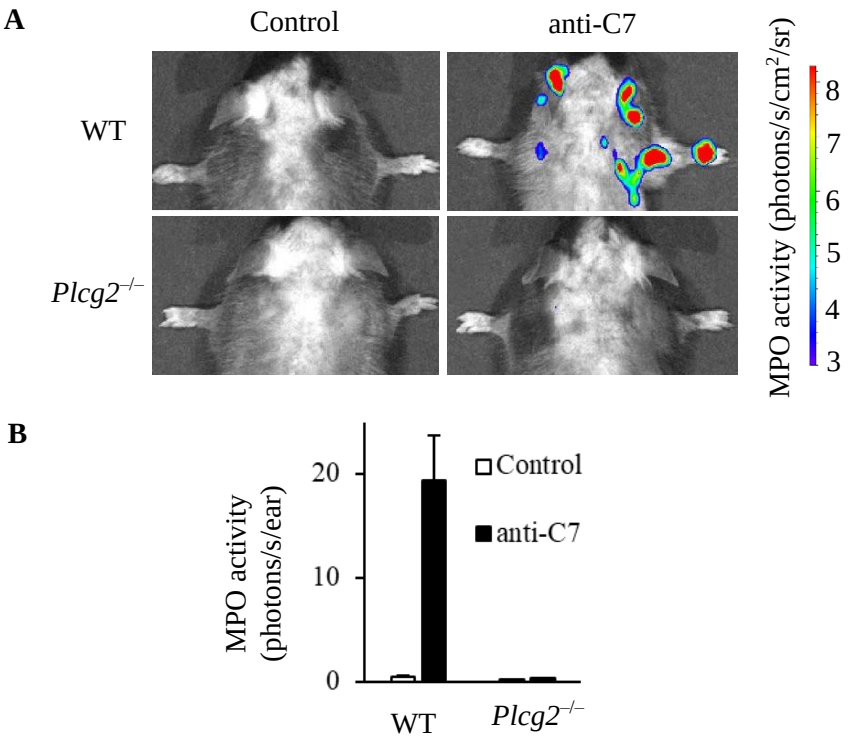

Figure 36. In vivo production of reactive oxygen species during anti-C7-induced skin blistering.

Wild-type and *Plcg2*$^{-/-}$ chimeras were subjected to skin blistering. Myeloperoxidase activity was measured on Day 8 with chemiluminescence-based in vivo imaging. Images (**A**) are representative of and quantitative data (**B**) show mean and SEM from 7-8 chimeras per group from 2 independent experiments. $p = 3.3\times10^{-7}$ [3]

To summarize this part of our experiments, we found that PLCγ2 is essential for the development of autoantibody-induced skin disease, including erosion formation, dermal-epidermal separation and leukocyte infiltration. PLCγ2 probably influences the development of the proinflammatory microenvironment without affecting cell-autonomous migration of myeloid cells. However, we do not know which cell type, or cell types are crucial to express PLCγ2 in order to drive anti-C7-induced skin blistering and inflammation.

4.4. IN VITRO FUNCTIONAL RESPONSES OF PLCγ2-DEFICIENT NEUTROPHILS

Neutrophils were massively accumulated in the skin of wild-type mice after anti-C7 administration (**Figure 28** and **Figure 29B**) and have been implicated by several studies to mediate autoimmune skin blistering in this model ([189, 205], discussed in section 1.5.3.5). Moreover, it has been shown that wild-type neutrophils can respond to immune complex stimuli by superoxide production and spreading [9], and may contribute to the development of the proinflammatory microenvironment, as well [236, 237]. However, there have been no studies so far investigating the role of PLCγ2 specifically in neutrophils regarding the pathogenesis of autoimmune skin blistering. Therefore, we continued our work to analyze in vitro functional responses of PLCγ2-deficient neutrophils relevant to skin blistering.

During these studies, we worked with primary bone marrow-derived neutrophils isolated from wild-type or *Plcg2*$^{-/-}$ mice. We subjected neutrophils to chemotactic or immune-complex stimuli relevant in autoimmune skin blistering. After that, we measured parameters that we also analyzed in our in vivo mouse model, namely their migratory capacity and ability to produce proinflammatory mediators (Sections 4.3.4 and 4.3.6).

4.4.1. Migration capacity

We tested neutrophil migration in a Transwell migration assay. Freshly isolated bone marrow-derived neutrophils were placed into Transwell inserts with 5 μm pores. Inserts were then placed into wells containing media supplemented with or without chemoattractants that were found in increased concentration in the ears of mice during skin blistering (namely MIP-2 and LTB_4). After 1 hour incubation at 37 °C, the amount of transmigrated neutrophils was determined in the lower compartment by an acid phosphatase assay. Although there was some spontaneous migration in the control-treated wells lacking any chemoattractants (**Figure 37A**), migration of wild-type neutrophils towards media containing 100 ng/ml MIP-2 was increased. *Plcg2*$^{-/-}$ neutrophils were also able to migrate towards MIP-2 to a similar extent as wild-type cells. When we used 50 ng/ml LTB_4 as chemoattractant, we found again no significant difference in the migrating ability between wild-type and *Plcg2*$^{-/-}$ neutrophils (**Figure 37B**).

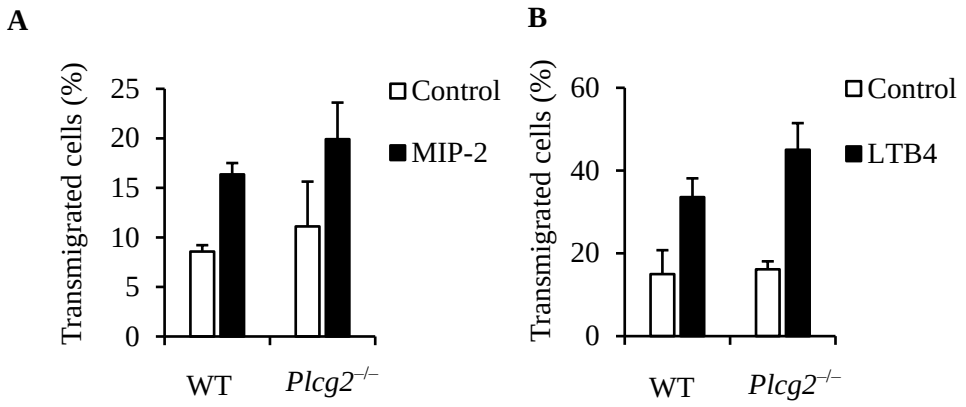

Figure 37. In vitro migration of *Plcg2*$^{-/-}$ neutrophils.
Bone marrow-derived wild-type and *Plcg2*$^{-/-}$ neutrophils were tested in a Transwell migration assay towards MIP-2 (**A**) or LTB_4 (**B**). Bar graphs show mean and SEM from 3 independent experiments. p = 0.87 (**A**) and 0.33 (**B**). [3]

4.4.2. Immune complex-induced release of proinflammatory mediators

We also investigated the production of different proinflammatory mediators by neutrophils, after we plated them onto immobilized C7/anti-C7 immune-complex surfaces. In these experiments, antigen (C7) treatment alone served as control. Thus, we mimicked immune-complex formation along the basement membrane occurring in vivo upon anti-C7 treatment.

When plated onto C7/anti-C7 surfaces, wild-type neutrophils produced significant amounts of MIP-2 after 4 hours of incubation. In sharp contrast, concentration of MIP-2 in supernatants of *Plcg2*$^{-/-}$ neutrophils remained beyond the detection limit (**Figure 38A**). In case of LTB_4, wild-type cells again released a massive amount of the lipid mediator upon immune complex stimuli. However, *Plcg2*$^{-/-}$ neutrophils completely failed to release LTB_4 under such conditions (**Figure 38B**).

According to our in vitro studies, *Plcg2*$^{-/-}$ neutrophils had preserved migration ability towards chemoattractants which were present also in the inflamed tissue in our EBA model. However, *Plcg2*$^{-/-}$ neutrophils were unable to produce those important inflammatory mediators upon C7/anti-C7 immune-complex stimulation. These findings are in line with our previous results that the intrinsic migration of neutrophils was not disturbed by PLCγ2 deficiency but the proinflammatory milieu failed to develop in *Plcg2*$^{-/-}$ mice after anti-C7 treatment (**Figure 33** and **Figure 35**).

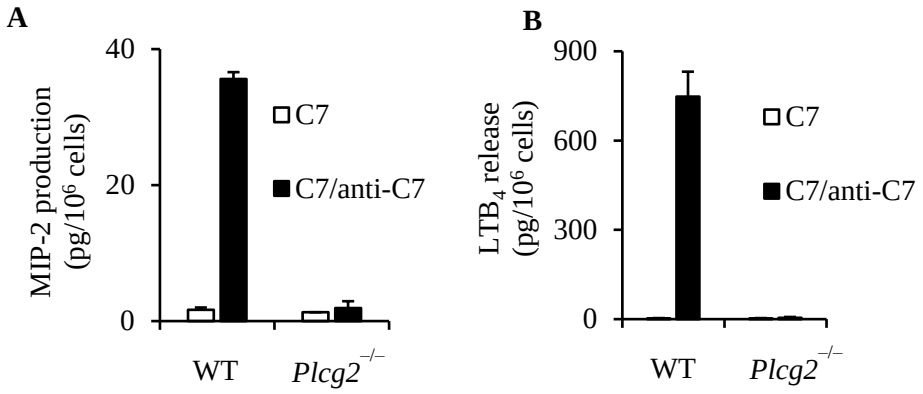

Figure 38. C7/anti-C7 immune complex-induced release of proinflammatory mediators from neutrophils.

Wild-type and *Plcg2*$^{-/-}$ neutrophils isolated from bone marrow were plated onto C7/ anti-C7 immune complex coated surfaces or antigen (C7)-coated surfaces as control. The release of MIP-2 (**A**) and LTB_4 (**B**) was measured from the supernatant by ELISA after 4 and 1 hour of incubation, respectively. Data show mean and SEM from 3 independent experiments. $p = 0.027$ (**A**) and 1.3×10^{-7} (**B**). [3]

4.5. LINEAGE-SPECIFIC ANALYSIS OF PLCγ2 IN ANTI-C7-INDUCED SKIN BLISTERING

The above in vitro results support the possibility that PLCγ2 expressed in neutrophils may be important during the effector phase of autoimmune skin blistering. Therefore, we next aimed to analyze the role of PLCγ2 specifically in neutrophils in our EBA model.

We chose again a transgenic approach to investigate which cell types are important to express PLCγ2 for the development of skin blistering. Namely, we utilized the Cre-loxP system to generate lineage-specific conditional knockout animals. Here, mice expressing Cre recombinase driven by a lineage-specific promoter are crossed with animals containing *Plcg2* alleles flanked by loxP sequences. Thus, Cre recombinase expressed only in certain cell lineages in the offspring, where the promoter is active, cleaves the DNA specifically at loxP sequences flanking *Plcg2*. This results in the deletion of the *Plcg2* allele. Based on our previous results, we aimed to test the effect of neutrophil-specific deletion of PLCγ2 in our model. Therefore, we used Cre recombinase driven by the neutrophil-specific promoter myeloid-related protein 8 (MRP8) to generate neutrophil-specific PLCγ2-deficient mice (**Figure 39**). The genotype of these mice were MRP8-Cre^{+} *Plcg2*$^{flox/flox}$ referred to as *Plcg2*$^{\Delta PMN}$ mice. The following results have not been published yet.

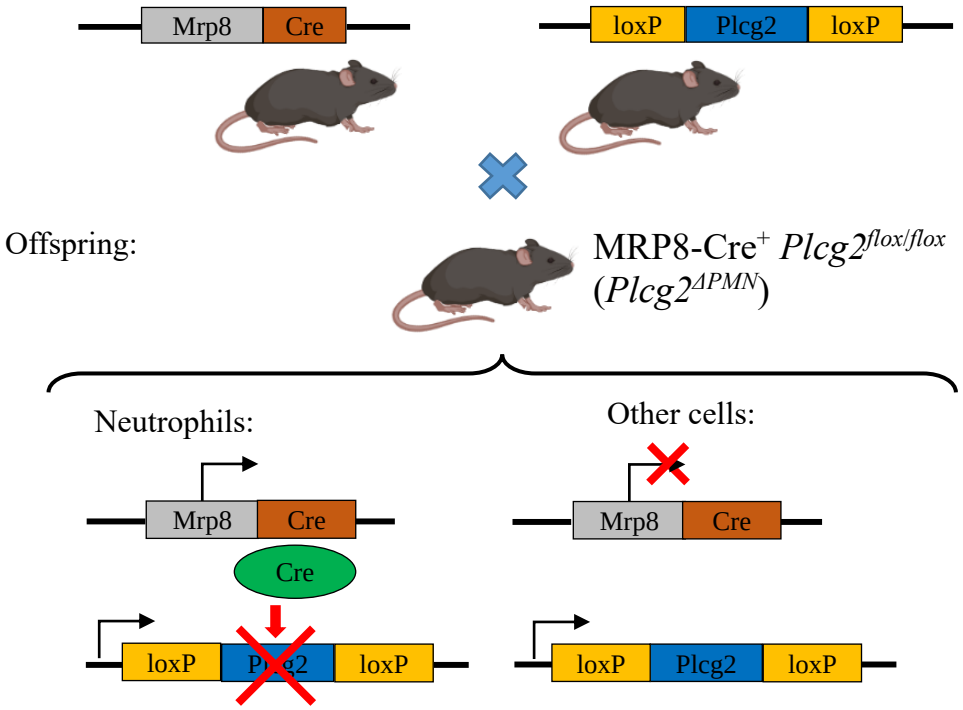

Figure 39. Generation of mice with neutrophil-specific *Plcg2* deletion.
Mice expressing Cre recombinase driven by the neutrophil-specific promoter (MRP8) were crossed with animals containing Plcg2 flanked by loxP sequences. In the offspring (*Plcg2*$^{\Delta PMN}$ mice), we assume that Cre recombinase is only expressed in neutrophils, leading to neutrophil-specific deletion of *Plcg2*.

4.5.1. Efficacy and specificity of *Plcg2* deletion in *Plcg2*$^{\Delta PMN}$ mice

First, we wanted to check the efficacy of Cre-mediated *Plcg2* deletion in neutrophils in *Plcg2*$^{\Delta PMN}$ mice. In addition, we also wanted to test whether there was any unspecific *Plcg2* deletion in other cell types. Therefore, we checked PLCγ2-expression in various circulating leukocyte populations using flow cytometry. These experiments were performed as a part of a study where we investigated *Plcg2*$^{\Delta PMN}$ mice in an autoantibody-mediated arthritis model [2]. In this paper, Krisztina Futosi and Orsolya Kása did the majority of the experiments. My contribution was to test the efficacy and specificity of *Plcg2* deletion in *Plcg2*$^{\Delta PMN}$ mice with flow cytometry.

As shown in **Figure 40A**, we compared PLCγ2 fluorescence intensity in circulating neutrophils, eosinophils, monocytes, B cells and T cells obtained from wild-type, *Plcg2*$^{-/-}$ and *Plcg2*$^{\Delta PMN}$ mice.

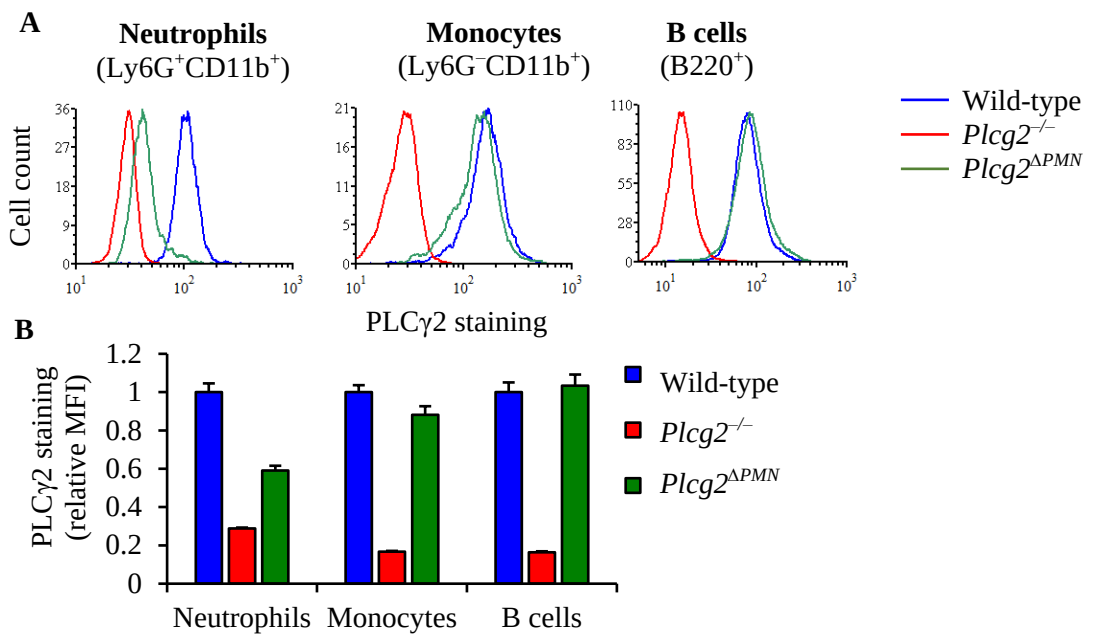

Figure 40. PLCγ2 expression in *Plcg2*$^{\Delta PMN}$ neutrophils, monocytes and B cells.
Expression of PLCγ2 was measured in circulating neutrophils, monocytes and B cells of wild-type, *Plcg2*$^{-/-}$ and *Plcg2*$^{\Delta PMN}$ mice, using flow cytometry. Histograms (**A**) are representative of and relative mean fluorescence intensity (MFI) data (**B**) show 3-7 mice per group from 3 independent experiments. WT vs. *Plcg2*$^{\Delta PMN}$ $p = 1.9\times10^{-6}$ (Neutrophils), p = 0.065 (Monocytes) and p = 0.68 (B cells) [2].

PLCγ2 staining of *Plcg2*$^{-/-}$ neutrophils, eosinophils, monocytes and B cells was strongly reduced compared to wild-type cells, similar to results seen in **Figure 15**. Regarding *Plcg2*$^{\Delta PMN}$ neutrophils, we observed a strong reduction in PLCγ2 staining compared to wild-type neutrophils. Nevertheless, the histogram of *Plcg2*$^{\Delta PMN}$ neutrophils remained shifted to the right compared to the histogram of *Plcg2*$^{-/-}$ neutrophils (**Figure 40A**). Circulating monocytes and B cells of *Plcg2*$^{\Delta PMN}$ mice, however, showed practically completely overlapping PLCγ2 staining with wild-type cells. We also quantified these results by measuring the mean fluorescent intensity (MFI) and normalizing it to the PLCγ2 staining of wild-type cells (**Figure 40B**). Relative MFI of PLCγ2 was efficiently reduced in neutrophils of *Plcg2*$^{\Delta PMN}$ mice compared to wild-type cells. Importantly, there was no substantial difference in other leukocyte subsets.

We also measured the expression of PLCγ2 in circulating eosinophils and T cells, in order to exclude Cre-mediated *Plcg2* deletion in these subsets (**Figure 41**). Eosinophils of *Plcg2*$^{\Delta PMN}$ mice showed completely overlapping PLCγ2 staining with wild-type cells. Circulating T cells, however, showed negative PLCγ2 staining in all genotypes.

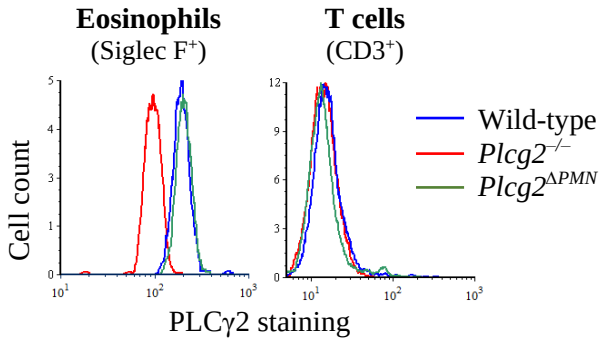

Figure 41. PLCγ2 expression in eosinophils and T cells.
Expression of PLCγ2 was measured in circulating eosinophils and T cells of wild-type, *Plcg2*$^{-/-}$ and *Plcg2*$^{\Delta PMN}$ mice using flow cytometry. Histograms are representative of 4-10 mice per group from 3 independent experiments.

Overall, these results showed that neutrophil-specific deletion in *Plcg2*$^{\Delta PMN}$ mice is efficient and specific, although not entirely complete.

4.5.2. Anti-C7-induced skin blistering in *Plcg2*$^{\Delta PMN}$ mice

Next, we subjected *Plcg2*$^{\Delta PMN}$ mice to our anti-C7-induced skin blistering model. Wild-type and *Plcg2*$^{-/-}$ animals served as controls. As shown in **Figure 42A**, wild-type mice consistently developed severe skin lesions upon anti-C7 treatment until Day 14. In contrast, *Plcg2*$^{\Delta PMN}$ animals did not show any signs of skin blistering, nor inflammation, similar to control-treated littermates.

To quantify the clinical phenotype over time, we measured the extent of affected skin area, severity of the lesions, the extent of erosions, as well as the ear thickness every second day. All these evaluated parameters increased over time in wild-type mice, while *Plcg2*$^{-/-}$ animals (used as a control in these experiments) remained fully protected, as expected (**Figure 42B-E**). *Plcg2*$^{\Delta PMN}$ animals were also almost completely protected regarding extent and severity of the disease. Only few of them developed some milder and smaller lesions in later phases of the experiment (**Figure 42B-C**). Neutrophil-specific PLCγ2-deficient mice were practically free from erosions, as well, similar to total PLCγ2-deficient mice. Ear thickening was also radically impaired in anti-C7-treated *Plcg2*$^{\Delta PMN}$ animals compared to the wild-type mice, showing only a slight increase over time.

Regarding microscopic signs of anti-C7-induced pathology, wild-type mice developed a massive epidermal hyperplasia and dermal infiltration on Day 8, suggesting severe

inflammation. In addition, we also observed the detachment of the epidermal layer at several parts of the ears, as a sign of blister formation (**Figure 43**). Compared to that, H&E stained ear sections of anti-C7-treated *Plcg2*$^{\Delta PMN}$ mice showed an overall normal microscopic phenotype. The epidermal layer was thin and only a few cells were found in the dermis (**Figure 43A**). Neutrophil-specific deletion of PLCγ2 also resulted in the massive reduction of anti-C7-induced D-E separation at the microscopic level, in contrast to wild-type mice (**Figure 43B**).

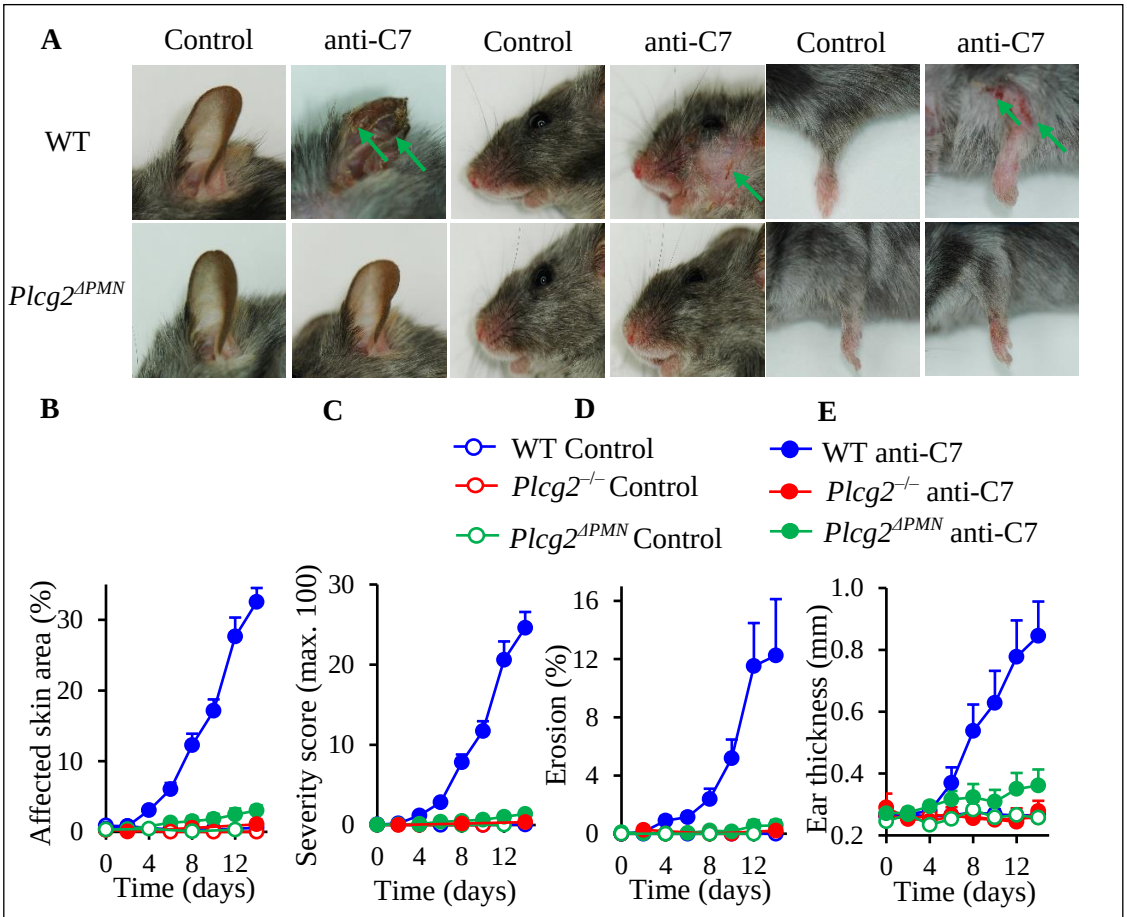

Figure 42. Impact of neutrophil-specific *Plcg2*-deletion on autoantibody-induced skin blistering.

Skin blistering was induced by repeated injections of anti-C7 on Days 0, 2, 4, 6 and 8 in wild-type, *Plcg2*$^{-/-}$ and *Plcg2*$^{\Delta PMN}$ mice. (**A**) Macroscopic phenotype on Day 14 of wild-type and *Plcg2*$^{\Delta PMN}$ mice. Green arrows indicate erosions. (**B**) Extent of affected skin area, $p = 3.40\times10^{-10}$. (**C**) Severity score, $p = 3.55\times10^{-13}$. (**D**) Percentage of erosions in particular, $p = 4.59\times10^{-3}$. (**E**) Evaluation of ear thickness, $p = 3.16\times10^{-3}$. Representative photographs and quantitative data show mean and SEM from, 5-8 mice per group from 4-5 individual experiments except *Plcg2*$^{-/-}$ mice where data of 2-3 mice from 2 experiments are shown due to the limited availability of *Plcg2*$^{-/-}$ animals.

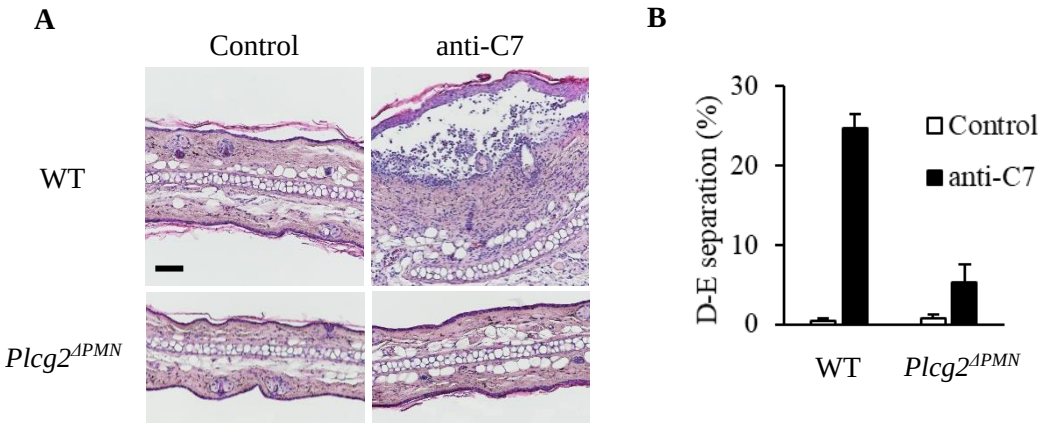

Figure 43. Microscopic phenotype of *Plcg2*$^{\Delta PMN}$ mice during anti-C7-induced skin blistering.

Ear samples were obtained from wild-type and *Plcg2*$^{\Delta PMN}$ mice 8 days after the first anti-C7 injection. (**A**) Paraffin-embedded sections stained with H&E. Scale bar: 100μm. (**B**) Percentage of dermal-epidermal (D-E) separation, $p = 4.40\times10^{-5}$. Histological images are representative of and quantitative data show mean and SEM from, 3-5 mice per group from 3 individual experiments.

4.5.3. Infiltration of leukocytes in *Plcg2*$^{\Delta PMN}$ mice

In order to quantitatively check the amount of accumulating leukocytes after anti-C7 treatment, ear tissue was removed on Day 8, digested, and analyzed by flow cytometry. As expected, the ears of wild-type mice became massively infiltrated with leukocytes. Among leukocytes, neutrophils were the dominant subset, but eosinophils and monocytes/macrophages were also recruited upon anti-C7 treatment (**Figure 44**). In case of total PLCγ2 deficiency, accumulation of all analyzed leukocyte subsets were absent in the ear samples. When PLCγ2 was deleted only from neutrophils, infiltration of all leukocytes was impaired, however not significantly reduced compared to the wild-type genotype (**Figure 44A**). The same partial reduction was observed regarding the infiltration of neutrophils and eosinophils, as well (**Figure 44B-C**). Infiltration of the monocytes/macrophage population in ears of *Plcg2*$^{\Delta PMN}$ mice was more similar to wild-type littermates (**Figure 44D**).

Taken together, our results showed that neutrophil-specific deletion of PLCγ2 resulted in an almost completely protected clinical phenotype of anti-C7-induced skin blistering, very similar to the phenotype of *Plcg2*$^{-/-}$ mice. Microscopic signs were also severely impaired if PLCγ2 was absent only in neutrophils. However, quantitative analysis of

infiltrating leukocytes showed only a tendency of reduced accumulation of myeloid subsets at the site of antibody deposition. This might be partly explained by the incomplete Cre-mediated deletion of PLCγ2 in neutrophils, as observed in **Figure 40**.

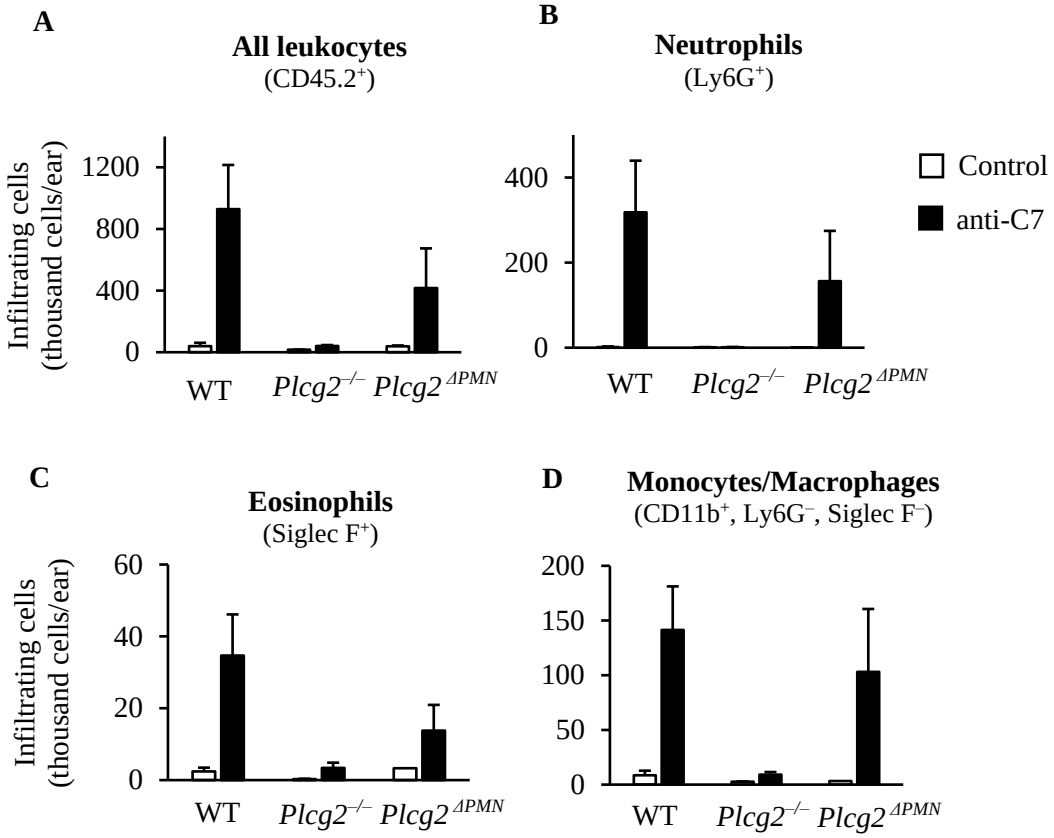

Figure 44. Quantitative analysis of infiltrating leukocyte subsets in the ears
Skin blistering was induced in wild-type and Plcg2$^{-/-}$ chimeras. Absolute number of CD45^{+} leukocytes (**A**, p = 0,289), Ly6G^{+} neutrophils (**B**, p = 0.487), Siglec F^{+} eosinophils (**C**, p = 0.213) and CD11b^{+}, Ly6G^{-}, Siglec F^{-} monocytes/macrophages (**D**, p = 0.691) was measured by flow cytometry in digested ear samples from Day 8. Data show mean and SEM from 2-6 mice per group from 3 independent experiments.

4.6. HUMAN EX VIVO DERMAL-EPIDERMAL SEPARATION

To extend our previous findings to human settings, we started to translate our studies and investigate human pathology. Namely, we set up a human neutrophil-mediated ex vivo dermal-epidermal separation assay. We investigated the effect of PLC inhibition in this model by a pharmacologic approach. In this assay, we preincubated cryosections of

healthy human skin with anti-C7 antibodies (same as the ones used to induce disease in mice) or normal IgG. After that, we treated the samples with freshly isolated human neutrophils obtained from healthy volunteers in the presence of the PLC inhibitor U73122 compound or vehicle.

After 1.5 hours of incubation, neutrophils accumulated at the DEJ and anti-C7-treated skin samples in the presence of vehicle alone. Moreover, separation could be observed between the dermal and epidermal layers of the skin, presumably at the site of anti-C7 deposition (**Figure 45A**). Importantly, we found no neutrophil accumulation or dermal-epidermal (D-E) separation in skin samples upon normal IgG treatment.

When we applied the PLC inhibitor U73122 during the coincubation of neutrophils and skin sections, we detected less neutrophils along the DEJ and rarely found any D-E separation in H&E stained skin sections (**Figure 45A**). Quantification of D-E separation along the entire length of the D-E interface revealed that anti-C7 preincubation led to a severe separation of the skin along the DEJ in vehicle-treated skin samples. 10 μM U73122 treatment was able to strongly reduce neutrophil-mediated D-E separation after anti-C7 treatment (**Figure 45B**).

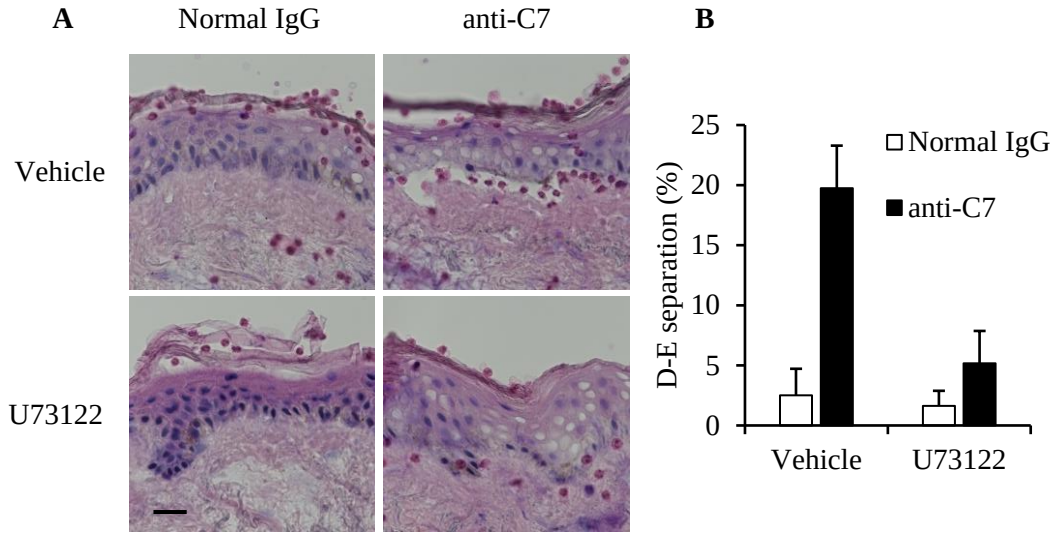

Figure 45. Effect of PLC inhibition on human ex vivo dermal-epidermal separation.

Freshly isolated human neutrophils were coincubated with cryosections of human skin pretreated with anti-C7 or normal IgG as control in the presence of a PLC inhibitor U73122 (10 μM) or vehicle alone (0.05% DMF). Ex vivo dermal-epidermal separation was evaluated after H&E staining. Microscopic images are representative of and quantitative data show mean and SEM from 4 independent experiments. $p = 0.020$. Scale bar: 50 μm [3].

Taken together, our results suggest that PLC enzymes have an important role in autoantibody-induced blister formation in human pemphigoid diseases, as well.

4.7. EFFECT OF TOFACITINIB TREATMENT ON ANTI-C7-INDUCED SKIN BLISTERING

Several lines of evidence showed, that immunoreceptor signaling is essential in the development of anti-C7-induced skin blistering. In this pathway, our workgroup have already described the indispensable role of Src-family kinases and the Syk tyrosine kinase. In this thesis, we presented and characterized the crucial role of PLCγ2 in anti-C7-induced skin blistering. Since therapeutic approaches are rather limited and quite unspecific in these disease entities, these molecules might serve as potential therapeutic targets, as well.

This line of thinking about possible therapeutic targets led us to another tyrosine kinase signaling pathway, namely Jak-Stat signaling. Janus kinases are involved in downstream signaling of various cytokine receptors. Nowadays, this pathway has been standing in the center of attention in clinical research [12]. Specific small molecule inhibitors are available blocking Jaks. They showed efficacy in immune-mediated disorders like rheumatoid arthritis, ulcerative colitis and atopic dermatitis, leading to the approval of tofacitinib for instance to treat severe forms of these diseases [12]. Jak inhibitors have been investigated in multiple other inflammatory skin diseases, as well, where the pathogenic role of several cytokines has been long established (see in detail in Section 1.4 and Szilveszter et al [1]).

In case of autoimmune blistering skin diseases, we found (in line with literature data discussed in section 1.5.3) that there is a complex proinflammatory milieu developing after anti-C7 treatment in the skin (**Figure 34**). This proinflammatory milieu involved the presence of multiple cytokines that signal through the Jak-Stat pathway, like G-CSF, IL-4 and IL-6. However, there are no clinical studies, nor preclinical data published so far about the effect of Jak inhibition on autoimmune blistering skin diseases. Based on these, we aimed to test Jak inhibition in the anti-C7-induced mouse model of EBA.

We treated wild-type mice twice a day (bid) with 0.4 mg or 1 mg tofacitinib by oral gavage. The drug was dissolved in 0.05% methylcellulose-containing tap water. Control mice received vehicle alone. Treatments started one day before the first anti-C7 injection

(on Day –1) and were carried on throughout the whole 14 days of the experiment.

Macroscopic phenotype of a representative vehicle-treated and a 0.4 mg tofacitinib-treated mouse from Day 14 is shown in **Figure 46A**.

Anti-C7 treatment resulted in a massive and severe disease phenotype in vehicle-treated wild-type mice, similar to what we usually observed. We found regions covered with alopecia, induration, erosion and crust formation in extended, confluent areas of the skin, usually most prominently in the ears and cheeks. In the 0.4 mg tofacitinib-treated group, the majority of mice developed milder skin symptoms following anti-C7 injections. Usually alopecia, scaling and induration occurred, but these were found in smaller areas of the skin. In some cases, we did not find areas containing erosions or crusts on Day 14 at all.

We also quantified different aspects of visible signs of skin blistering every second day for 14 days. As expected, the affected skin area and the severity of lesions increased robustly over time in case of vehicle- and anti-C7-treated mice (**Figure 46B** and **C**). Tofacitinib-treatment was able to diminish, in a dose-dependent manner, both the extent and the severity of the lesions induced by anti-C7 injections (**Figure 46B** and **C**). The affected skin area was significantly reduced in the 1 mg tofacitinib-treated group. Both 0.4 mg and 1 mg tofacitinib bid was able to significantly reduce the severity score compared to the vehicle-treated mice. We found that the extent of erosions also tended to be reduced in a dose dependent manner upon tofacitinib treatment. This suggests that blister formation itself might be influenced by tofacitinib. However, those differences did not become significant, probably due to the small number of animals used so far (**Figure 46D**). Lastly, there was no significant difference between the average ear thickening of anti-C7-treated groups over time. This means that tofacitinib treatment could not reduce ear thickening, in particular (**Figure 46E**).

Taken together, in this small study we found that tofacitinib treatment was able to reduce the extent and severity of skin lesions in a mouse model of anti-C7-induced skin blistering in a dose dependent manner. It further supports the need for additional studies to delineate the role of Jaks in the pathogenesis of autoimmune skin blistering.

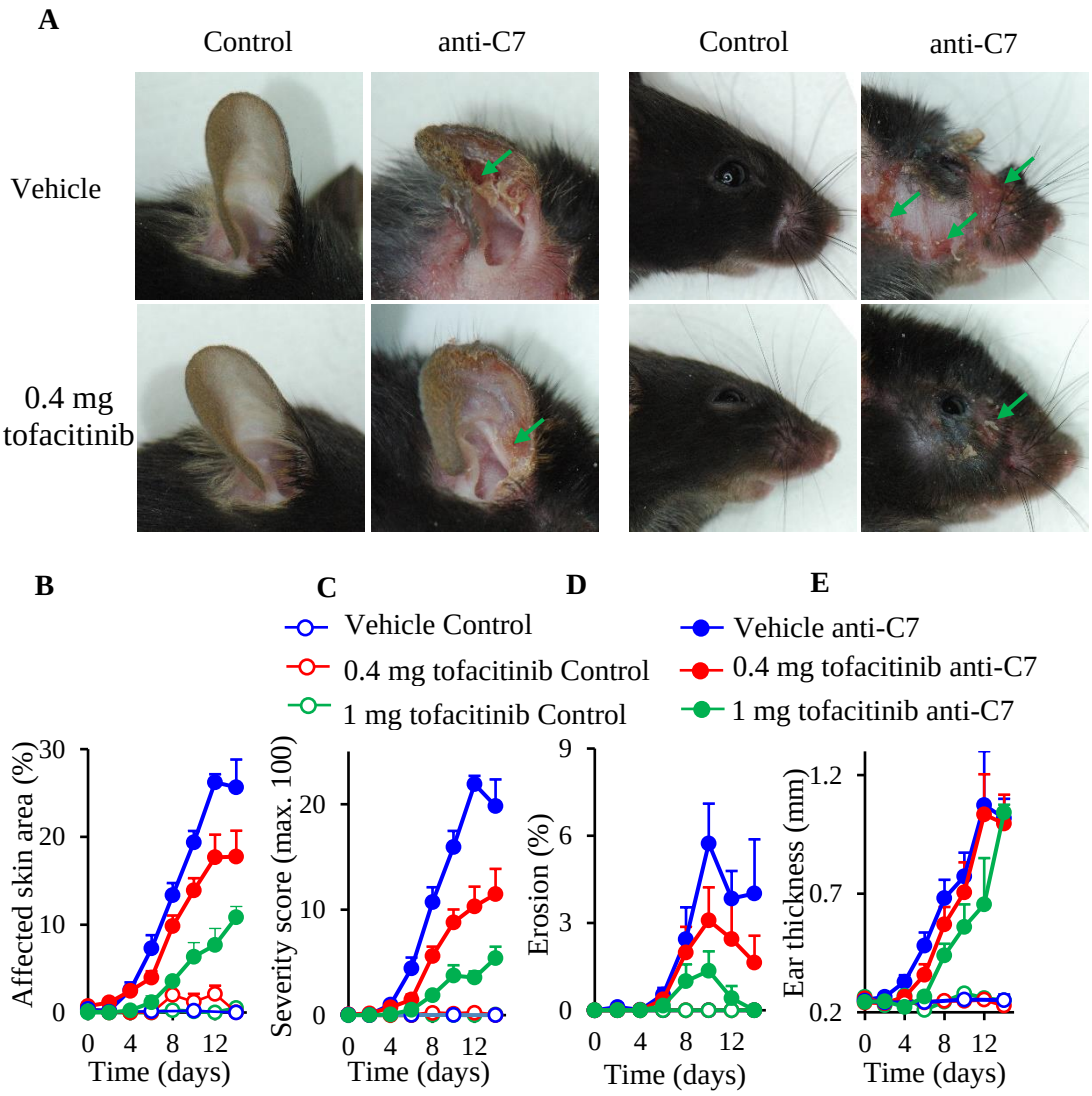

Figure 46. Effect of tofacitinib on autoantibody-induced skin blistering.

Skin blistering was induced by repeated injections of anti-C7 on Days 0, 2, 4, 6 and 8 in wild-type mice treated with vehicle, 0.4 mg or 1 mg tofacitinib bid throughout the experiment. (**A**) Macroscopic phenotype on Day 14. Green arrows indicate erosions. (**B**) Extent of affected skin area, p = 0.059 (vehicle vs. 0.4 mg tofacitinib), p = 0.011 (vehicle vs. 1 mg tofacitinib). (**C**) Severity score, p = 0.022 (vehicle vs. 0.4 mg tofacitinib), p = 0.0078 (vehicle vs. 1 mg tofacitinib). (**D**) Percentage of erosions in particular, p = 0.153 (vehicle vs. 0.4 mg tofacitinib), p = 0.304 (vehicle vs. 1 mg tofacitinib). (**E**) Evaluation of ear thickness, p = 0.182 (vehicle vs. 0.4 mg tofacitinib), p = 0.168 (vehicle vs. 1 mg tofacitinib). Representative photographs and quantitative data show mean and SEM from, 3-4 mice per group from 2-3 individual experiments. Only one mouse was measured in the 1 mg tofacitinib-treated control group due to the limited availability of the drug.

5. DISCUSSION

Our experiments showed that PLCγ2 is critical for the development of anti-C7-induced skin blistering in mice, mimicking the inflammatory form of epidermolysis bullosa acquisita. Our results also indicate that neutrophil-specific expression of PLCγ2 is essential to induce macroscopic and microscopic signs of skin blistering in mice. Moreover, according to our human ex vivo studies, inhibition of PLC could be a plausible target in the therapy of anti-C7-induced pathology, as well.

5.1. CHARACTERIZATION OF *Plcg2*$^{-/-}$ MICE

The survival defect detected in *Plcg2*$^{-/-}$ embryos and newborn pups (**Figure 13**) were in line with the previous findings of Wang and colleagues [84] and with the *Plcg2*^{al} mouse strain containing a spontaneous loss-of-function mutation in *Plcg2* [95]. Both studies showed a subcutaneous hemorrhaging-like phenotype in embryos and surviving adults. This phenotype developed possibly due to the aberrant separation of blood and lymphatic vessels, creating blood-filled lymphatics in the skin and intestines [95]. Similarly, adult *Plcg2*$^{-/-}$ mice usually develop subcutaneous edema in our facility. Edema is mostly visible in the paws and could indicate defective lymphatic drainage. Importantly, however, no literature data supports increased susceptibility to infections, nor could we detect such defects. Animals remained healthy even if they were kept in conventional facility for longer time periods.

We demonstrated that PLCγ2 is expressed in most major circulating leukocyte subsets, namely neutrophils, eosinophils and monocytes, as well as in B cells, but not in T cells (**Figure 15**). These findings are in line with the literature, as T cells have been reported to predominantly express PLCγ1 [79]. We did not investigate it, but other leukocyte subsets like NK cells and dendritic cells have been shown to express functionally relevant PLCγ2 [88, 91].

Circulating leukocyte numbers were similar in the wild-type and *Plcg2*$^{-/-}$ mice (**Figure 16**). Importantly, side-by-side analysis of the number and expression profile of multiple different circulating leukocyte subsets (especially eosinophils) have not been performed so far in this regard.

Wang and colleagues showed that most hematopoietic lineages are not affected in the

bone marrow of *Plcg2*$^{-/-}$ mice, except a defect in B cell maturation [84]. There are studies implicating a role of PLCγ2 in hematopoietic stem cell and myeloid progenitor differentiation [238, 239]. However, these studies use pharmacologic approach, namely the same PLC inhibitor U73122 that we used in our human experiments. U73122 has, unfortunately, rather limited selectivity, blocking several other phospholipase isoforms apart from PLCγ2.

The role of PLCγ2 in B cell differentiation and function has been well studied. PLCγ2 has a critical role in BCR signaling, therefore it contributes to B cell maturation and function [84, 85, 240, 241]. Moreover, it has been proposed that PLCγ2 deficiency may render pre-B cells stuck in that early maturation state, making them susceptible to malignant transformation [242]. However, increased susceptibility to malignant transformation was not described upon PLCγ2 deficiency.

We did not analyze B cell maturation markers and function thoroughly; but focused on analyzing different activation and maturation markers of myeloid lineages. Namely, we analyzed neutrophils, eosinophils and monocytes, since they are considered to be key players during the effector phase of pemphigoid diseases. We did not find any significant maturation defect based on the expression of Ly6G in neutrophils, Siglec-F in eosinophils or Ly6C polarization marker on monocytes (**Figure 17**). Expression of several FcγRs and integrin chains were also the same in wild-type and *Plcg2*$^{-/-}$ cells in all subsets (**Figure 17**). This is also in line with the previous studies of our group where the expression of a few cell surface molecules was measured in circulating *Plcg2*$^{-/-}$ neutrophils [81].

Taken together, our results indicate that there is no substantial defect in the differentiation or survival of *Plcg2*$^{-/-}$ leukocytes that would affect circulating cell numbers. Moreover, such maturation- or cell surface expression-profile cannot explain the observed protected phenotype in anti-C7-induced skin blistering in *Plcg2*$^{-/-}$ mice.

5.2. ANTI-C7-INDUCED SKIN BLISTERING IN *Plcg2*$^{-/-}$ MICE

In order to investigate the role of PLCγ2 in the development of the effector phase of skin blistering, we utilized a widely used antibody-induced mouse model resembling the inflammatory form of epidermolysis bullosa acquisita.

After repeated subcutaneous injections of anti-C7, we evaluated and scored the extent of affected skin area and the severity of lesions every second day for 2 weeks. This kind

of evaluation of skin lesions has similarities compared to the clinical scoring systems used in BP. Such commonly used, reliable scoring approaches are ABSIS (Autoimmune Bullous Skin Disorder Intensity Score) and BPDAI (BP Disease Area Index) [221]. ABSIS takes into account the extent of affected body surface area weighted by the quality of lesions [243]. This is similar to the severity score that we used to evaluate skin blistering in mice. In addition, we also quantified the extent of erosions in particular, as a direct measure of blister formation without the masking effect of further secondary elementary lesions. Mice usually did not show intact blisters, probably due to their intense scratching behavior. Ear thickness was also assessed as a more objective measure of disease development.

Importantly, intact *Plcg2*$^{-/-}$ mice remained completely protected against the repeated subcutaneous injections of anti-C7 antibodies, regarding all signs and measures of macroscopic skin blistering (**Figure 22**). *Plcg2*$^{-/-}$ bone-marrow chimeras (where PLCγ2 was absent only in cells of hematopoietic origin) showed the same protection against all clinical signs of skin blistering. This suggests that PLCγ2 expressed in the hematopoietic compartment is crucial for the development of anti-C7-induced skin pathology.

Our laboratory has shown that other components of the FcγR pathway are essential during the effector phase of antibody-induced skin blistering, namely Src-family kinases [8] and the Syk tyrosine kinase [9]. We and others showed that PLCγ2 is also an important element of FcγR signaling in vitro, and it supposedly lays downstream from those mentioned tyrosine kinases [80, 81]. Our current results indicate that PLCγ2 has an equally important role like Src-family kinases and Syk during the effector phase of skin blistering in mice. Our workgroup has also investigated the adaptor molecule CARD9 and identified that FcγR signaling diverges into a CARD9-dependent and a CARD9-independent arm [28]. In line with that, CARD9-deficient mice were only partially protected from anti-C7-induced skin blistering [28]. Based on the full protection we observed in *Plcg2*$^{-/-}$ mice, it seems that PLCγ2 lays upstream from CARD9. Our current hypothesis about the FcγR signaling pathway is also demonstrated in **Figure 47**.

PLCγ2 deficiency protected mice not only from macroscopic, but from the microscopic signs of skin blistering, such as dermal infiltration of cells, and, importantly, dermal-epidermal separation (**Figure 25**).Histological evaluation and other mechanistic studies were usually performed on the ear samples of mice from Day 8. We chose this

time point, because this was the peak of acute inflammatory and erosive lesions, which we consider specific for this disease. Later on lesions tend to develop into more severe, aspecific secondary lesions, like crust formation, histologically appearing mainly as necrotic cell debris.

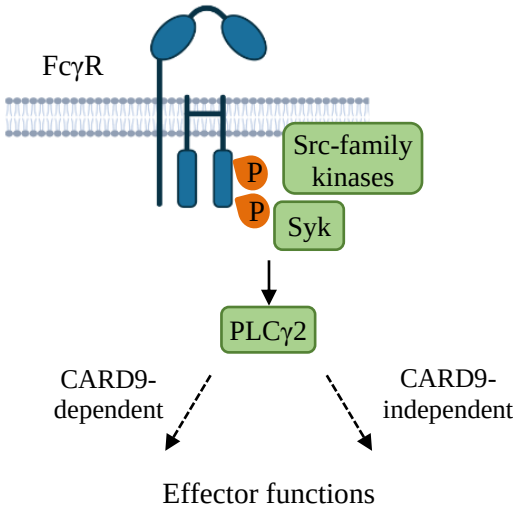

Figure 47. Proposed mechanism of FcγR signaling in myeloid cells during anti-C7-induced skin blistering.

PLCγ2 was not required to maintain circulating anti-C7 levels, nor did it affect the deposition of injected anti-C7 antibodies at the dermal-epidermal junction (**Figure 26** and **Figure 27**). This is in line with our concept, that PLCγ2 is important after autoantibody deposition and regulates the function of the effector cells.

Indeed, the presence of PLCγ2 was indispensable for the dermal recruitment of all tested leukocyte populations induced by anti-C7 treatment. This was shown by the immunofluorescent analysis of neutrophils in ear sections (**Figure 28**), as well as quantified by flow cytometry after digestion of extracellular components of the ears (**Figure 29**). To investigate the mechanism behind this leukocyte accumulation defect, we set up two hypotheses. First, accumulation could be abrogated due to a defect in the migratory capacity of the cells themselves. It would be plausible since extravasation is an integrin-dependent process utilizing immunoreceptor-like signaling [56-59]. Second, defective development of a proinflammatory milieu could also result in the abrogation of leukocyte recruitment.

When wild-type cells were also present in the same animals (using mixed bone-marrow chimeras), even *Plcg2*$^{-/-}$ neutrophils, eosinophils and monocytes/macrophages were able to migrate into the inflamed tissue upon anti-C7 treatment **(Figure 33)**. According to these results, the accumulation defect in total *Plcg2*$^{-/-}$ mice was likely not due to an impaired endogenous migratory capability of those leukocytes. In line with that, *Plcg2*$^{-/-}$ neutrophils migrated also normally in an in vitro transwell migration assay (**Figure 37**). We used either MIP-2 or LTB_4 as chemotactic stimulus in these assays, since

these were also implicated to drive neutrophil recruitment during autoimmune skin blistering in vivo [194].

Instead of affecting the intrinsic ability of migration, PLCγ2 was shown to be essential for the generation of a proinflammatory milieu at the site of anti-C7 deposition (**Figure 34** and **Figure 35**). Based on the cytokine array we used, there was a substantial increase in the concentration of multiple proinflammatory mediators in the affected ear tissues of wild-type mice, with C5/C5a and MIP-2 being among the mediators showing the highest increase in concentrations (**Figure 34**). These findings are in line with the important role of C5a during the recruitment and activation of neutrophils in the EBA model [185] and with the elevated concentration of IL-8 (the human analog for MIP-2) in the blister fluid of BP patients [191]. Moreover, there were also several other cytokines, that were found increased in the ear tissue in our model and also in the blister fluid of patients with BP. Such cytokines included IL-4, IL-6 (described in [220] and we detected more than 2-fold increase in our model according to **Table 4**) and IL-1β and M-CSF (described in [204, 235] and we measured more than 10-fold increase in our model according to **Table 4**).

Importantly, in ear samples of anti-C7-treated *Plcg2*$^{-/-}$ chimeras, none of the analyzed mediators showed any difference from control (**Figure 34** and **Table 4**). Moreover, we observed the same finding during the quantitative analysis of IL-1β, MIP-2 and the lipid mediator LTB_4 using ELISA, since their accumulation in the ears was also completely abrogated in the absence of PLCγ2 (**Figure 35**).

The above mentioned results were in line with the previous observations of our laboratory regarding other components of the immunoreceptor signaling. It was shown that β_2 integrin signaling diverges to a Src-family- and Syk-dependent adherent activation; and a tyrosine kinase independent migration of neutrophils in vitro [57]. In addition, Syk was also dispensable for cell-autonomous migration of neutrophils, but crucial for the development of the proinflammatory milieu in the EBA model [9]. Similar in vivo results has been published about Src-family kinases but in an autoantibody-induced arthritis model [8]. Taken together, it seems that PLCγ2 acts in a similar manner to Src-family kinases and Syk, and affects the development of the proinflammatory milieu rather than the intrinsic migratory capacity of myeloid cells.

In addition to inflammatory mediators, we also investigated the production of reactive oxygen species by the analysis of MPO activity in vivo. ROS production has also been

shown to be crucial in the development of skin blistering in mice [189]. ROS can be considered as another participant of the proinflammatory microenvironment, as well as a contributor to tissue damage and dermal-epidermal separation. According to our results, in vivo ROS production is also dependent on the presence of PLCγ2 (**Figure 36**).

Our in vitro experiments suggested that these proinflammatory mediators are produced in a PLCγ2-dependent manner at least in part by neutrophils (**Figure 38**). In this study, we also investigated C7/anti-C7-induced spreading and ROS production of murine and human neutrophils, which were also dependent on PLCγ2 [3]. These experiments were performed mainly by Simon Vikár, therefore, I did not include these results in the current thesis.

5.3. NEUTROPHIL-SPECIFIC ANALYSIS OF PLCγ2 DURING EXPERIMENTAL EBA

We have shown the essential role of PLCγ2 in anti-C7-induced skin blistering in mice in section 4.3. Those experiments did not allow us to identify which specific cellular players expressing PLCγ2 are crucial for the development of this phenotype. Since we used bone-marrow chimeras in the majority of our experiments, it seems that PLCγ2 expressed in hematopoietic cells is important. Tissue resident immune cells, such as dermal macrophages, Langerhans cells and mast cells are quite radioresistant. It means, that these cells probably remained wild-type in the bone-marrow chimeras we used in our experiment. This makes it less likely that PLCγ2 expressed in these cells has critical role in disease development. However, their direct analysis using lineage-specific PLCγ2-deficient mice would answer this question most suitably. PLCγ2 is expressed mainly in hematopoietic cells, but there are some exceptions like in certain endothelial cells and in the central nervous system (see also in section 1.3.1). We did not test "vice versa" chimeras, in which wild-type bone marrow cells were transplanted into *Plcg2*$^{-/-}$ recipients. Such experiment would be useful to reliably exclude the role of PLCγ2 expressed in nonhematopoietic cells. Notably, such chimeras were tested in an autoantibody-induced arthritis model, and disease phenotype did not differ compared to wild-type littermates [2].

Neutrophils represent the most prevalent cells recruited to the dermis in patients with inflammatory EBA [144] and they are abundant in BP lesions, as well [204]. It is also the

case in the anti-C7-induced model we used. Moreover, depletion of neutrophils, as well as genetic neutrophil deficiency protected mice from anti-C7-induced pathology [189, 194, 205]. However, until now there was no information about the role of neutrophil-specific PLCγ2 expression regarding autoimmune skin blistering.

Therefore, we investigated the neutrophil-specific deletion of PLCγ2, utilizing the Cre-lox transgenic approach. Notably, Cre-mediated deletion of *Plcg2* gene in neutrophils was effective but not complete (**Figure 40**). This indicates that some neutrophils may have at least partially reserved PLCγ2 expression in *Plcg2*$^{\Delta PMN}$ mice. Importantly, PLCγ2 expression of other major leukocyte populations were unaffected, indicating the specific nature of the Cre-mediated deletion (**Figure 40** and **Figure 41**). These results were published by Futosi and Kása et al, where I contributed to the work as a co-author [2].

During the anti-C7-induced skin blistering, *Plcg2*$^{\Delta PMN}$ mice were also highly protected from macroscopic and microscopic signs of blister formation, closely resembling *Plcg2*$^{-/-}$ mice (**Figure 42** and **Figure 43**). However, quantitative analysis of infiltrating leukocyte subsets showed only partial reduction in ears in case of neutrophil-specific PLCγ2-deficiency (**Figure 44**). This findings might be due to the incomplete Cre-mediated deletion of PLCγ2 from neutrophils, or the relatively low sample size. However we cannot exclude that other cells expressing PLCγ2 also contribute to leukocyte recruitment.

More detailed lineage-specific studies were also performed in our laboratory, in order to identify cell types in which PLCγ2 is needed for arthritis development [2]. I contributed to this study not only by measuring PLCγ2 expression in leukocytes (**Figure 40**), but also analyzed the concentration of different proinflammatory mediators in the inflamed joints after arthritis induction. I chose not to include these findings in my thesis, since it is not closely related to the main topic. Briefly, we found, that PLCγ2 expressed in myeloid cells, especially in neutrophils, is crucial for arthritis development. Myeloid-specific and neutrophil-specific deletion of *Plcg2* resulted in the same protection as in complete *Plcg2*$^{-/-}$ mice. On the other hand, neither mast cell-, nor platelet-specific PLCγ2-deficiency affected arthritis development [2].

There are other leukocytes in which PLCγ2 expression may be relevant during experimental EBA, in addition to neutrophils. Since we focus on the pathomechanism of the effector phase of the disease, it is rather unlikely that PLCγ2 in B cells are important.

In other myeloid cells, like eosinophils, mast cells and macrophages, however, PLCγ2 expression might be relevant. The role of PLCγ2 in eosinophils would be especially interesting in models of BP, since human BP is the one characterized by the dominant infiltration of eosinophils. Mast cells were long considered as crucial participants driving initial changes upon antibody-deposition in BP models [218]. However, they were found dispensable in the anti-C7-induced EBA model [219], questioning the importance of PLCγ2 expressed by mast cells in our experimental setup.

Taken together, we showed that PLCγ2 expressed in neutrophils is crucial for the development of anti-C7-induced skin blistering in mice. However, we cannot rule out the potential contribution of PLCγ2 expressed by other cell types.

Based on our results and previous literature data, I would also like to present a possible mechanism for how PLCγ2 drives anti-C7-induced skin blistering in mice, also summarized schematically in **Figure 48**. Deposition of anti-C7 at the DEJ supposedly activates tissue resident leukocytes (and maybe keratinocytes, as well). They subsequently release proinflammatory mediators recruiting further leukocytes, mostly neutrophils (as well as eosinophils and monocytes/macrophages) to the dermis. Activation of these early recruited neutrophils then might lead to the amplification of inflammatory response via a positive feedback mechanism. This would be in line with the already described potential of neutrophils to induce feedback amplification in autocrine, paracrine and more complex routes reviewed in [237]. Importantly, it has been also shown by Hundt et al using fluorescently labeled myeloid cells, that neutrophils are recruited to the dermis in a biphasic manner during anti-C7-induced skin blistering in mice [244]. PLCγ2 is crucial most likely during the amplification of inflammation at the site of anti-C7 deposition, including the recruitment of further leukocytes, acting mainly in neutrophils (and possibly other myeloid cells).

One of the crucial proinflammatory mediators described essential in this feedback amplification is LTB_4 [194]. Our results implicate that the tissue accumulation of LTB_4 was dependent on PLCγ2 (**Figure 35**), as well as the release of LTB_4 by neutrophils upon C7/anti-C7-mediated activation in vitro (**Figure 38**). This pathway supposedly at least partially contributes to the abolishment of skin blistering in *Plcg2*$^{-/-}$ mice.

In addition, PLCγ2 might also contribute directly to tissue destruction through influencing the production of reactive oxygen species and possibly proteases, since in

vivo ROS production was dependent on PLCγ2 in our model (**Figure 36**).

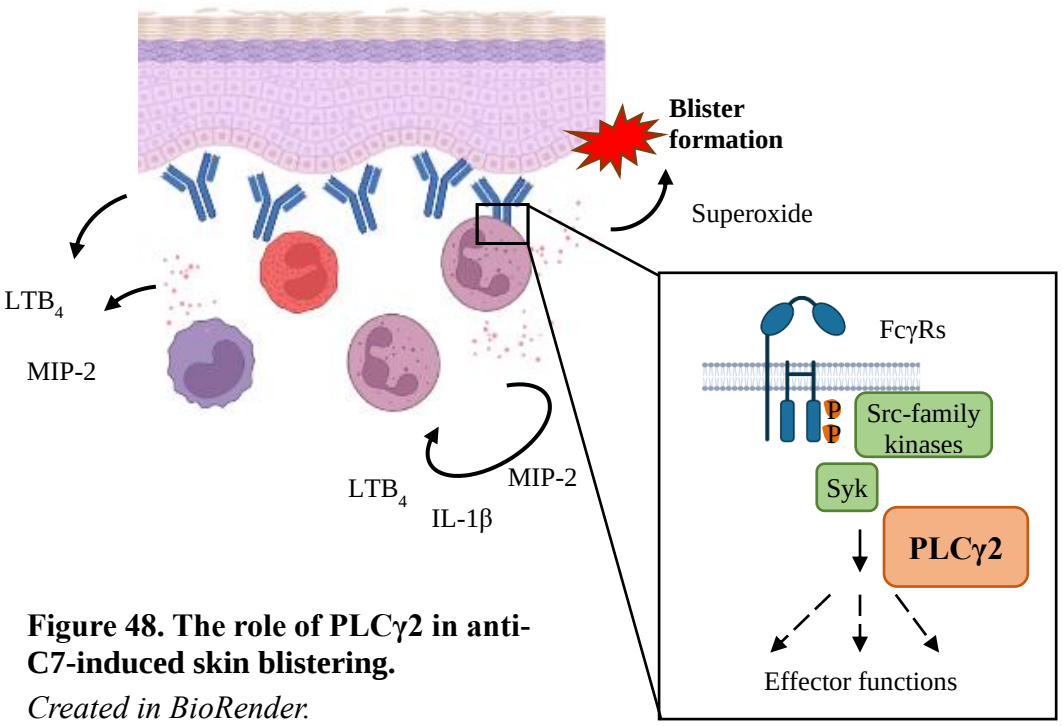

Figure 48. The role of PLCγ2 in anti-C7-induced skin blistering.
Created in BioRender.

5.4. HUMAN RELEVANCE OF OUR STUDIES

Translating experimental results from mice into human disease have to be considered with great caution. There are multiple differences between mice and humans in the types and structures of molecules. In this case, autoantigens, antibodies, proinflammatory mediators and Fc receptors, among others have major interspecies differences that might affect the pathogenic processes.

Interestingly, gain-of-function mutations of *PLCG2* in APLAID patients also caused skin lesions often referred to epidermolysis-bullosa-like eruptions. Such lesions were often accompanied by the infiltration of neutrophils (Section 1.3.3.1). Similarly, skin lesions with dermal inflammation were also described in mice with gain-of-function mutations of *Plcg2* (Section 1.3.2.2). These data further support the role of PLCγ2 in the pathogenesis of the inflammatory form of EBA.

To better understand the human relevance of our studies, we moved to the direction of a human ex vivo model. Thus, we were able to investigate the role of PLC enzymes in an experimental setup involving human skin and human neutrophils. Since there is no specific PLCγ2 inhibitor available, we used the U73122 compound (1-(6-((17beta-3-

methoxyestra-1,3,5(10)-trien-17-yl)amino)hexyl)-1H-pyrrole-2,5-dione). This is a widely used and potent PLC inhibitor under in vitro conditions [245, 246]. U73122 inhibited several effector functions of human neutrophils in vitro, induced by a variety of agonists. IC50 ranged between ~ 0.1-5 μM [247]. It is in line with our observations that, immune complex-induced superoxide production of human neutrophils were dose-dependently suppressed within the range of 0.1-10 μM [3]. Such experiments were performed mainly by Simon Vikár, therefore the results are not presented in this thesis.

We showed, that U73122 applied at 10 μM concentration inhibited ex vivo neutrophil-mediated separation of anti-C7-treated cryosections of human skin (**Figure 45**). This suggests that our findings in the mouse model may be relevant in the pathogenesis of the human disease, as well. Moreover, it also indicates that PLC enzymes (and possibly PLCγ2 within) may also play a direct role in tissue damage and the separation of the DEJ upon anti-C7 treatment.

Our human ex vivo studies using pharmacological inhibition of PLC also suggests a potential therapeutic application in this rare disease. U73122 has been administered to experimental animals without reporting any major toxicity issues. Studies were using systemic administration of U73122 in 3-30 mg/kg dose. For example, U73122 was able to reduce carrageenan-induced hind paw edema in rats and inflammatory peritonitis in mice [247]. In addition, it dose-dependently inhibited irritant-induced inflammatory ear edema in mice [247]. These results support that this compound could be investigated in our animal model of skin blistering, as well. Topical application of PLC inhibitors would be also a plausible application form to minimize systemic side effects.

The generation of a selective PLCγ2 inhibitor is possibly hindered because enzymatic region of PLC enzymes are relatively conserved. Specificity between the subtypes usually relies on the different regulatory domains, which are more difficult to inhibit. Interfering with the adapter function of PLCγ2 might be useful in the development of new more selective inhibitors. Recently published human mutations in the *PLCG2* gene (either gain- or loss-of-function, discussed in section 1.3.3) can possibly give us a hint about which are the potential regions that may be worth targeting therapeutically.

5.5. RELEVANCE OF OUR STUDIES REGARDING OTHER AUTOIMMUNE DISEASES

We chose the anti-C7-induced passive transfer model of subepidermal skin blistering to study the role of PLCγ2 because it seems to be a widely-used, reliable and useful approach compared to other animal models that are available mimicking pemphigoid diseases (described and compared in Section 1.5.2.3). This mouse model mimics the inflammatory form of EBA. It is also important to mention that EBA is often presented in a mechanobullous form, which does not involve inflammation. Therefore, our results cannot be adapted to that disease form. The mechanism of skin blistering in the mechanobullous form of EBA is incompletely understood. The factors that would commit patients to the presentation of the mechanobullous or the inflammatory form of EBA are also currently unknown.

There are multiple similarities, as well as differences between the pathomechanism of BP and EBA (see in detail in Section 1.5). Both of them are mediated by autoantibodies, with a crucial role of FcγRs. However, for instance, eosinophil-rich dermal infiltrate occurs in BP, but neutrophil-dominated accumulation happens during EBA. These data further underline, that our findings about the role of PLCγ2 cannot be directly implicated for the pathogenesis of BP. It would be useful to investigate the role of PLCγ2 in a reliable model of BP, as well.

Comparing the role of PLCγ2 in disease models of skin blistering versus autoimmune arthritis, our workgroup previously showed that PLCγ2 is crucial during the effector phase of autoimmune arthritis in vivo [81]. In line with that, we revealed in this thesis that PLCγ2 is also essential in antibody-induced skin blistering. Moreover, neutrophil-specific expression of PLCγ2 was also essential both in antibody-induced arthritis [2] and in skin blistering (Section 4.5).

5.6. EFFECT OF JAK INHIBITION IN EXPERIMENTAL EBA

In addition to the detailed characterization of the role of PLCγ2, we also tested the role of Janus kinases in experimental EBA using a pharmacological approach. We used a first-generation Jak inhibitor tofacitinib which is currently approved for the treatment of autoimmune diseases such as rheumatoid arthritis and ulcerative colitis. Tofacitinib is

highly selective for Janus kinases, however, relatively less selective between different Jaks, compared to other next generation drugs [1].

We applied two different doses of tofacitinib via oral gavage twice daily. Mice received this treatment during the entire 2-week experimental procedure starting a day before the first anti-C7 injection. Mice treated with 1 mg tofacitinib and anti-C7 antibodies presented significantly reduced skin lesions both in size and severity compared to vehicle-treated littermates (**Figure 46A-C**). The extent of erosions tended to be also reduced dose-dependently by Jak inhibition, however, that was not significant (**Figure 46D**). Tofacitinib treatment did not reduce ear thickening of anti-C7-treated mice (**Figure 46E**). Notably, these are still early findings with low sample sizes. Nevertheless, they show that inhibition of Janus kinases could be promising. Further investigation, increasing sample size and additional mechanistic experiments would be beneficial to elucidate the relevance of Jak inhibition in anti-C7-induced skin blistering.

There is increasing evidence regarding the role of Janus kinases in the development of prevalent inflammatory skin diseases [1] (see also in section 1.4). Despite that, such studies are still missing in pemphigoid diseases. Since current treatment regimens in pemphigoid diseases might have quite serious side effects, targeted therapy could be beneficial, and topical treatment options could be useful to reduce the probability of side effects. Based on our initial results, Jak inhibitors could be beneficial in these diseases.

Taken together, we presented in this thesis that PLCγ2, in particular when expressed in neutrophils, is essential for the development of skin blistering in mice, mediating dermal-epidermal separation, leukocyte accumulation and proinflammatory mediator production. In addition, we also showed that Jak inhibitors could reduce signs of anti-C7-induced skin blistering in mice. These results improve our understanding of the pathomechanism of anti-C7-induced skin pathology and can point to new possible therapeutic targets for pemphigoid diseases.

6. CONCLUSIONS

To conclude my work, I investigated the role of PLCγ2 and, in less detail, Janus kinases during the effector phase of autoantibody-induced skin blistering, using multiple models of epidermolysis bullosa acquisita. I list my findings in the same order as it was presented in the objectives section.

1. Adult *Plcg2*$^{-/-}$ mice have normal numbers of circulating leukocyte subsets and normal expression of major leukocyte antigens.
2. Intact *Plcg2*$^{-/-}$ mice, as well as *Plcg2*$^{-/-}$ bone-marrow chimeras are completely protected from macroscopic and microscopic signs of anti-C7-induced skin blistering. PLCγ2 is indispensable for dermal-epidermal separation and leukocyte accumulation at the site of antibody deposition, through influencing the development of the proinflammatory microenvironment without affecting the endogenous migration capacity of myeloid cells.
3. PLCγ2 is essential for the C7/anti-C7-induced inflammatory mediator release, but not for the migration of neutrophils in vitro.
4. Neutrophil-specific deletion of PLCγ2 is effective and specific, however, not complete. *Plcg2*$^{\Delta PMN}$ mice are almost completely protected from clinical and microscopic signs of anti-C7-induced skin blistering. This suggests that PLCγ2 expressed specifically by neutrophils has an essential role during the effector phase of experimental EBA.
5. Pharmacological inhibition of PLC successfully diminishes neutrophil-mediated dermal-epidermal separation of anti-C7-treated human skin. This underlines the human relevance of our studies and suggests a potential therapeutic application.
6. Inhibition of Janus kinases by the systemic administration of tofacitinib is able to dose-dependently reduce the extent and severity of skin lesions induced by anti-C7 treatment.

7. SUMMARY

Subepidermal autoimmune blistering skin diseases are often severe and treatment-resistant disorders. They are characterized by autoantibody formation against components of the dermal-epidermal junction (DEJ), leading to blister formation. Such conditions exert serious impact on the quality of life, without an available effective targeted therapy. Elucidation of the molecular mechanisms driving autoantibody-induced pathology and the identification of targetable pathways are particularly important. Therefore, we aimed to characterize the role of phospholipase Cγ2 (PLCγ2), an enzyme involved in immunoreceptor signaling, and in less detail Janus kinases in the development of autoantibody-induced skin blistering.

Plcg2$^{-/-}$ mice, as well as chimeras with *Plcg2*$^{-/-}$ hematopoietic system remained completely protected from autoantibody-induced skin blistering. Disease was induced by the passive transfer of anti-C7 antibodies recognizing the crucial DEJ component collagen type VII. PLCγ2 deficiency prevented dermal-epidermal separation and the infiltration of multiple myeloid cells including neutrophils to the skin, without affecting autoantibody deposition. The intrinsic migratory capacity of myeloid cells remained intact in *Plcg2*$^{-/-}$ mice, but in vivo accumulation of proinflammatory mediators, as well as the in vivo production of reactive oxygen species were completely blocked in the absence of PLCγ2. In vitro C7/anti-C7 immune complex-induced release of proinflammatory mediators from neutrophils was also dependent on PLCγ2. Moreover, neutrophil-specific deletion of PLCγ2 strongly diminished macroscopic and microscopic signs of anti-C7-induced skin blistering in vivo. Underlining the human relevance of our studies, we demonstrated that pharmacological inhibition of PLC enzymes was able to inhibit dermal-epidermal separation in an ex vivo human skin separation assay.

Pharmacological inhibition of Janus kinases by tofacitinib also dose-dependently reduced macroscopic signs of anti-C7-induced skin blistering in mice.

Our results identify PLCγ2 as a critical component of anti-C7-induced skin blistering. PLCγ2, in particular when expressed in neutrophils, is supposedly involved in creating the proinflammatory milieu after autoantibody deposition in the skin. Our results also suggests that Janus kinases also have an important role in the development of this model.

8. ÖSSZEFOGLALÁS

A szubepidermális autoimmun hólyagos bőrbetegségek sokszor súlyos, nehezen kezelhető állapotok. A betegség során autoantitestek keletkeznek a bőr felső két rétegét összetartó struktúra bizonyos komponensei ellen, melyek lerakódva a dermo-epidermális junkció (DEJ) gyengüléséhez, végső soron hólyagképződéshez vezetnek. A kórképek molekuláris patomechanizmusának minél mélyebb feltérképezése alapvető fontosságú esetleges terápiás célpontok azonosítása szempontjából. Ezek alapján célul tűztük ki egy immunreceptorok jelátvitelében kulcsfontosságú enzim, a foszfolipáz Cγ2 (PLCγ2) szerepének részletes, illetve a Janus kinázok rövid vizsgálatát az autoantitest-indukált hólyagos bőrbetegségek kialakulásában.

Kimutattuk, hogy mind a PLCγ2-hiányos intakt egerek, mind a PLCγ2-hiányos csontvelői kimérák védettnek bizonyultak az autoantitest-indukált hólyagos bőrgyulladás kialakulásával szemben. A betegséget a DEJ egyik kulcsfontosságú fehérjéje, a VII-es típusú kollagén-ellenes antitestek (anti-C7) beadásával hoztuk létre. PLCγ2 hiányában elmaradt a dermo-epidermális szeparáció, valamint a bőr mieloid-sejtes, főleg neutrofileket tartalmazó infiltrációja, de nem változott az anti-C7 lerakódása. A különböző mieloid sejtek endogén migrációs képessége nem változott PLCγ2 hiányában, viszont teljes mértékben elmaradt a különböző gyulladásos mediátorok szöveti felhalmozódása és a reaktív oxigén származékok termelődése in vivo. A neutrofilekből in vitro C7/anti-C7 immunkomplexek hatására PLCγ2-függő módon történt a gyulladásos mediátorok felszabadulása. Kimutattuk továbbá, hogy a PLCγ2 neutrofilekből történő törlése esetén szintén elmaradt az anti-C7-indukált bőrtünetek kialakulása egerekben. Az eredményeink humán relevanciáját alátámasztja, hogy a PLC farmakológiai gátlása képes volt csökkenteni a dermo-epidermális szeparációt egy humán ex vivo bőrszeparációs modellben.

A Janus kinázokat gátló tofacitinib alkalmazása dózisfüggő módon csökkentette egerekben az anti-C7-kiváltotta hólyagos bőrbetegség makroszkópos tüneteit.

Eredményeink alapján elmondhatjuk, hogy a PLCγ2 kulcsfontosságú szerepet tölt be az anti-C7-indukált hólyagos bőrbetegség patogenezisében, feltehetően a gyulladásos mikrokörnyezet kialakításán keresztül. Kezdeti kísérleteink szintén felvetik a Janus kinázok szerepét ezen állatmodell kialakulásában.

9. REFERENCES

1. Szilveszter, K. P., Németh, T. and Mócsai, A., *Tyrosine Kinases in Autoimmune and Inflammatory Skin Diseases.* **Front Immunol**, 2019. 10: p. 1862.
2. Futosi, K., Kása, O., Szilveszter, K. P. and Mócsai, A., *Neutrophil Phospholipase Cγ2 Drives Autoantibody-Induced Arthritis Through the Generation of the Inflammatory Microenvironment.* **Arthritis Rheumatol**, 2021. 73(9): p. 1614-1625.
3. Szilveszter, K. P., Vikár, S., Horváth, A. I., Helyes, Z., Sárdy, M. and Mócsai, A., *Phospholipase Cγ2 Is Essential for Experimental Models of Epidermolysis Bullosa Acquisita.* **J Invest Dermatol**, 2022. 142(4): p. 1114-1125.
4. Németh, T., Futosi, K., Szilveszter, K., Vilinovszki, O., Kiss-Pápai, L. and Mócsai, A., *Lineage-Specific Analysis of Syk Function in Autoantibody-Induced Arthritis.* **Front Immunol**, 2018. 9: p. 555.
5. Bach, J. F., *The hygiene hypothesis in autoimmunity: the role of pathogens and commensals.* **Nat Rev Immunol**, 2018. 18(2): p. 105-120.
6. Baker, K. F. and Isaacs, J. D., *Novel therapies for immune-mediated inflammatory diseases: What can we learn from their use in rheumatoid arthritis, spondyloarthritis, systemic lupus erythematosus, psoriasis, Crohn's disease and ulcerative colitis?* **Ann Rheum Dis**, 2018. 77(2): p. 175-187.
7. Mócsai, A., Kovács, L. and Gergely, P., *What is the future of targeted therapy in rheumatology: biologics or small molecules?* **BMC Med**, 2014. 12: p. 43.
8. Kovács, M., Németh, T., Jakus, Z., Sitaru, C., Simon, E., Futosi, K., Botz, B., Helyes, Z., Lowell, C. A. and Mócsai, A., *The Src family kinases Hck, Fgr, and Lyn are critical for the generation of the in vivo inflammatory environment without a direct role in leukocyte recruitment.* **J Exp Med**, 2014. 211(10): p. 1993-2011.
9. Németh, T., Virtic, O., Sitaru, C. and Mócsai, A., *The Syk Tyrosine Kinase Is Required for Skin Inflammation in an In Vivo Mouse Model of Epidermolysis Bullosa Acquisita.* **J Invest Dermatol**, 2017. 137(10): p. 2131-2139.

10. Jakus, Z., Simon, E., Balázs, B. and Mócsai, A., *Genetic deficiency of Syk protects mice from autoantibody-induced arthritis.* **Arthritis Rheum**, 2010. 62(7): p. 1899-910.
11. O'Shea, J. J. and Plenge, R., *JAK and STAT signaling molecules in immunoregulation and immune-mediated disease.* **Immunity**, 2012. 36(4): p. 542-50.
12. O'Shea, J. J., Schwartz, D. M., Villarino, A. V., Gadina, M., McInnes, I. B. and Laurence, A., *The JAK-STAT pathway: impact on human disease and therapeutic intervention.* **Annu Rev Med**, 2015. 66: p. 311-28.
13. O'Connell, K. E., Mikkola, A. M., Stepanek, A. M., Vernet, A., Hall, C. D., Sun, C. C., Yildirim, E., Staropoli, J. F., Lee, J. T. and Brown, D. E., *Practical murine hematopathology: a comparative review and implications for research.* **Comp Med**, 2015. 65(2): p. 96-113.
14. Kolaczkowska, E. and Kubes, P., *Neutrophil recruitment and function in health and inflammation.* **Nat Rev Immunol**, 2013. 13(3): p. 159-75.
15. Ley, K., Laudanna, C., Cybulsky, M. I. and Nourshargh, S., *Getting to the site of inflammation: the leukocyte adhesion cascade updated.* **Nat Rev Immunol**, 2007. 7(9): p. 678-89.
16. Mócsai, A., Walzog, B. and Lowell, C. A., *Intracellular signalling during neutrophil recruitment.* **Cardiovasc Res**, 2015. 107(3): p. 373-85.
17. Subramanian, B. C., Melis, N., Chen, D., Wang, W., Gallardo, D., Weigert, R. and Parent, C. A., *The LTB4-BLT1 axis regulates actomyosin and β2-integrin dynamics during neutrophil extravasation.* **J Cell Biol**, 2020. 219(10).
18. Colotta, F., Re, F., Polentarutti, N., Sozzani, S. and Mantovani, A., *Modulation of granulocyte survival and programmed cell death by cytokines and bacterial products.* **Blood**, 1992. 80(8): p. 2012-20.
19. Nourshargh, S., Renshaw, S. A. and Imhof, B. A., *Reverse Migration of Neutrophils: Where, When, How, and Why?* **Trends Immunol**, 2016. 37(5): p. 273-286.
20. Nordenfelt, P. and Tapper, H., *Phagosome dynamics during phagocytosis by neutrophils.* **J Leukoc Biol**, 2011. 90(2): p. 271-84.

21. Leto, T. L. and Geiszt, M., *Role of Nox family NADPH oxidases in host defense.* **Antioxid Redox Signal**, 2006. 8(9-10): p. 1549-61.
22. Amulic, B., Cazalet, C., Hayes, G. L., Metzler, K. D. and Zychlinsky, A., *Neutrophil function: from mechanisms to disease.* **Annu Rev Immunol**, 2012. 30: p. 459-89.
23. Faurschou, M. and Borregaard, N., *Neutrophil granules and secretory vesicles in inflammation.* **Microbes Infect**, 2003. 5(14): p. 1317-27.
24. Kjeldsen, L., Bjerrum, O. W., Askaa, J. and Borregaard, N., *Subcellular localization and release of human neutrophil gelatinase, confirming the existence of separate gelatinase-containing granules.* **Biochem J**, 1992. 287 (Pt 2): p. 603-10.
25. Borregaard, N., Miller, L. J. and Springer, T. A., *Chemoattractant-regulated mobilization of a novel intracellular compartment in human neutrophils.* **Science**, 1987. 237(4819): p. 1204-6.
26. Tecchio, C. and Cassatella, M. A., *Neutrophil-derived chemokines on the road to immunity.* **Semin Immunol**, 2016. 28(2): p. 119-28.
27. Mantovani, A., Cassatella, M. A., Costantini, C. and Jaillon, S., *Neutrophils in the activation and regulation of innate and adaptive immunity.* **Nat Rev Immunol**, 2011. 11(8): p. 519-31.
28. Németh, T., Futosi, K., Sitaru, C., Ruland, J. and Mócsai, A., *Neutrophil-specific deletion of the CARD9 gene expression regulator suppresses autoantibody-induced inflammation in vivo.* **Nat Commun**, 2016. 7: p. 11004.
29. Kolonics, F., Szeifert, V., Timar, C. I., Ligeti, E. and Lorincz, A. M., *The Functional Heterogeneity of Neutrophil-Derived Extracellular Vesicles Reflects the Status of the Parent Cell.* **Cells**, 2020. 9(12).
30. Timár, C. I., Lőrincz, A. M., Csépányi-Komi, R., Vályi-Nagy, A., Nagy, G., Buzás, E. I., Iványi, Z., Kittel, A., Powell, D. W., McLeish, K. R. and Ligeti, E., *Antibacterial effect of microvesicles released from human neutrophilic granulocytes.* **Blood**, 2013. 121(3): p. 510-8.
31. Brinkmann, V., Reichard, U., Goosmann, C., Fauler, B., Uhlemann, Y., Weiss, D. S., Weinrauch, Y. and Zychlinsky, A., *Neutrophil extracellular traps kill bacteria.* **Science**, 2004. 303(5663): p. 1532-5.

32. Castanheira, F. V. S. and Kubes, P., *Neutrophils and NETs in modulating acute and chronic inflammation.* **Blood**, 2019. 133(20): p. 2178-2185.
33. Papayannopoulos, V., *Neutrophil extracellular traps in immunity and disease.* **Nat Rev Immunol**, 2018. 18(2): p. 134-147.
34. Németh, T., Sperandio, M. and Mócsai, A., *Neutrophils as emerging therapeutic targets.* **Nat Rev Drug Discov**, 2020.
35. Dinauer, M. C., *Primary immune deficiencies with defects in neutrophil function.* **Hematology Am Soc Hematol Educ Program**, 2016. 2016(1): p. 43-50.
36. Németh, T. and Mócsai, A., *The role of neutrophils in autoimmune diseases.* **Immunol Lett**, 2012. 143(1): p. 9-19.
37. Németh, T., Mócsai, A. and Lowell, C. A., *Neutrophils in animal models of autoimmune disease.* **Semin Immunol**, 2016. 28(2): p. 174-86.
38. Chiang, C. C., Cheng, W. J., Korinek, M., Lin, C. Y. and Hwang, T. L., *Neutrophils in Psoriasis.* **Front Immunol**, 2019. 10: p. 2376.
39. Soehnlein, O., *Multiple roles for neutrophils in atherosclerosis.* **Circ Res**, 2012. 110(6): p. 875-88.
40. Snelgrove, R. J., Jackson, P. L., Hardison, M. T., Noerager, B. D., Kinloch, A., Gaggar, A., Shastry, S., Rowe, S. M., Shim, Y. M., Hussell, T. and Blalock, J. E., *A critical role for LTA4H in limiting chronic pulmonary neutrophilic inflammation.* **Science**, 2010. 330(6000): p. 90-4.
41. Panettieri, R. A., Jr., *The Role of Neutrophils in Asthma.* **Immunol Allergy Clin North Am**, 2018. 38(4): p. 629-638.
42. Noubouossie, D. F., Reeves, B. N., Strahl, B. D. and Key, N. S., *Neutrophils: back in the thrombosis spotlight.* **Blood**, 2019. 133(20): p. 2186-2197.
43. Giese, M. A., Hind, L. E. and Huttenlocher, A., *Neutrophil plasticity in the tumor microenvironment.* **Blood**, 2019. 133(20): p. 2159-2167.
44. Mócsai, A., Ruland, J. and Tybulewicz, V. L., *The SYK tyrosine kinase: a crucial player in diverse biological functions.* **Nat Rev Immunol**, 2010. 10(6): p. 387-402.
45. Abram, C. L. and Lowell, C. A., *Shp1 function in myeloid cells.* **J Leukoc Biol**, 2017. 102(3): p. 657-675.

46. Turner, M., Mee, P. J., Costello, P. S., Williams, O., Price, A. A., Duddy, L. P., Furlong, M. T., Geahlen, R. L. and Tybulewicz, V. L., *Perinatal lethality and blocked B-cell development in mice lacking the tyrosine kinase Syk.* **Nature**, 1995. 378(6554): p. 298-302.

47. Cheng, A. M., Rowley, B., Pao, W., Hayday, A., Bolen, J. B. and Pawson, T., *Syk tyrosine kinase required for mouse viability and B-cell development.* **Nature**, 1995. 378(6554): p. 303-6.

48. Nimmerjahn, F. and Ravetch, J. V., *Fcγ receptors as regulators of immune responses.* **Nat Rev Immunol**, 2008. 8(1): p. 34-47.

49. Bruhns, P. and Jonsson, F., *Mouse and human FcR effector functions.* **Immunol Rev**, 2015. 268(1): p. 25-51.

50. Németh, T., Futosi, K., Szabó, M., Aradi, P., Saito, T., Mócsai, A. and Jakus, Z., *Importance of Fc Receptor γ-Chain ITAM Tyrosines in Neutrophil Activation and in vivo Autoimmune Arthritis.* **Frontiers in Immunology**, 2019. 10(252).

51. Jakus, Z., Németh, T., Verbeek, J. S. and Mócsai, A., *Critical but overlapping role of FcγRIII and FcγRIV in activation of murine neutrophils by immobilized immune complexes.* **J Immunol**, 2008. 180(1): p. 618-29.

52. Kiefer, F., Brumell, J., Al-Alawi, N., Latour, S., Cheng, A., Veillette, A., Grinstein, S. and Pawson, T., *The Syk protein tyrosine kinase is essential for Fcgamma receptor signaling in macrophages and neutrophils.* **Mol Cell Biol**, 1998. 18(7): p. 4209-20.

53. Harburger, D. S. and Calderwood, D. A., *Integrin signalling at a glance.* **J Cell Sci**, 2009. 122(Pt 2): p. 159-63.

54. Bouti, P., Webbers, S. D. S., Fagerholm, S. C., Alon, R., Moser, M., Matlung, H. L. and Kuijpers, T. W., *β2 Integrin Signaling Cascade in Neutrophils: More Than a Single Function.* **Front Immunol**, 2020. 11: p. 619925.

55. Abram, C. L. and Lowell, C. A., *The ins and outs of leukocyte integrin signaling.* **Annu Rev Immunol**, 2009. 27: p. 339-62.

56. Mócsai, A., Abram, C. L., Jakus, Z., Hu, Y., Lanier, L. L. and Lowell, C. A., *Integrin signaling in neutrophils and macrophages uses adaptors containing immunoreceptor tyrosine-based activation motifs.* **Nat Immunol**, 2006. 7(12): p. 1326-33.

57. Mócsai, A., Zhou, M., Meng, F., Tybulewicz, V. L. and Lowell, C. A., *Syk is required for integrin signaling in neutrophils.* **Immunity**, 2002. 16(4): p. 547-58.
58. Mócsai, A., Ligeti, E., Lowell, C. A. and Berton, G., *Adhesion-dependent degranulation of neutrophils requires the Src family kinases Fgr and Hck.* **J Immunol**, 1999. 162(2): p. 1120-6.
59. Jakus, Z., Fodor, S., Abram, C. L., Lowell, C. A. and Mócsai, A., *Immunoreceptor-like signaling by β2 and β3 integrins.* **Trends Cell Biol**, 2007. 17(10): p. 493-501.
60. Bowen, T. J., Ochs, H. D., Altman, L. C., Price, T. H., Van Epps, D. E., Brautigan, D. L., Rosin, R. E., Perkins, W. D., Babior, B. M., Klebanoff, S. J. and Wedgwood, R. J., *Severe recurrent bacterial infections associated with defective adherence and chemotaxis in two patients with neutrophils deficient in a cell-associated glycoprotein.* **J Pediatr**, 1982. 101(6): p. 932-40.
61. Baker, S. J., Rane, S. G. and Reddy, E. P., *Hematopoietic cytokine receptor signaling.* **Oncogene**, 2007. 26(47): p. 6724-37.
62. Renauld, J. C., *Class II cytokine receptors and their ligands: key antiviral and inflammatory modulators.* **Nat Rev Immunol**, 2003. 3(8): p. 667-76.
63. Rodig, S. J., Meraz, M. A., White, J. M., Lampe, P. A., Riley, J. K., Arthur, C. D., King, K. L., Sheehan, K. C., Yin, L., Pennica, D., Johnson, E. M., Jr. and Schreiber, R. D., *Disruption of the Jak1 gene demonstrates obligatory and nonredundant roles of the Jaks in cytokine-induced biologic responses.* **Cell**, 1998. 93(3): p. 373-83.
64. Neubauer, H., Cumano, A., Muller, M., Wu, H., Huffstadt, U. and Pfeffer, K., *Jak2 deficiency defines an essential developmental checkpoint in definitive hematopoiesis.* **Cell**, 1998. 93(3): p. 397-409.
65. Macchi, P., Villa, A., Giliani, S., Sacco, M. G., Frattini, A., Porta, F., Ugazio, A. G., Johnston, J. A., Candotti, F., O'Shea, J. J. and et al., *Mutations of Jak-3 gene in patients with autosomal severe combined immune deficiency (SCID).* **Nature**, 1995. 377(6544): p. 65-8.
66. Russell, S. M., Tayebi, N., Nakajima, H., Riedy, M. C., Roberts, J. L., Aman, M. J., Migone, T. S., Noguchi, M., Markert, M. L., Buckley, R. H., O'Shea, J. J. and

Leonard, W. J., *Mutation of Jak3 in a patient with SCID: essential role of Jak3 in lymphoid development.* **Science**, 1995. 270(5237): p. 797-800.

67. Nosaka, T., van Deursen, J. M., Tripp, R. A., Thierfelder, W. E., Witthuhn, B. A., McMickle, A. P., Doherty, P. C., Grosveld, G. C. and Ihle, J. N., *Defective lymphoid development in mice lacking Jak3.* **Science**, 1995. 270(5237): p. 800-2.
68. Park, S. Y., Saijo, K., Takahashi, T., Osawa, M., Arase, H., Hirayama, N., Miyake, K., Nakauchi, H., Shirasawa, T. and Saito, T., *Developmental defects of lymphoid cells in Jak3 kinase-deficient mice.* **Immunity**, 1995. 3(6): p. 771-82.
69. Shimoda, K., Kato, K., Aoki, K., Matsuda, T., Miyamoto, A., Shibamori, M., Yamashita, M., Numata, A., Takase, K., Kobayashi, S., Shibata, S., Asano, Y., Gondo, H., Sekiguchi, K., Nakayama, K., Nakayama, T., Okamura, T., Okamura, S., Niho, Y. and Nakayama, K., *Tyk2 plays a restricted role in IFNα signaling, although it is required for IL-12-mediated T cell function.* **Immunity**, 2000. 13(4): p. 561-71.
70. Urzainqui, A., Serrador, J. M., Viedma, F., Yanez-Mo, M., Rodriguez, A., Corbi, A. L., Alonso-Lebrero, J. L., Luque, A., Deckert, M., Vazquez, J. and Sanchez-Madrid, F., *ITAM-based interaction of ERM proteins with Syk mediates signaling by the leukocyte adhesion receptor PSGL-1.* **Immunity**, 2002. 17(4): p. 401-12.
71. Zarbock, A., Abram, C. L., Hundt, M., Altman, A., Lowell, C. A. and Ley, K., *PSGL-1 engagement by E-selectin signals through Src kinase Fgr and ITAM adapters DAP12 and FcRγ to induce slow leukocyte rolling.* **J Exp Med**, 2008. 205(10): p. 2339-47.
72. Mócsai, A., Zhang, H., Jakus, Z., Kitaura, J., Kawakami, T. and Lowell, C. A., *G-protein-coupled receptor signaling in Syk-deficient neutrophils and mast cells.* **Blood**, 2003. 101(10): p. 4155-63.
73. Kadamur, G. and Ross, E. M., *Mammalian phospholipase C.* **Annu Rev Physiol**, 2013. 75: p. 127-54.
74. Jackson, J. T., Mulazzani, E., Nutt, S. L. and Masters, S. L., *The role of PLCγ2 in immunological disorders, cancer, and neurodegeneration.* **J Biol Chem**, 2021. 297(2): p. 100905.

75. Gresset, A., Hicks, S. N., Harden, T. K. and Sondek, J., *Mechanism of phosphorylation-induced activation of phospholipase Cγ isozymes.* **J Biol Chem**, 2010. 285(46): p. 35836-47.

76. Wilde, J. I. and Watson, S. P., *Regulation of phospholipase Cγ isoforms in haematopoietic cells: why one, not the other?* **Cell Signal**, 2001. 13(10): p. 691-701.

77. Ji, Q. S., Winnier, G. E., Niswender, K. D., Horstman, D., Wisdom, R., Magnuson, M. A. and Carpenter, G., *Essential role of the tyrosine kinase substrate phospholipase Cγ1 in mammalian growth and development.* **Proc Natl Acad Sci U S A**, 1997. 94(7): p. 2999-3003.

78. Liao, H. J., Kume, T., McKay, C., Xu, M. J., Ihle, J. N. and Carpenter, G., *Absence of erythrogenesis and vasculogenesis in Plcg1-deficient mice.* **J Biol Chem**, 2002. 277(11): p. 9335-41.

79. Fu, G., Chen, Y., Yu, M., Podd, A., Schuman, J., He, Y., Di, L., Yassai, M., Haribhai, D., North, P. E., Gorski, J., Williams, C. B., Wang, D. and Wen, R., *Phospholipase Cγ1 is essential for T cell development, activation, and tolerance.* **J Exp Med**, 2010. 207(2): p. 309-18.

80. Takata, M., Sabe, H., Hata, A., Inazu, T., Homma, Y., Nukada, T., Yamamura, H. and Kurosaki, T., *Tyrosine kinases Lyn and Syk regulate B cell receptor-coupled Ca2+ mobilization through distinct pathways.* **EMBO J**, 1994. 13(6): p. 1341-9.

81. Jakus, Z., Simon, E., Frommhold, D., Sperandio, M. and Mócsai, A., *Critical role of phospholipase Cγ2 in integrin and Fc receptor-mediated neutrophil functions and the effector phase of autoimmune arthritis.* **J Exp Med**, 2009. 206(3): p. 577-93.

82. Fluckiger, A. C., Li, Z., Kato, R. M., Wahl, M. I., Ochs, H. D., Longnecker, R., Kinet, J. P., Witte, O. N., Scharenberg, A. M. and Rawlings, D. J., *Btk/Tec kinases regulate sustained increases in intracellular Ca2+ following B-cell receptor activation.* **EMBO J**, 1998. 17(7): p. 1973-85.

83. Piechulek, T., Rehlen, T., Walliser, C., Vatter, P., Moepps, B. and Gierschik, P., *Isozyme-specific stimulation of phospholipase Cγ2 by Rac GTPases.* **J Biol Chem**, 2005. 280(47): p. 38923-31.

84. Wang, D., Feng, J., Wen, R., Marine, J. C., Sangster, M. Y., Parganas, E., Hoffmeyer, A., Jackson, C. W., Cleveland, J. L., Murray, P. J. and Ihle, J. N., *Phospholipase Cγ2 is essential in the functions of B cell and several Fc receptors.* **Immunity**, 2000. 13(1): p. 25-35.

85. Hashimoto, A., Takeda, K., Inaba, M., Sekimata, M., Kaisho, T., Ikehara, S., Homma, Y., Akira, S. and Kurosaki, T., *Cutting edge: essential role of phospholipase Cγ2 in B cell development and function.* **J Immunol**, 2000. 165(4): p. 1738-42.

86. Wen, R., Jou, S. T., Chen, Y., Hoffmeyer, A. and Wang, D., *Phospholipase Cγ2 is essential for specific functions of FcεR and FcγR.* **J Immunol**, 2002. 169(12): p. 6743-52.

87. Tassi, I., Presti, R., Kim, S., Yokoyama, W. M., Gilfillan, S. and Colonna, M., *Phospholipase Cγ2 is a critical signaling mediator for murine NK cell activating receptors.* **J Immunol**, 2005. 175(2): p. 749-54.

88. Caraux, A., Kim, N., Bell, S. E., Zompi, S., Ranson, T., Lesjean-Pottier, S., Garcia-Ojeda, M. E., Turner, M. and Colucci, F., *Phospholipase Cγ2 is essential for NK cell cytotoxicity and innate immunity to malignant and virally infected cells.* **Blood**, 2006. 107(3): p. 994-1002.

89. Wonerow, P., Pearce, A. C., Vaux, D. J. and Watson, S. P., *A critical role for phospholipase Cγ2 in αIIbβ3-mediated platelet spreading.* **J Biol Chem**, 2003. 278(39): p. 37520-9.

90. Tassi, I., Cella, M., Castro, I., Gilfillan, S., Khan, W. N. and Colonna, M., *Requirement of phospholipase Cγ2 (PLCγ2) for Dectin-1-induced antigen presentation and induction of TH1/TH17 polarization.* **Eur J Immunol**, 2009. 39(5): p. 1369-78.

91. Xu, S., Huo, J., Lee, K. G., Kurosaki, T. and Lam, K. P., *Phospholipase Cγ2 is critical for Dectin-1-mediated Ca^{2+} flux and cytokine production in dendritic cells.* **J Biol Chem**, 2009. 284(11): p. 7038-46.

92. Gorjestani, S., Yu, M., Tang, B., Zhang, D., Wang, D. and Lin, X., *Phospholipase Cγ2 (PLCγ2) is key component in Dectin-2 signaling pathway, mediating anti-fungal innate immune responses.* **J Biol Chem**, 2011. 286(51): p. 43651-9.

93. Kertész, Z., Győri, D., Körmendi, S., Fekete, T., Kis-Tóth, K., Jakus, Z., Schett, G., Rajnavölgyi, E., Dobó-Nagy, C. and Mócsai, A., *Phospholipase Cγ2 is required for basal but not oestrogen deficiency-induced bone resorption.* **Eur J Clin Invest**, 2012. 42(1): p. 49-60.

94. Chiang, C. Y., Veckman, V., Limmer, K. and David, M., *Phospholipase Cγ2 and intracellular calcium are required for lipopolysaccharide-induced Toll-like receptor 4 (TLR4) endocytosis and interferon regulatory factor 3 (IRF3) activation.* **J Biol Chem**, 2012. 287(6): p. 3704-9.

95. Ichise, H., Ichise, T., Ohtani, O. and Yoshida, N., *Phospholipase Cγ2 is necessary for separation of blood and lymphatic vasculature in mice.* **Development**, 2009. 136(2): p. 191-5.

96. Yu, P., Constien, R., Dear, N., Katan, M., Hanke, P., Bunney, T. D., Kunder, S., Quintanilla-Martinez, L., Huffstadt, U., Schroder, A., Jones, N. P., Peters, T., Fuchs, H., de Angelis, M. H., Nehls, M., Grosse, J., Wabnitz, P., Meyer, T. P., Yasuda, K., Schiemann, M., Schneider-Fresenius, C., Jagla, W., Russ, A., Popp, A., Josephs, M., Marquardt, A., Laufs, J., Schmittwolf, C., Wagner, H., Pfeffer, K. and Mudde, G. C., *Autoimmunity and inflammation due to a gain-of-function mutation in phospholipase Cγ2 that specifically increases external Ca^{2+} entry.* **Immunity**, 2005. 22(4): p. 451-65.

97. Abe, K., Fuchs, H., Boersma, A., Hans, W., Yu, P., Kalaydjiev, S., Klaften, M., Adler, T., Calzada-Wack, J., Mossbrugger, I., Rathkolb, B., Rozman, J., Prehn, C., Maraslioglu, M., Kametani, Y., Shimada, S., Adamski, J., Busch, D. H., Esposito, I., Klingenspor, M., Wolf, E., Wurst, W., Gailus-Durner, V., Katan, M., Marschall, S., Soewarto, D., Wagner, S. and de Angelis, M. H., *A novel N-ethyl-N-nitrosourea-induced mutation in phospholipase Cγ2 causes inflammatory arthritis, metabolic defects, and male infertility in vitro in a murine model.* **Arthritis Rheum**, 2011. 63(5): p. 1301-11.

98. Everett, K. L., Bunney, T. D., Yoon, Y., Rodrigues-Lima, F., Harris, R., Driscoll, P. C., Abe, K., Fuchs, H., de Angelis, M. H., Yu, P., Cho, W. and Katan, M., *Characterization of phospholipase Cγ enzymes with gain-of-function mutations.* **J Biol Chem**, 2009. 284(34): p. 23083-93.

99. Ombrello, M. J., Remmers, E. F., Sun, G., Freeman, A. F., Datta, S., Torabi-Parizi, P., Subramanian, N., Bunney, T. D., Baxendale, R. W., Martins, M. S., Romberg, N., Komarow, H., Aksentijevich, I., Kim, H. S., Ho, J., Cruse, G., Jung, M. Y., Gilfillan, A. M., Metcalfe, D. D., Nelson, C., O'Brien, M., Wisch, L., Stone, K., Douek, D. C., Gandhi, C., Wanderer, A. A., Lee, H., Nelson, S. F., Shianna, K. V., Cirulli, E. T., Goldstein, D. B., Long, E. O., Moir, S., Meffre, E., Holland, S. M., Kastner, D. L., Katan, M., Hoffman, H. M. and Milner, J. D., *Cold urticaria, immunodeficiency, and autoimmunity related to PLCG2 deletions.* **N Engl J Med**, 2012. 366(4): p. 330-8.

100. Aderibigbe, O. M., Priel, D. L., Lee, C. C., Ombrello, M. J., Prajapati, V. H., Liang, M. G., Lyons, J. J., Kuhns, D. B., Cowen, E. W. and Milner, J. D., *Distinct Cutaneous Manifestations and Cold-Induced Leukocyte Activation Associated With PLCG2 Mutations.* **JAMA Dermatol**, 2015. 151(6): p. 627-34.

101. Zhou, Q., Lee, G. S., Brady, J., Datta, S., Katan, M., Sheikh, A., Martins, M. S., Bunney, T. D., Santich, B. H., Moir, S., Kuhns, D. B., Long Priel, D. A., Ombrello, A., Stone, D., Ombrello, M. J., Khan, J., Milner, J. D., Kastner, D. L. and Aksentijevich, I., *A hypermorphic missense mutation in PLCG2, encoding phospholipase Cγ2, causes a dominantly inherited autoinflammatory disease with immunodeficiency.* **Am J Hum Genet**, 2012. 91(4): p. 713-20.

102. Neves, J. F., Doffinger, R., Barcena-Morales, G., Martins, C., Papapietro, O., Plagnol, V., Curtis, J., Martins, M., Kumararatne, D., Cordeiro, A. I., Neves, C., Borrego, L. M., Katan, M. and Nejentsev, S., *Novel PLCG2 Mutation in a Patient With APLAID and Cutis Laxa.* **Front Immunol**, 2018. 9: p. 2863.

103. Moran-Villasenor, E., Saez-de-Ocariz, M., Torrelo, A., Arostegui, J. I., Yamazaki-Nakashimada, M. A., Alcantara-Ortigoza, M. A., Gonzalez-Del-Angel, A., Velazquez-Aragon, J. A., Lopez-Herrera, G., Berron-Ruiz, L. and Garcia-Romero, M. T., *Expanding the Clinical Features of Autoinflammation and PLCγ2-associated Antibody Deficiency and Immune Dysregulation by description of a Novel Patient.* **J Eur Acad Dermatol Venereol**, 2019.

104. Novice, T., Kariminia, A., Del Bel, K. L., Lu, H., Sharma, M., Lim, C. J., Read, J., Lugt, M. V., Hannibal, M. C., O'Dwyer, D., Hosler, M., Scharnitz, T., Rizzo, J. M., Zacur, J., Priatel, J., Abdossamadi, S., Bohm, A., Junker, A., Turvey, S. E.,

Schultz, K. R. and Rozmus, J., *A Germline Mutation in the C2 Domain of PLCγ2 Associated with Gain-of-Function Expands the Phenotype for PLCG2-Related Diseases.* **J Clin Immunol**, 2020. 40(2): p. 267-276.

105. Khabbazi, A., Rahbar Kafshboran, H., Nasiri Aghdam, M., Nouri Nojadeh, J., Daghagh, H., Daneshmandpour, Y., Kazemzadeh, M., Hamzeiy, H. and Sakhinia, E., *A new report of autoinflammation and PLCG2-associated antibody deficiency and immune dysregulation (APLAID) with a homozygous pattern from Iran.* **Immunol Lett**, 2020. 221: p. 27-32.
106. Martin-Nalda, A., Fortuny, C., Rey, L., Bunney, T. D., Alsina, L., Esteve-Sole, A., Bull, D., Anton, M. C., Basagana, M., Casals, F., Deya, A., Garcia-Prat, M., Gimeno, R., Juan, M., Martinez-Banaclocha, H., Martinez-Garcia, J. J., Mensa-Vilaro, A., Rabionet, R., Martin-Begue, N., Rudilla, F., Yague, J., Estivill, X., Garcia-Patos, V., Pujol, R. M., Soler-Palacin, P., Katan, M., Pelegrin, P., Colobran, R., Vicente, A. and Arostegui, J. I., *Severe Autoinflammatory Manifestations and Antibody Deficiency Due to Novel Hypermorphic PLCG2 Mutations.* **J Clin Immunol**, 2020. 40(7): p. 987-1000.
107. Park, H. S., Oh, A., Keum, C. W., Lee, J., Lee, J. K., Son, B. R., Shin, K. S. and Hahn, Y. S., *A novel likely pathogenic PLCG2 variant in a patient with a recurrent skin blistering disease and B-cell lymphopenia.* **Eur J Med Genet**, 2021. 65(1): p. 104387.
108. Mahajan, R., Bishnoi, A., Manjunath, S., Vignesh, P., Suri, D., Gopal, M., Chatterjee, D., Jamwal, M., De, D., Das, R., Handa, S., Kubba, A., Batrani, M. and Radotra, B. D., *Severe epidermolysis bullosa/Kindler syndrome-like phenotype of an autoinflammatory syndrome in a child.* **Clin Exp Dermatol**, 2021. 46(4): p. 795-799.
109. Byrd, J. C., Furman, R. R., Coutre, S. E., Flinn, I. W., Burger, J. A., Blum, K. A., Grant, B., Sharman, J. P., Coleman, M., Wierda, W. G., Jones, J. A., Zhao, W., Heerema, N. A., Johnson, A. J., Sukbuntherng, J., Chang, B. Y., Clow, F., Hedrick, E., Buggy, J. J., James, D. F. and O'Brien, S., *Targeting BTK with ibrutinib in relapsed chronic lymphocytic leukemia.* **N Engl J Med**, 2013. 369(1): p. 32-42.

110. Walliser, C., Hermkes, E., Schade, A., Wiese, S., Deinzer, J., Zapatka, M., Desire, L., Mertens, D., Stilgenbauer, S. and Gierschik, P., *The Phospholipase Cγ2 Mutants R665W and L845F Identified in Ibrutinib-resistant Chronic Lymphocytic Leukemia Patients Are Hypersensitive to the Rho GTPase Rac2 Protein.* **J Biol Chem**, 2016. 291(42): p. 22136-22148.

111. Walliser, C., Wist, M., Hermkes, E., Zhou, Y., Schade, A., Haas, J., Deinzer, J., Desire, L., Li, S. S. C., Stilgenbauer, S., Milner, J. D. and Gierschik, P., *Functional characterization of phospholipase Cγ2 mutant protein causing both somatic ibrutinib resistance and a germline monogenic autoinflammatory disorder*. **Oncotarget**, 2018. 9(76): p. 34357-34378.

112. Magno, L., Lessard, C. B., Martins, M., Lang, V., Cruz, P., Asi, Y., Katan, M., Bilsland, J., Lashley, T., Chakrabarty, P., Golde, T. E. and Whiting, P. J., *Alzheimer's disease phospholipase Cγ2 (PLCG2) protective variant is a functional hypermorph.* **Alzheimers Res Ther**, 2019. 11(1): p. 16.

113. Andreone, B. J., Przybyla, L., Llapashtica, C., Rana, A., Davis, S. S., van Lengerich, B., Lin, K., Shi, J., Mei, Y., Astarita, G., Di Paolo, G., Sandmann, T., Monroe, K. M. and Lewcock, J. W., *Alzheimer's-associated PLCγ2 is a signaling node required for both TREM2 function and the inflammatory response in human microglia.* **Nat Neurosci**, 2020. 23(8): p. 927-938.

114. Maguire, E., Menzies, G. E., Phillips, T., Sasner, M., Williams, H. M., Czubala, M. A., Evans, N., Cope, E. L., Sims, R., Howell, G. R., Lloyd-Evans, E., Williams, J., Allen, N. D. and Taylor, P. R., *PIP2 depletion and altered endocytosis caused by expression of Alzheimer's disease-protective variant PLCγ2 R522.* **EMBO J**, 2021. 40(17): p. e105603.

115. Cremasco, V., Graham, D. B., Novack, D. V., Swat, W. and Faccio, R., *Vav/Phospholipase Cγ2-mediated control of a neutrophil-dependent murine model of rheumatoid arthritis.* **Arthritis Rheum**, 2008. 58(9): p. 2712-22.

116. Cremasco, V., Benasciutti, E., Cella, M., Kisseleva, M., Croke, M. and Faccio, R., *Phospholipase Cγ2 is critical for development of a murine model of inflammatory arthritis by affecting actin dynamics in dendritic cells.* **PLoS One**, 2010. 5(1): p. e8909.

117. Afroz, S., Giddaluru, J., Vishwakarma, S., Naz, S., Khan, A. A. and Khan, N., *A Comprehensive Gene Expression Meta-analysis Identifies Novel Immune Signatures in Rheumatoid Arthritis Patients.* **Front Immunol**, 2017. 8: p. 74.

118. Mahajan, S., Decker, C. E., Yang, Z., Veis, D., Mellins, E. D. and Faccio, R., *Plcγ2/Tmem178 dependent pathway in myeloid cells modulates the pathogenesis of cytokine storm syndrome.* **J Autoimmun**, 2019. 100: p. 62-74.

119. Berger, M., Wraith, K., Woodward, C., Aburima, A., Raslan, Z., Hindle, M. S., Moellmann, J., Febbraio, M. and Naseem, K. M., *Dyslipidemia-associated atherogenic oxidized lipids induce platelet hyperactivity through phospholipase Cγ2-dependent reactive oxygen species generation.* **Platelets**, 2019. 30(4): p. 467-472.

120. Throm, A. A., Alinger, J. B., Pingel, J. T., Daugherty, A. L., Pachman, L. M. and French, A. R., *Dysregulated NK cell PLCγ2 signaling and activity in juvenile dermatomyositis.* **JCI Insight**, 2018. 3(22).

121. Weidinger, S., Beck, L. A., Bieber, T., Kabashima, K. and Irvine, A. D., *Atopic dermatitis.* **Nat Rev Dis Primers**, 2018. 4(1): p. 1.

122. Wohlmann, A., Sebastian, K., Borowski, A., Krause, S. and Friedrich, K., *Signal transduction by the atopy-associated human thymic stromal lymphopoietin (TSLP) receptor depends on Janus kinase function.* **Biol Chem**, 2010. 391(2-3): p. 181-6.

123. Jin, H., He, R., Oyoshi, M. and Geha, R. S., *Animal models of atopic dermatitis.* **J Invest Dermatol**, 2009. 129(1): p. 31-40.

124. Howell, M. D., Kim, B. E., Gao, P., Grant, A. V., Boguniewicz, M., Debenedetto, A., Schneider, L., Beck, L. A., Barnes, K. C. and Leung, D. Y., *Cytokine modulation of atopic dermatitis filaggrin skin expression.* **J Allergy Clin Immunol**, 2007. 120(1): p. 150-5.

125. Bao, L., Shi, V. Y. and Chan, L. S., *IL-4 up-regulates epidermal chemotactic, angiogenic, and pro-inflammatory genes and down-regulates antimicrobial genes in vivo and in vitro: relevant in the pathogenesis of atopic dermatitis.* **Cytokine**, 2013. 61(2): p. 419-25.

126. Oetjen, L. K., Mack, M. R., Feng, J., Whelan, T. M., Niu, H., Guo, C. J., Chen, S., Trier, A. M., Xu, A. Z., Tripathi, S. V., Luo, J., Gao, X., Yang, L., Hamilton,

S. L., Wang, P. L., Brestoff, J. R., Council, M. L., Brasington, R., Schaffer, A., Brombacher, F., Hsieh, C. S., Gereau, R. W. t., Miller, M. J., Chen, Z. F., Hu, H., Davidson, S., Liu, Q. and Kim, B. S., *Sensory Neurons Co-opt Classical Immune Signaling Pathways to Mediate Chronic Itch.* **Cell**, 2017. 171(1): p. 217-228 e13.

127. Yasuda, T., Fukada, T., Nishida, K., Nakayama, M., Matsuda, M., Miura, I., Dainichi, T., Fukuda, S., Kabashima, K., Nakaoka, S., Bin, B. H., Kubo, M., Ohno, H., Hasegawa, T., Ohara, O., Koseki, H., Wakana, S. and Yoshida, H., *Hyperactivation of JAK1 tyrosine kinase induces stepwise, progressive pruritic dermatitis.* **J Clin Invest**, 2016. 126(6): p. 2064-76.

128. Cartron, A. M., Nguyen, T. H., Roh, Y. S., Kwatra, M. M. and Kwatra, S. G., *Janus kinase inhibitors for atopic dermatitis: a promising treatment modality.* **Clin Exp Dermatol**, 2021. 46(5): p. 820-824.

129. Reich, K., Teixeira, H. D., de Bruin-Weller, M., Bieber, T., Soong, W., Kabashima, K., Werfel, T., Zeng, J., Huang, X., Hu, X., Hendrickson, B. A., Ladizinski, B., Chu, A. D. and Silverberg, J. I., *Safety and efficacy of upadacitinib in combination with topical corticosteroids in adolescents and adults with moderate-to-severe atopic dermatitis (AD Up): results from a randomised, double-blind, placebo-controlled, phase 3 trial.* **Lancet**, 2021. 397(10290): p. 2169-2181.

130. Guttman-Yassky, E., Teixeira, H. D., Simpson, E. L., Papp, K. A., Pangan, A. L., Blauvelt, A., Thaci, D., Chu, C. Y., Hong, H. C., Katoh, N., Paller, A. S., Calimlim, B., Gu, Y., Hu, X., Liu, M., Yang, Y., Liu, J., Tenorio, A. R., Chu, A. D. and Irvine, A. D., *Once-daily upadacitinib versus placebo in adolescents and adults with moderate-to-severe atopic dermatitis (Measure Up 1 and Measure Up 2): results from two replicate double-blind, randomised controlled phase 3 trials.* **Lancet**, 2021. 397(10290): p. 2151-2168.

131. Melo, A., Carrascosa, J. M. and Torres, T., *Baricitinib for the treatment of atopic dermatitis.* **J Dermatolog Treat**, 2021: p. 1-10.

132. Papp, K., Szepietowski, J. C., Kircik, L., Toth, D., Eichenfield, L. F., Leung, D. Y. M., Forman, S. B., Venturanza, M. E., Sun, K., Kuligowski, M. E. and Simpson, E. L., *Efficacy and safety of ruxolitinib cream for the treatment of atopic*

dermatitis: Results from 2 phase 3, randomized, double-blind studies. **J Am Acad Dermatol**, 2021. 85(4): p. 863-872.

133. Chiou, C., *Incyte Announces U.S. FDA Approval of Opzelura™ (ruxolitinib) Cream, a Topical JAK Inhibitor, for the Treatment of Atopic Dermatitis (AD)*. 2021, Incyte press releases.
134. Novak, N., Tepel, C., Koch, S., Brix, K., Bieber, T. and Kraft, S., *Evidence for a differential expression of the FcεRIγ chain in dendritic cells of atopic and nonatopic donors.* **J Clin Invest**, 2003. 111(7): p. 1047-56.
135. Greb, J. E., Goldminz, A. M., Elder, J. T., Lebwohl, M. G., Gladman, D. D., Wu, J. J., Mehta, N. N., Finlay, A. Y. and Gottlieb, A. B., *Psoriasis.* **Nat Rev Dis Primers**, 2016. 2: p. 16082.
136. Di Cesare, A., Di Meglio, P. and Nestle, F. O., *The IL-23/Th17 Axis in the Immunopathogenesis of Psoriasis.* **J Invest Dermatol**, 2009. 129(6): p. 1339-1350.
137. Dainichi, T., Kitoh, A., Otsuka, A., Nakajima, S., Nomura, T., Kaplan, D. H. and Kabashima, K., *The epithelial immune microenvironment (EIME) in atopic dermatitis and psoriasis.* **Nat Immunol**, 2018. 19(12): p. 1286-1298.
138. Ishizaki, M., Muromoto, R., Akimoto, T., Sekine, Y., Kon, S., Diwan, M., Maeda, H., Togi, S., Shimoda, K., Oritani, K. and Matsuda, T., *Tyk2 is a therapeutic target for psoriasis-like skin inflammation.* **Int Immunol**, 2014. 26(5): p. 257-67.
139. Works, M. G., Yin, F., Yin, C. C., Yiu, Y., Shew, K., Tran, T. T., Dunlap, N., Lam, J., Mitchell, T., Reader, J., Stein, P. L. and D'Andrea, A., *Inhibition of TYK2 and JAK1 ameliorates imiquimod-induced psoriasis-like dermatitis by inhibiting IL-22 and the IL-23/IL-17 axis.* **J Immunol**, 2014. 193(7): p. 3278-87.
140. Fridman, J. S., Scherle, P. A., Collins, R., Burn, T., Neilan, C. L., Hertel, D., Contel, N., Haley, P., Thomas, B., Shi, J., Collier, P., Rodgers, J. D., Shepard, S., Metcalf, B., Hollis, G., Newton, R. C., Yeleswaram, S., Friedman, S. M. and Vaddi, K., *Preclinical evaluation of local JAK1 and JAK2 inhibition in cutaneous inflammation.* **J Invest Dermatol**, 2011. 131(9): p. 1838-44.
141. Funk, P. J., Perche, P. O., Singh, R., Kelly, K. A. and Feldman, S. R., *Comparing available JAK inhibitors for treating patients with psoriasis.* **Expert Rev Clin Immunol**, 2022: p. 1-14.

142. LeibundGut-Landmann, S., Gross, O., Robinson, M. J., Osorio, F., Slack, E. C., Tsoni, S. V., Schweighoffer, E., Tybulewicz, V., Brown, G. D., Ruland, J. and Sousa, C. R. E., *Syk- and CARD9-dependent coupling of innate immunity to the induction of T helper cells that produce interleukin 17.* **Nature Immunology**, 2007. 8(6): p. 630-638.

143. Muro, R., Nitta, T., Nakano, K., Okamura, T., Takayanagi, H. and Suzuki, H., *γδTCR recruits the Syk/PI3K axis to drive proinflammatory differentiation program.* **J Clin Invest**, 2018. 128(1): p. 415-426.

144. Montagnon, C. M., Tolkachjov, S. N., Murrell, D. F., Camilleri, M. J. and Lehman, J. S., *Subepithelial autoimmune blistering dermatoses: Clinical features and diagnosis.* **J Am Acad Dermatol**, 2021. 85(1): p. 1-14.

145. Deng, G. M., Liu, L., Bahjat, F. R., Pine, P. R. and Tsokos, G. C., *Suppression of Skin and Kidney Disease by Inhibition of Spleen Tyrosine Kinase in Lupus-Prone Mice.* **Arthritis and Rheumatism**, 2010. 62(7): p. 2086-2092.

146. Chalmers, S. A., Wen, J., Doerner, J., Stock, A., Cuda, C. M., Makinde, H. M., Perlman, H., Bosanac, T., Webb, D., Nabozny, G., Fine, J. S., Klein, E., Ramanujam, M. and Putterman, C., *Highly selective inhibition of Bruton's tyrosine kinase attenuates skin and brain disease in murine lupus.* **Arthritis Res Ther**, 2018. 20(1): p. 10.

147. Chan, E. S., Herlitz, L. C. and Jabbari, A., *Ruxolitinib Attenuates Cutaneous Lupus Development in a Mouse Lupus Model.* **J Invest Dermatol**, 2015. 135(7): p. 1912-1915.

148. Nesterovitch, A. B., Szanto, S., Gonda, A., Bardos, T., Kis-Toth, K., Adarichev, V. A., Olasz, K., Ghassemi-Najad, S., Hoffman, M. D., Tharp, M. D., Mikecz, K. and Glant, T. T., *Spontaneous insertion of a b2 element in the ptpn6 gene drives a systemic autoinflammatory disease in mice resembling neutrophilic dermatosis in humans.* **Am J Pathol**, 2011. 178(4): p. 1701-14.

149. Gurung, P., Fan, G., Lukens, J. R., Vogel, P., Tonks, N. K. and Kanneganti, T. D., *Tyrosine Kinase SYK Licenses MyD88 Adaptor Protein to Instigate IL-1α-Mediated Inflammatory Disease.* **Immunity**, 2017. 46(4): p. 635-648.

150. Schmidt, E. and Zillikens, D., *Pemphigoid diseases.* **Lancet**, 2013. 381(9863): p. 320-32.

151. Hammers, C. M. and Stanley, J. R., *Mechanisms of Disease: Pemphigus and Bullous Pemphigoid.* **Annu Rev Pathol**, 2016. 11: p. 175-97.
152. Egami, S., Yamagami, J. and Amagai, M., *Autoimmune bullous skin diseases, pemphigus and pemphigoid.* **J Allergy Clin Immunol**, 2020. 145(4): p. 1031-1047.
153. Kridin, K. and Ludwig, R. J., *The Growing Incidence of Bullous Pemphigoid: Overview and Potential Explanations.* **Front Med (Lausanne)**, 2018. 5: p. 220.
154. Sitaru, C., Mihai, S., Otto, C., Chiriac, M. T., Hausser, I., Dotterweich, B., Saito, H., Rose, C., Ishiko, A. and Zillikens, D., *Induction of dermal-epidermal separation in mice by passive transfer of antibodies specific to type VII collagen.* **J Clin Invest**, 2005. 115(4): p. 870-8.
155. Koga, H., Prost-Squarcioni, C., Iwata, H., Jonkman, M. F., Ludwig, R. J. and Bieber, K., *Epidermolysis Bullosa Acquisita: The 2019 Update.* **Front Med (Lausanne)**, 2018. 5: p. 362.
156. Chen, M., O'Toole, E. A., Sanghavi, J., Mahmud, N., Kelleher, D., Weir, D., Fairley, J. A. and Woodley, D. T., *The epidermolysis bullosa acquisita antigen (type VII collagen) is present in human colon and patients with crohn's disease have autoantibodies to type VII collagen.* **J Invest Dermatol**, 2002. 118(6): p. 1059-64.
157. Nusbaum, K. B., Korman, A. M., Tyler, K., Kaffenberger, J., Trinidad, J. and Kaffenberger, B. H., *In vitro diagnostics for the medical dermatologist. Part I: Autoimmune tests.* **J Am Acad Dermatol**, 2021. 85(2): p. 287-298.
158. Feliciani, C., Joly, P., Jonkman, M. F., Zambruno, G., Zillikens, D., Ioannides, D., Kowalewski, C., Jedlickova, H., Karpati, S., Marinovic, B., Mimouni, D., Uzun, S., Yayli, S., Hertl, M. and Borradori, L., *Management of bullous pemphigoid: the European Dermatology Forum consensus in collaboration with the European Academy of Dermatology and Venereology*. **Br J Dermatol**, 2015. 172(4): p. 867-77.
159. Schmidt, E., Reimer, S., Kruse, N., Jainta, S., Brocker, E. B., Marinkovich, M. P., Giudice, G. J. and Zillikens, D., *Autoantibodies to BP180 associated with bullous pemphigoid release interleukin-6 and interleukin-8 from cultured human keratinocytes.* **J Invest Dermatol**, 2000. 115(5): p. 842-8.

160. Gammon, W. R., Merritt, C. C., Lewis, D. M., Sams, W. M., Jr., Carlo, J. R. and Wheeler, C. E., Jr., *An in vitro model of immune complex-mediated basement membrane zone separation caused by pemphigoid antibodies, leukocytes, and complement.* **J Invest Dermatol**, 1982. 78(4): p. 285-90.

161. Sitaru, C., Kromminga, A., Hashimoto, T., Brocker, E. B. and Zillikens, D., *Autoantibodies to type VII collagen mediate Fcγ-dependent neutrophil activation and induce dermal-epidermal separation in cryosections of human skin.* **Am J Pathol**, 2002. 161(1): p. 301-11.

162. Csorba, K., Sesarman, A., Oswald, E., Feldrihan, V., Fritsch, A., Hashimoto, T. and Sitaru, C., *Cross-reactivity of autoantibodies from patients with epidermolysis bullosa acquisita with murine collagen VII.* **Cell Mol Life Sci**, 2010. 67(8): p. 1343-51.

163. Liu, Z., Diaz, L. A., Troy, J. L., Taylor, A. F., Emery, D. J., Fairley, J. A. and Giudice, G. J., *A passive transfer model of the organ-specific autoimmune disease, bullous pemphigoid, using antibodies generated against the hemidesmosomal antigen, BP180.* **J Clin Invest**, 1993. 92(5): p. 2480-8.

164. Liu, Z., Sui, W., Zhao, M., Li, Z., Li, N., Thresher, R., Giudice, G. J., Fairley, J. A., Sitaru, C., Zillikens, D., Ning, G., Marinkovich, M. P. and Diaz, L. A., *Subepidermal blistering induced by human autoantibodies to BP180 requires innate immune players in a humanized bullous pemphigoid mouse model.* **J Autoimmun**, 2008. 31(4): p. 331-8.

165. Nishie, W., Sawamura, D., Goto, M., Ito, K., Shibaki, A., McMillan, J. R., Sakai, K., Nakamura, H., Olasz, E., Yancey, K. B., Akiyama, M. and Shimizu, H., *Humanization of autoantigen.* **Nat Med**, 2007. 13(3): p. 378-83.

166. Oswald, E., Sesarman, A., Franzke, C. W., Wolfle, U., Bruckner-Tuderman, L., Jakob, T., Martin, S. F. and Sitaru, C., *The flavonoid luteolin inhibits Fcγ-dependent respiratory burst in granulocytes, but not skin blistering in a new model of pemphigoid in adult mice.* **PLoS One**, 2012. 7(2): p. e31066.

167. Schulze, F. S., Beckmann, T., Nimmerjahn, F., Ishiko, A., Collin, M., Kohl, J., Goletz, S., Zillikens, D., Ludwig, R. and Schmidt, E., *Fcγ receptors III and IV mediate tissue destruction in a novel adult mouse model of bullous pemphigoid.* **Am J Pathol**, 2014. 184(8): p. 2185-96.

168. Woodley, D. T., Chang, C., Saadat, P., Ram, R., Liu, Z. and Chen, M., *Evidence that anti-type VII collagen antibodies are pathogenic and responsible for the clinical, histological, and immunological features of epidermolysis bullosa acquisita.* **J Invest Dermatol**, 2005. 124(5): p. 958-64.

169. Woodley, D. T., Ram, R., Doostan, A., Bandyopadhyay, P., Huang, Y., Remington, J., Hou, Y., Keene, D. R., Liu, Z. and Chen, M., *Induction of epidermolysis bullosa acquisita in mice by passive transfer of autoantibodies from patients.* **J Invest Dermatol**, 2006. 126(6): p. 1323-30.

170. Vorobyev, A., Ujiie, H., Recke, A., Buijsrogge, J. J. A., Jonkman, M. F., Pas, H. H., Iwata, H., Hashimoto, T., Kim, S. C., Hoon Kim, J., Groves, R., Samavedam, U., Gupta, Y., Schmidt, E., Zillikens, D., Shimizu, H. and Ludwig, R. J., *Autoantibodies to Multiple Epitopes on the Non-Collagenous-1 Domain of Type VII Collagen Induce Blisters.* **J Invest Dermatol**, 2015. 135(6): p. 1565-1573.

171. Hirose, M., Recke, A., Beckmann, T., Shimizu, A., Ishiko, A., Bieber, K., Westermann, J., Zillikens, D., Schmidt, E. and Ludwig, R. J., *Repetitive immunization breaks tolerance to type XVII collagen and leads to bullous pemphigoid in mice.* **J Immunol**, 2011. 187(3): p. 1176-83.

172. Ujiie, H., Shibaki, A., Nishie, W., Sawamura, D., Wang, G., Tateishi, Y., Li, Q., Moriuchi, R., Qiao, H., Nakamura, H., Akiyama, M. and Shimizu, H., *A novel active mouse model for bullous pemphigoid targeting humanized pathogenic antigen.* **J Immunol**, 2010. 184(4): p. 2166-74.

173. Sitaru, C., Chiriac, M. T., Mihai, S., Buning, J., Gebert, A., Ishiko, A. and Zillikens, D., *Induction of complement-fixing autoantibodies against type VII collagen results in subepidermal blistering in mice.* **J Immunol**, 2006. 177(5): p. 3461-8.

174. Iwata, H., Bieber, K., Tiburzy, B., Chrobok, N., Kalies, K., Shimizu, A., Leineweber, S., Ishiko, A., Vorobyev, A., Zillikens, D., Kohl, J., Westermann, J., Seeger, K., Manz, R. and Ludwig, R. J., *B cells, dendritic cells, and macrophages are required to induce an autoreactive CD4 helper T cell response in experimental epidermolysis bullosa acquisita.* **J Immunol**, 2013. 191(6): p. 2978-88.

175. Hurskainen, T., Kokkonen, N., Sormunen, R., Jackow, J., Loffek, S., Soininen, R., Franzke, C. W., Bruckner-Tuderman, L. and Tasanen, K., *Deletion of the major bullous pemphigoid epitope region of collagen XVII induces blistering, autoimmunization, and itching in mice.* **J Invest Dermatol**, 2015. 135(5): p. 1303-1310.

176. Ludwig, R. J., Recke, A., Bieber, K., Muller, S., Marques Ade, C., Banczyk, D., Hirose, M., Kasperkiewicz, M., Ishii, N., Schmidt, E., Westermann, J., Zillikens, D. and Ibrahim, S. M., *Generation of antibodies of distinct subclasses and specificity is linked to H2s in an active mouse model of epidermolysis bullosa acquisita.* **J Invest Dermatol**, 2011. 131(1): p. 167-76.

177. Sitaru, A. G., Sesarman, A., Mihai, S., Chiriac, M. T., Zillikens, D., Hultman, P., Solbach, W. and Sitaru, C., *T cells are required for the production of blister-inducing autoantibodies in experimental epidermolysis bullosa acquisita.* **J Immunol**, 2010. 184(3): p. 1596-603.

178. Freire, P. C., Munoz, C. H. and Stingl, G., *IgE autoreactivity in bullous pemphigoid: eosinophils and mast cells as major targets of pathogenic immune reactants.* **Br J Dermatol**, 2017. 177(6): p. 1644-1653.

179. Sesarman, A., Sitaru, A. G., Olaru, F., Zillikens, D. and Sitaru, C., *Neonatal Fc receptor deficiency protects from tissue injury in experimental epidermolysis bullosa acquisita.* **J Mol Med (Berl)**, 2008. 86(8): p. 951-9.

180. Kasprick, A., Hofrichter, M., Smith, B., Ward, P., Bieber, K., Shock, A., Ludwig, R. J. and Schmidt, E., *Treatment with anti-neonatal Fc receptor (FcRn) antibody ameliorates experimental epidermolysis bullosa acquisita in mice.* **Br J Pharmacol**, 2020. 177(10): p. 2381-2392.

181. Karsten, C. M., Beckmann, T., Holtsche, M. M., Tillmann, J., Tofern, S., Schulze, F. S., Heppe, E. N., Ludwig, R. J., Zillikens, D., Konig, I. R., Kohl, J. and Schmidt, E., *Tissue Destruction in Bullous Pemphigoid Can Be Complement Independent and May Be Mitigated by C5aR2.* **Front Immunol**, 2018. 9: p. 488.

182. Nelson, K. C., Zhao, M., Schroeder, P. R., Li, N., Wetsel, R. A., Diaz, L. A. and Liu, Z., *Role of different pathways of the complement cascade in experimental bullous pemphigoid.* **J Clin Invest**, 2006. 116(11): p. 2892-900.

183. Mihai, S., Chiriac, M. T., Takahashi, K., Thurman, J. M., Holers, V. M., Zillikens, D., Botto, M. and Sitaru, C., *The alternative pathway of complement activation is critical for blister induction in experimental epidermolysis bullosa acquisita.* **J Immunol**, 2007. 178(10): p. 6514-21.

184. Mihai, S., Hirose, M., Wang, Y., Thurman, J. M., Holers, V. M., Morgan, B. P., Kohl, J., Zillikens, D., Ludwig, R. J. and Nimmerjahn, F., *Specific Inhibition of Complement Activation Significantly Ameliorates Autoimmune Blistering Disease in Mice.* **Front Immunol**, 2018. 9: p. 535.

185. Sadik, C. D., Miyabe, Y., Sezin, T. and Luster, A. D., *The critical role of C5a as an initiator of neutrophil-mediated autoimmune inflammation of the joint and skin.* **Semin Immunol**, 2018. 37: p. 21-29.

186. Rosetti, F. and Mayadas, T. N., *The many faces of Mac-1 in autoimmune disease.* **Immunol Rev**, 2016. 269(1): p. 175-93.

187. Liu, Z., Zhao, M., Li, N., Diaz, L. A. and Mayadas, T. N., *Differential roles for β2 integrins in experimental autoimmune bullous pemphigoid.* **Blood**, 2006. 107(3): p. 1063-9.

188. Deng, F. Y., Chen, Y., Zheng, J. F., Huang, Q. N. A., Cao, X. T., Zillikens, D., Petersen, F. and Yu, X. H., *CD11b-deficient mice exhibit an increased severity in the late phase of antibody transfer-induced experimental epidermolysis bullosa acquisita.* **Experimental Dermatology**, 2017. 26(12): p. 1175-1178.

189. Chiriac, M. T., Roesler, J., Sindrilaru, A., Scharffetter-Kochanek, K., Zillikens, D. and Sitaru, C., *NADPH oxidase is required for neutrophil-dependent autoantibody-induced tissue damage.* **J Pathol**, 2007. 212(1): p. 56-65.

190. Yu, X. H., Akbarzadeh, R., Pieper, M., Scholzen, T., Gehrig, S., Schultz, C., Zillikens, D., Konig, P. and Petersen, F., *Neutrophil Adhesion Is a Prerequisite for Antibody-Mediated Proteolytic Tissue Damage in Experimental Models of Epidermolysis Bullosa Acquisita.* **Journal of Investigative Dermatology**, 2018. 138(9): p. 1990-1998.

191. Schmidt, E., Ambach, A., Bastian, B., Brocker, E. B. and Zillikens, D., *Elevated levels of interleukin-8 in blister fluid of bullous pemphigoid compared with suction blisters of healthy control subjects.* **J Am Acad Dermatol**, 1996. 34(2 Pt 1): p. 310-2.

192. Sezin, T., Murthy, S., Attah, C., Seutter, M., Holtsche, M. M., Hammers, C. M., Schmidt, E., Meshrkey, F., Mousavi, S., Zillikens, D., Nunn, M. A. and Sadik, C. D., *Dual inhibition of complement factor 5 and leukotriene B4 synergistically suppresses murine pemphigoid disease.* **JCI Insight**, 2019. 4(15).

193. Kawana, S., Ueno, A. and Nishiyama, S., *Increased levels of immunoreactive leukotriene B4 in blister fluids of bullous pemphigoid patients and effects of a selective 5-lipoxygenase inhibitor on experimental skin lesions.* **Acta Derm Venereol**, 1990. 70(4): p. 281-5.

194. Sezin, T., Krajewski, M., Wutkowski, A., Mousavi, S., Chakievska, L., Bieber, K., Ludwig, R. J., Dahlke, M., Rades, D., Schulze, F. S., Schmidt, E., Kalies, K., Gupta, Y., Schilf, P., Ibrahim, S. M., Konig, P., Schwudke, D., Zillikens, D. and Sadik, C. D., *The Leukotriene B4 and its Receptor BLT1 Act as Critical Drivers of Neutrophil Recruitment in Murine Bullous Pemphigoid-Like Epidermolysis Bullosa Acquisita.* **J Invest Dermatol**, 2017. 137(5): p. 1104-1113.

195. Kasperkiewicz, M., Nimmerjahn, F., Wende, S., Hirose, M., Iwata, H., Jonkman, M. F., Samavedam, U., Gupta, Y., Moller, S., Rentz, E., Hellberg, L., Kalies, K., Yu, X., Schmidt, E., Hasler, R., Laskay, T., Westermann, J., Kohl, J., Zillikens, D. and Ludwig, R. J., *Genetic identification and functional validation of FcγRIV as key molecule in autoantibody-induced tissue injury.* **J Pathol**, 2012. 228(1): p. 8-19.

196. Kovacs, B., Tillmann, J., Freund, L. C., Nimmerjahn, F., Sadik, C. D., Bieber, K., Ludwig, R. J., Karsten, C. M. and Kohl, J., *Fcγ Receptor IIB Controls Skin Inflammation in an Active Model of Epidermolysis Bullosa Acquisita.* **Front Immunol**, 2019. 10: p. 3012.

197. Iwata, H., Pipi, E., Mockel, N., Sondermann, P., Vorobyev, A., van Beek, N., Zillikens, D. and Ludwig, R. J., *Recombinant soluble CD32 suppresses disease progression in experimental epidermolysis bullosa acquisita.* **J Invest Dermatol**, 2015. 135(3): p. 916-919.

198. Zhao, M. L., Trimbeger, M. E., Li, N., Diaz, L. A., Shapiro, S. D. and Liu, Z., *Role of FcRs in animal model of autoimmune bullous pemphigoid.* **Journal of Immunology**, 2006. 177(5): p. 3398-3405.

199. Yu, X., Holdorf, K., Kasper, B., Zillikens, D., Ludwig, R. J. and Petersen, F., *FcγRIIA and FcγRIIIB are required for autoantibody-induced tissue damage in experimental human models of bullous pemphigoid.* **J Invest Dermatol**, 2010. 130(12): p. 2841-4.

200. Samavedam, U. K., Mitschker, N., Kasprick, A., Bieber, K., Schmidt, E., Laskay, T., Recke, A., Goletz, S., Vidarsson, G., Schulze, F. S., Armbrust, M., Dieckhoff, K. S., Pas, H. H., Jonkman, M. F., Kalies, K., Zillikens, D., Gupta, Y., Ibrahim, S. M. and Ludwig, R. J., *Whole-genome expression profiling in skin reveals SYK as a key regulator of inflammation in experimental epidermolysis bullosa acquisita.* **Frontiers in Immunology**, 2018. 9: p. 16.

201. Kulkarni, S., Sitaru, C., Jakus, Z., Anderson, K. E., Damoulakis, G., Davidson, K., Hirose, M., Juss, J., Oxley, D., Chessa, T. A., Ramadani, F., Guillou, H., Segonds-Pichon, A., Fritsch, A., Jarvis, G. E., Okkenhaug, K., Ludwig, R., Zillikens, D., Mócsai, A., Vanhaesebroeck, B., Stephens, L. R. and Hawkins, P. T., *PI3Kβ plays a critical role in neutrophil activation by immune complexes.* **Sci Signal**, 2011. 4(168): p. ra23.

202. Koga, H., Kasprick, A., Lopez, R., Auli, M., Pont, M., Godessart, N., Zillikens, D., Bieber, K., Ludwig, R. J. and Balague, C., *Therapeutic Effect of a Novel Phosphatidylinositol-3-Kinase delta Inhibitor in Experimental Epidermolysis Bullosa Acquisita.* **Front Immunol**, 2018. 9: p. 1558.

203. Lin, L., Hwang, B., Culton, D. A., Li, N., Burette, S., Koller, B. H., Messingham, K. A., Fairley, J. A., Lee, J. J., Hall, R. P., An, L. J., Diaz, L. A. and Liu, Z., *Eosinophils Mediate Tissue Injury in the Autoimmune Skin Disease Bullous Pemphigoid.* **Journal of Investigative Dermatology**, 2018. 138(5): p. 1032-1043.

204. Margaroli, C., Bradley, B., Thompson, C., Brown, M. R., Giacalone, V. D., Bhatt, L., Stoff, B., Ahuja, S., Springman, E., Tirouvanziam, R. and Feldman, R. J., *Distinct compartmentalization of immune cells and mediators characterizes bullous pemphigoid disease.* **Exp Dermatol**, 2020. 29(12): p. 1191-1198.

205. Csepregi, J. Z., Orosz, A., Zajta, E., Kása, O., Németh, T., Simon, E., Fodor, S., Csonka, K., Baratki, B. L., Kövesdi, D., He, Y. W., Gácser, A. and Mócsai, A., *Myeloid-Specific Deletion of Mcl-1 Yields Severely Neutropenic Mice That*

Survive and Breed in Homozygous Form. **J Immunol**, 2018. 201(12): p. 3793-3803.

206. Samavedam, U. K., Iwata, H., Muller, S., Schulze, F. S., Recke, A., Schmidt, E., Zillikens, D. and Ludwig, R. J., *GM-CSF modulates autoantibody production and skin blistering in experimental epidermolysis bullosa acquisita.* **J Immunol**, 2014. 192(2): p. 559-71.
207. Czech, W., Schaller, J., Schopf, E. and Kapp, A., *Granulocyte activation in bullous diseases: release of granular proteins in bullous pemphigoid and pemphigus vulgaris.* **J Am Acad Dermatol**, 1993. 29(2 Pt 1): p. 210-5.
208. D'Auria, L., Pietravalle, M., Cordiali-Fei, P. and Ameglio, F., *Increased tryptase and myeloperoxidase levels in blister fluids of patients with bullous pemphigoid: correlations with cytokines, adhesion molecules and anti-basement membrane zone antibodies.* **Exp Dermatol**, 2000. 9(2): p. 131-7.
209. Liu, Z., Shipley, J. M., Vu, T. H., Zhou, X., Diaz, L. A., Werb, Z. and Senior, R. M., *Gelatinase B-deficient mice are resistant to experimental bullous pemphigoid.* **J Exp Med**, 1998. 188(3): p. 475-82.
210. Liu, Z., Shapiro, S. D., Zhou, X., Twining, S. S., Senior, R. M., Giudice, G. J., Fairley, J. A. and Diaz, L. A., *A critical role for neutrophil elastase in experimental bullous pemphigoid.* **J Clin Invest**, 2000. 105(1): p. 113-23.
211. Lin, L., Betsuyaku, T., Heimbach, L., Li, N., Rubenstein, D., Shapiro, S. D., An, L., Giudice, G. J., Diaz, L. A., Senior, R. M. and Liu, Z., *Neutrophil elastase cleaves the murine hemidesmosomal protein BP180/type XVII collagen and generates degradation products that modulate experimental bullous pemphigoid.* **Matrix Biol**, 2012. 31(1): p. 38-44.
212. Shimanovich, I., Mihai, S., Oostingh, G. J., Ilenchuk, T. T., Brocker, E. B., Opdenakker, G., Zillikens, D. and Sitaru, C., *Granulocyte-derived elastase and gelatinase B are required for dermal-epidermal separation induced by autoantibodies from patients with epidermolysis bullosa acquisita and bullous pemphigoid.* **J Pathol**, 2004. 204(5): p. 519-27.
213. Wakugawa, M., Nakamura, K., Hino, H., Toyama, K., Hattori, N., Okochi, H., Yamada, H., Hirai, K., Tamaki, K. and Furue, M., *Elevated levels of eotaxin and*

interleukin-5 in blister fluid of bullous pemphigoid: correlation with tissue eosinophilia. **Br J Dermatol**, 2000. 143(1): p. 112-6.

214. Solimani, F., Didona, D., Li, J., Bao, L., Patel, P. M., Gasparini, G., Kridin, K., Cozzani, E., Hertl, M. and Amber, K. T., *Characterizing the proteome of bullous pemphigoid blister fluid utilizing tandem mass tag labeling coupled with LC-MS/MS.* **Arch Dermatol Res**, 2021.
215. Messingham, K. N., Wang, J. W., Holahan, H. M., Srikantha, R., Aust, S. C. and Fairley, J. A., *Eosinophil localization to the basement membrane zone is autoantibody- and complement-dependent in a human cryosection model of bullous pemphigoid.* **Exp Dermatol**, 2016. 25(1): p. 50-5.
216. de Graauw, E., Sitaru, C., Horn, M., Borradori, L., Yousefi, S., Simon, H. U. and Simon, D., *Evidence for a role of eosinophils in blister formation in bullous pemphigoid.* **Allergy**, 2017. 72(7): p. 1105-1113.
217. Fang, H., Zhang, Y., Li, N., Wang, G. and Liu, Z., *The Autoimmune Skin Disease Bullous Pemphigoid: The Role of Mast Cells in Autoantibody-Induced Tissue Injury*. **Front Immunol**, 2018. 9: p. 407.
218. Heimbach, L., Li, Z., Berkowitz, P., Zhao, M., Li, N., Rubenstein, D. S., Diaz, L. A. and Liu, Z., *The C5a receptor on mast cells is critical for the autoimmune skin-blistering disease bullous pemphigoid.* **J Biol Chem**, 2011. 286(17): p. 15003-9.
219. Kasprick, A., Yu, X., Scholten, J., Hartmann, K., Pas, H. H., Zillikens, D., Ludwig, R. J. and Petersen, F., *Conditional depletion of mast cells has no impact on the severity of experimental epidermolysis bullosa acquisita.* **Eur J Immunol**, 2015. 45(5): p. 1462-70.
220. Schmidt, E., Bastian, B., Dummer, R., Tony, H. P., Brocker, E. B. and Zillikens, D., *Detection of elevated levels of IL-4, IL-6, and IL-10 in blister fluid of bullous pemphigoid.* **Arch Dermatol Res**, 1996. 288(7): p. 353-7.
221. Montagnon, C. M., Lehman, J. S., Murrell, D. F., Camilleri, M. J. and Tolkachjov, S. N., *Subepithelial autoimmune bullous dermatoses disease activity assessment and therapy.* **J Am Acad Dermatol**, 2021. 85(1): p. 18-27.
222. Kremer, N., Snast, I., Cohen, E. S., Hodak, E., Mimouni, D., Lapidoth, M., Mazor, S. and Levi, A., *Rituximab and Omalizumab for the Treatment of Bullous*

Pemphigoid: A Systematic Review of the Literature. **Am J Clin Dermatol**, 2019. 20(2): p. 209-216.

223. Rashid, H., Meijer, J. M., Bolling, M. C. and Horvath, B., *Clinical response of rituximab and improvement of quality of life in patients with bullous pemphigoid and mucous membrane pemphigoid.* **Br J Dermatol**, 2021.
224. Zhang, Y., Xu, Q., Chen, L., Chen, J., Zhang, J., Zou, Y., Gong, T. and Ji, C., *Efficacy and Safety of Dupilumab in Moderate-to-Severe Bullous Pemphigoid.* **Front Immunol**, 2021. 12: p. 738907.
225. Abdat, R., Waldman, R. A., de Bedout, V., Czernik, A., McLeod, M., King, B., Gordon, S., Ahmed, R., Nichols, A., Rothe, M. and Rosmarin, D., *Dupilumab as a novel therapy for bullous pemphigoid: A multicenter case series.* **J Am Acad Dermatol**, 2020. 83(1): p. 46-52.
226. Majima, Y., Yagi, H., Tateishi, C., Groth, S., Schmidt, E., Zillikens, D., Koga, H., Hashimoto, T. and Tokura, Y., *A successful treatment with ustekinumab in a case of antilaminin-γ1 pemphigoid associated with psoriasis.* **Br J Dermatol**, 2013. 168(6): p. 1367-9.
227. Le Guern, A., Alkeraye, S., Vermersch-Langlin, A., Coupe, P. and Vonarx, M., *Bullous pemphigoid during ustekinumab therapy.* **JAAD Case Rep**, 2015. 1(6): p. 359-60.
228. Izumi, K., Bieber, K. and Ludwig, R. J., *Current Clinical Trials in Pemphigus and Pemphigoid.* **Frontiers in Immunology**, 2019. 10(978).
229. Simon, D., Yousefi, S., Cazzaniga, S., Burgler, C., Radonjic, S., Houriet, C., Heidemeyer, K., Klotgen, H. W., Kozlowski, E., Borradori, L. and Simon, H. U., *Mepolizumab failed to affect bullous pemphigoid: A randomized, placebo-controlled, double-blind phase 2 pilot study.* **Allergy**, 2020. 75(3): p. 669-672.
230. Kahn, J. S., Moody, K. and Rosmarin, D., *Significant improvement of dermatitis herpetiformis with tofacitinib.* **Dermatol Online J**, 2021. 27(7).
231. Ludwig, R. J., Kalies, K., Kohl, J., Zillikens, D. and Schmidt, E., *Emerging treatments for pemphigoid diseases.* **Trends Mol Med**, 2013. 19(8): p. 501-12.
232. Ichise, H., Ichise, T. and Yoshida, N., *Phospholipase Cγ2 Is Required for Luminal Expansion of the Epididymal Duct during Postnatal Development in Mice.* **PLoS One**, 2016. 11(3): p. e0150521.

233. Passegue, E., Wagner, E. F. and Weissman, I. L., *JunB deficiency leads to a myeloproliferative disorder arising from hematopoietic stem cells.* **Cell**, 2004. 119(3): p. 431-43.

234. Gross, S., Gammon, S. T., Moss, B. L., Rauch, D., Harding, J., Heinecke, J. W., Ratner, L. and Piwnica-Worms, D., *Bioluminescence imaging of myeloperoxidase activity in vivo.* **Nat Med**, 2009. 15(4): p. 455-61.

235. Schmidt, E., Mittnacht, A., Schomig, H., Dummer, R., Brocker, E. B. and Zillikens, D., *Detection of IL-1α, IL-1β and IL-1 receptor antagonist in blister fluid of bullous pemphigoid.* **J Dermatol Sci**, 1996. 11(2): p. 142-7.

236. Mócsai, A., *Diverse novel functions of neutrophils in immunity, inflammation, and beyond.* **J Exp Med**, 2013. 210(7): p. 1283-99.

237. Németh, T. and Mócsai, A., *Feedback Amplification of Neutrophil Function.* **Trends Immunol**, 2016. 37(6): p. 412-424.

238. Leon, C. M., Barbosa, C. M., Justo, G. Z., Borelli, P., Resende, J. D., Jr., de Oliveira, J. S., Ferreira, A. T. and Paredes-Gamero, E. J., *Requirement for PLCγ2 in IL-3 and GM-CSF-stimulated MEK/ERK phosphorylation in murine and human hematopoietic stem/progenitor cells.* **J Cell Physiol**, 2011. 226(7): p. 1780-92.

239. Barbosa, C. M., Bincoletto, C., Barros, C. C., Ferreira, A. T. and Paredes-Gamero, E. J., *PLCγ2 and PKC are important to myeloid lineage commitment triggered by M-SCF and G-CSF.* **J Cell Biochem**, 2014. 115(1): p. 42-51.

240. Kurosaki, T., Maeda, A., Ishiai, M., Hashimoto, A., Inabe, K. and Takata, M., *Regulation of the phospholipase Cγ2 pathway in B cells.* **Immunol Rev**, 2000. 176: p. 19-29.

241. Bai, L., Chen, Y., He, Y., Dai, X., Lin, X., Wen, R. and Wang, D., *Phospholipase Cγ2 contributes to light-chain gene activation and receptor editing.* **Mol Cell Biol**, 2007. 27(17): p. 5957-67.

242. Wen, R., Chen, Y., Bai, L., Fu, G., Schuman, J., Dai, X., Zeng, H., Yang, C., Stephan, R. P., Cleveland, J. L. and Wang, D., *Essential role of phospholipase Cγ2 in early B-cell development and Myc-mediated lymphomagenesis.* **Mol Cell Biol**, 2006. 26(24): p. 9364-76.

243. Daniel, B. S., Hertl, M., Werth, V. P., Eming, R. and Murrell, D. F., *Severity score indexes for blistering diseases.* **Clin Dermatol**, 2012. 30(1): p. 108-13.

244. Hundt, J. E., Iwata, H., Pieper, M., Pfundl, R., Bieber, K., Zillikens, D., Konig, P. and Ludwig, R. J., *Visualization of autoantibodies and neutrophils in vivo identifies novel checkpoints in autoantibody-induced tissue injury.* **Sci Rep**, 2020. 10(1): p. 4509.

245. Mao, D., Epple, H., Uthgenannt, B., Novack, D. V. and Faccio, R., *PLCγ2 regulates osteoclastogenesis via its interaction with ITAM proteins and GAB2.* **J Clin Invest**, 2006. 116(11): p. 2869-79.

246. Bleasdale, J. E., Thakur, N. R., Gremban, R. S., Bundy, G. L., Fitzpatrick, F. A., Smith, R. J. and Bunting, S., *Selective inhibition of receptor-coupled phospholipase C-dependent processes in human platelets and polymorphonuclear neutrophils.* **J Pharmacol Exp Ther**, 1990. 255(2): p. 756-68.

247. Hou, C., Kirchner, T., Singer, M., Matheis, M., Argentieri, D. and Cavender, D., *In vivo activity of a phospholipase C inhibitor, 1-(6-((17beta-3-methoxyestra-1,3,5(10)-trien-17-yl)amino)hexyl)-1H-pyrrole-2,5-di one (U73122), in acute and chronic inflammatory reactions.* **J Pharmacol Exp Ther**, 2004. 309(2): p. 697-704.

10. BIBLIOGRAPHY OF CANDIDATE'S PUBLICATIONS

10.1. PUBLICATIONS RELATED TO THESIS

[1] **Szilveszter, K. P.**, Németh, T., and Mócsai, A., *Tyrosine Kinases in Autoimmune and Inflammatory Skin Diseases.* **Front Immunol**, 2019. 10: p. 1862.

IF: 5.085

[2] Futosi, K., Kása, O., **Szilveszter, K. P.**, and Mócsai, A., *Neutrophil Phospholipase Cγ2 Drives Autoantibody-Induced Arthritis Through the Generation of the Inflammatory Microenvironment.* **Arthritis Rheumatol**, 2021. 73(9): p. 1614-1625.

IF: 15.483

[3] **Szilveszter, K. P.,** Vikár, S., Horváth, A. I., Helyes, Z., Sárdy, M. and Mócsai, A., *Phospholipase Cγ2 Is Essential for Experimental Models of Epidermolysis Bullosa Acquisita.* **J Invest Dermatol**, 2022. 142(4): p. 1114-1125.

IF: 7.590

10.2. PUBLICATIONS NOT RELATED TO THESIS

[4] Németh, T., Futosi, K., **Szilveszter, K.**, Vilinovszki, O., Kiss-Pápai, L., and Mócsai, A., *Lineage-Specific Analysis of Syk Function in Autoantibody-Induced Arthritis*. **Front Immunol**, 2018. 9: p. 555.

IF: 4.716

11. ACKNOWLEDGEMENTS

I would like to express my gratitude to all the below mentioned people who helped me along the exciting journey of my PhD studies.

First, I am very grateful that I could call Professor Attila Mócsai my supervisor. He kindly guided me with his invaluable scientific expertise and outstanding warm-hearted personality.

I would like to thank Prof. László Hunyady, the former head of the Department of Physiology, for welcoming me into the Department, and Professors Erzsébet Ligeti and Péter Enyedi, heads of the Doctoral School and the Doctoral Program for their welcoming attitude and professional guidance.

I also thank Prof. Zsuzsanna Helyes and Dr. Ádám Horváth for their help during the in vivo imaging experiments, Dr. László Hiripi and Dr. Péter Major for their support during rabbit immunizations and Prof. Miklós Sárdy for his active collaboration and valuable advice regarding the human ex vivo studies.

My special thanks go to every member of the Department of Physiology supporting me with unconditional help and useful advice any time. Most of all, I am very grateful for the support of all the former and current members of the Inflammatory Research group. They provided a unique environment with kind and friendly atmosphere where I was happy to enter day by day. I would like to highlight Dr. Tamás Németh, who introduced me to this fascinating world when I joined the lab as a research student and kindly supported me from the very beginning.

My thanks also go to my talented research students Dr. Lukács Lesinszki, Simon Vikár and Petra Koncz for enthusiastically helping me in our experiments.

I deeply thank Dr. Anita Orosz, Nikolett Szénási, Klaudia Kiss and Dr. Domonkos Cseh for their continuous support both intellectually and personally throughout these years. I feel fortunate that we became not only good colleges but true friends, as well.

I am grateful for my family who were always standing by my side. I thank my parents for teaching me that I can achieve anything I can imagine. I am thankful for my husband for making a peaceful, loving home together and being there for me whenever I need. Last but definitely not least, I am grateful for my soon-to-be-born baby daughter for patiently waiting for my full attention.